Development of Intelligent GNSS-based Land Vehicle Localisation Systems

Von der Fakultät für Maschinenbau der
Technischen Universität Carolo-Wilhelmina zu Braunschweig

zur Erlangung der Würde
eines Doktor-Ingenieurs (Dr.-Ing.)
genehmigte Dissertation

von: Ing. Federico Grasso Toro
aus: San Juan, Argentina

eingereicht am:	7. April 2015
mündliche Prüfung am:	29. Mai 2015
Referenten:	Prof. Dr.-Ing. Dr. h. c. mult. Eckehard Schnieder
	Prof. Dr.-Ing. Jürgen Beyer
Vorsitzender:	Prof. Dr. Karsten Lemmer

2015

Declaration of Authorship

This thesis was written during my work at the Institute for Traffic Safety and Automation Engineering (Institut für Verkehrssicherheit und Automatisierungstechnik) at the TU-Braunschweig (Technischen Universität Carolo-Wilhelmina zu Braunschweig).
The thesis follows a long tradition of research focused on satellite-based vehicle localisation systems.

Signed: _____

Date: _____

"I believe in the value of the book,
which keeps something irreplaceable,
and in the necessity of fighting
to secure its respect."

Jacques Derrida,
Paper Machine

Zusammenfassung

Die Nutzung der globalen Navigationssatellitensysteme (GNSS) zu Lokalisierungszwecken erfordert eine ständige Auswertung der generierten Positionsinformationen sowie eine standardisierte Validierungsmethodik und anschließende Qualitätskontrollverfahren der GNSS-Empfänger. Die Verwendung eines unabhängigen Referenzsystems sollte genügend Informationen liefern, um das Lokalisierungssystem zu validieren, aber das Fehlen sowohl einer angemessenen Auswertung als auch entsprechender Verfahren stellen erhebliche Lücken für zukünftige Anwendungen sowohl dem Empfänger und der Referenz dar.
Um diese Probleme zu lösen, wird ein Ansatz mit Künstlicher Intelligenz (KI) vorgestellt. Die Entwicklung KI-basierter Validierungstools sowie Filtertechniken zur Positionsbestimmung, um das Bezugssystem zu unterstützen, führt zu erheblichen Verbesserungen insofern, als dass ein GNSS-abhängiges Referenzsystem erstellt werden kann, wenn keine unabhängigen Referenzsysteme verfügbar sein sollten.
Diese zusätzlichen Elemente sind die Grundlagen für zukünftige intelligente GNSS-basierte Lokalisierungssysteme. Die vorgestellten Methoden vereinen fortschrittliche Partikelfilter (PF) für die Positionsbestimmung mit der neuentwickelten Mahalanobis-Ellipsen-Filter (MEF)-Methodik für die genauigkeitsbasierte Datenauswertung, sowie einen Künstlichen-Neuronalen-Netze (KNN)-Ansatz für sowohl qualitative als auch quantitative Validierungstools.
Im Rahmen des BMW-Prinzips (kurz für Beschreibungsmittel, Methoden und Werkzeuge) werden die Grundlagen für ein KI-basiertes System für GNSS-basierte Lokalisierungssysteme vorgestellt und im Rahmen dieser Arbeit entwickelt. Das sich ergebende intelligente GNSS-basierte Lokalisierungssystem wird in einem Demonstrator-Werkzeug angewendet, um das entwickelte System auf der Software- und Hardware-Ebene zu validieren. Abschließend wird eine Risikoanalyse des Demonstrators präsentiert.
Diese Methoden zur Entwicklung eines intelligenten GNSS-basierten Lokalisierungssystems werden zukünftige sicherheitsrelevante Anwendungen in Bereichen wie Bordunsicherheitsermittlung in der Fahrzeuglokalisierung, Fahrassistenzsysteme und GNSS-basierte Fahrzeugortung mit intelligenten Karten für eine spurselektive Lokalisierung ermöglichen.
Die wichtigsten wissenschaftlichen Beiträge und Leistungen:
Meilenstein für intelligente GNSS-basierte Lokalisierungssysteme.
Das modellierte, entwickelte und angewandte System in dieser Dissertation entspricht einem ersten Schritt in Richtung KI-basierter Anwendung für die Auswertung und Überprüfung GNSS-basierter Lokalisierungssysteme.

Abstract

The usage of Global Navigation Satellites Systems (GNSS) for localisation purposes demands a permanent evaluation of the position information provided for the receiver, as well as a standardised GNSS-Receivers validation methodology and subsequently quality control procedures oriented to land vehicles within the ergodic hypothesis.
The use of an independent reference system should provide enough information to validate the localisation system, but the lack of proper evaluation and procedures presents significant blind spots for future applications in both the GNSS-Receiver and the correspondent reference system. To solve these problems an approach based on artificial intelligence (AI) is presented.
Also the development of an advanced filter technique for positioning estimation results in significant improvements of the reference system, even allowing a standalone GNSS-dependent reference system when no independent systems are available.
The presented developments are the bases for future intelligent GNSS-based localisation systems. The methodologies combine the advanced Particle Filter (PF) for positioning estimation with the newly developed Mahalanobis Ellipses Filter (MEF) methodology for accuracy-based data evaluation and the Artificial Neural Networks (ANN) models for both quantitative and qualitative validation.
In this thesis the bases of the intelligent GNSS-based localisation system are presented and developed follows the BMW principle. In German the BMW principle stands for *Beschreibungsmittel* (means of description), *Methode* (methods) and *Werkzeug* (tool).
The resulting system described along the thesis is applied and tested in a demonstrator tool, validating the developed methodologies in both software and hardware level.
The proposed methodologies for the development of an intelligent GNSS-based localisation system are a substantial contribution for intelligent GNSS-based validation tools that will enable future safety-relevant applications, in field such as on-board uncertainty evaluation of vehicle localisation; advanced driver assistance systems; and GNSS-based vehicle localisation with intelligent maps for track selective enabled-localisation.

Major scientific contributions and achievements:

General achievement: Substantial contribution for intelligent GNSS-based localisation systems. The modeled, developed and applied system in this thesis corresponds to a first step in an AI-based application for GNSS-based localisation system evaluation and verification.

Scientific contributions:

- Standarised quality based certification process for GNSS-Receivers for usage within GNSS-based localisation system. (Chapter 3)
- Mahalanobis Ellipses Filter (MEF) methodology for accuracy-based GNSS receivers quality description, by means of deviation evaluation and MEF-based Statistical Quality Control (SQC) methodology. (Chapter 4)
- Particle Filter (PF) approach for GNSS-Receivers positioning estimation for self-reference systems and independent reference systems validation. (Chapter 5)
- Artificial Neural Networks (ANN) validation tools for quantitative and qualitative accuracy-based analysis of GNSS-based localisation systems. (Chapter 6)
- Demonstrator-Tool of the developed intelligent GNSS-based localisation system. (Chapter 7)

Acknowledgements

During the years I've lived in Braunschweig, Germany I've learned not only how to be a researcher and a teacher in a second language, but also how to be part of a multicultural working team.

For that my deepest thanks to Prof. Dr.-Ing. Dr. h.c. mult. Eckehard Schnieder, who allowed me to become part of his family of researchers, and to all the people I've worked with in the Institut für Verkehrssicherheit und Automatisierungstechnik, especially to Lisandro Quiroga, Hansjörg Manz, Debiao Lu and my friends Damián Eduardo Díaz Fuentes and Adam Lipski, who helped me create my new life in Germany. An especial thank to Zuzana Raichlova, for her never-ending friendship and her illustration "What is the current location?", used as the cover of this book.

Finally a special recognition to Prof. Dr.-Ing. Jürgen Beyer for all his help and the hours of stimulating conversation.

This doctoral thesis is dedicated to both my parents, Prof. Ing. Alberto Bartolo Grasso and Prof. Ing. María Eugenia Toro.

Contents

List of Figures

List of Tables

Abbreviations

AAIM	**A**ircraft **A**utonomous **I**ntegrity **M**onitoring
AARI	**A**vailability-**A**ccuracy-**R**eliability-**I**ntegrity
A/D	**A**nalog-to-**D**igital
A-J	**A**nti-**J**amming
A-S	**A**nti-**S**poofing
AWGN	**A**dditive **W**hite **G**aussian **N**oise
AI	**A**rtificial **I**intelligence
AIMA	**A**utonomous **I**ntegrity **M**onitoring and **A**ssurance
AL	**A**lert **L**imit
AQF	**A**ccuracy-based **Q**uality **F**unction
BMW	**B**eschreibungsmittel, **M**ethoden, **W**erkzeuge
ANN	**A**rtificial **N**eural **N**etworks
BT	**B**elief, **T**heory
CDMA	**C**ode **D**ivision **M**ultiple **A**ccess
CEP	**C**ircular **E**rror **P**robable
CSW	**C**umulative **S**um of **W**eights
CRL	**C**oefficient of **R**acial **L**ikeness
DIN	**D**eutsches **I**nstitut für **N**ormung
DFR	**D**etection **F**alse **R**ate
DGPS	**D**ifferential **G**lobal **P**ositioning **S**ystem
DMR	**D**etection **M**issed **R**ate
DMS	**D**ynamic **M**easurement **S**ystem
drms	**D**istance **R**oot **M**ean **S**quared
ED	**E**uclidean **D**istance
EGNOS	**E**uropean **G**eostationary **N**avigation **O**verlay **S**ervice

EKF	**E**xtended **K**alman **F**ilter
FDMA	**F**requency **D**ivision **M**ultiple **A**ccess
FFNN	**F**eed **F**orward **N**eural **N**etwork
FL	**F**uzzy **L**ogic
FNP	**F**ault **N**on-isolation **P**robability
FRP	**F**ederal **R**adionavigation **P**lan
GEO	**Ge**ostationary **O**rbit
GK	**G**auss **K**rüeger
GNSS	**G**lobal **N**avigation **S**atellite **S**ystems
GNSS-R	**G**lobal **N**avigation **S**atellite **S**ystems **R**eceiver
GPRS	**G**eneral **P**acket **R**adio **S**ervice
GPS	**G**lobal **P**ositioning **S**ystem
GLONASS	**Gl**obal **O**rbiting **Na**vigation **S**atellite **S**ystem
GUM	**G**uide to the Expression of **U**ncertainty in **M**easurement
HDOP	**H**orizontal **D**ilution **o**f **P**recision
iglos	**i**ntelligent **glos**sary
iAQF	**I**ntelligent **A**ccuracy-based **Q**uality **F**unction
iEKF	**i**terated **E**xtended **K**alman **F**ilter
ITS	**I**ntelligent **T**ransportation **S**ystem
iUKF	**i**terated **U**nscented **K**alman **F**ilter
KF	**K**alman **F**ilter
LE	**L**ocation **E**rror
LocAv	**Loc**ation **Av**ailability
MD	**M**ahalanobis **D**istance
MCM	**M**onte **C**arlo **M**ethod
MCS	**M**onte **C**arlo **S**imulation
MEF	**M**ahalanobis **E**llipses **F**ilter
MEO	**M**edium **E**arth **O**rbit
MMSE	**M**inimum **M**ean **S**quare **E**rror
MSL	**M**ean **S**ea **L**evel
MTB	**M**ean **T**ime **B**etween
NMEA	**N**ational **M**arine **E**lectronics **A**ssociation
PF	**P**article **F**ilter

PL	**P**rotection **L**evel
PN	**P**etri **N**ets
PNT	**P**osition **N**avigation and **T**iming
PPP	**P**recise **P**oint **P**ositioning
PPS	**P**recise **P**ositioning **S**ervice
PTB	**P**hysikalisch **T**echnische **B**undesanstalt
RNN	**R**ecurrent **N**eural **N**etwork
RMS	**R**oot **M**ean **S**quare
RS	**R**eference **S**ystem
RTK	**R**eal **T**ime **K**inematic
SIR	**S**ampling **I**mportance **R**esampling
SIS	**S**equential **I**mportance **S**ampling
SNR	**S**ignal **N**oise **R**atio
SMC	**S**equential **M**onte **C**arlo
SoL	**S**afety-**o**f-**L**ife
SPS	**S**tandard **P**ositioning **S**ervice
TLS	**T**rain **L**ocalisation **S**ystem
TTFF	**T**ime **T**o **F**irst **F**ix
TTSF	**T**ime **T**o **S**ubsequent **F**ix
UKF	**U**nscented **K**alman **F**ilter
UML	**U**nified **M**odeling **L**anguage
UTC	**C**oordinated **U**niversal **T**ime

Chapter 1

Introduction

"Begin, be bold, and venture to be wise."

Horace

The Global Navigation Satellite System (GNSS) spectrum has expanded during the last decades [1]. In addition to the already established Global Positioning System (GPS), operational since 1978 and globally available since 1994 [2] and the GLObal NAvigation Satellite System (GLONASS) with fully functional navigation constellation from 1995 [3], new systems in development such as the Galileo Positioning System [4] and Compass (BeiDou) [5] present the perfect opportunity for GNSS-based localisation applications. Table 1.1 presents a comparison of the four systems mentioned above.

More and more GNSS-based localisation systems have been developed during the last decade, since the expansion of the GNSS spectrum for both road [6] and railway [7] applications, and also the imminent crossover of these developed localisation systems from the research field into the final user application area should be specially oriented to safety-relevant applications [8].

However, before these systems are completely accepted for safety relevant civilian usage, many previous steps must be fully solved, regarding themes such as certification of GNSS-Receivers [9], the standardization of procedures for validation of quality on real time applications, as well as the verification of GNSS-based localisation systems for safety-relevant applications [10].

TABLE 1.1: Comparison of Global Navigation Satellite Systems [11]

System	**GPS**	**GLONASS**	**BeiDou**	**Galileo**
Political Entity	United States of America	Russian Federation	P.R. China	European Union
Coding	CDMA	FDMA/CDMA	CDMA	CDMA
Orbital height	20,180 km (12,540 mi)	19,130 km (11,890 mi)	21,150 km (13,140 mi)	23,220 km (14,430 mi)
Period	11.97 hours (11h 58m)	11.26 hours (11h 16m)	12.63 hours (12h 38m)	14.08 hours (14h 5m)
Evolution per sidereal day	2	17/8	17/9	17/10
Number of satellites	24	24 (operational)	5 GEO satellites, 30 MEO satellites	4 test bed satellites in orbit, 22 operational satellites budgeted
Frequency	1.57542 GHz (L1 signal) 1.2276 GHz (L2 signal)	Around 1.602 GHz (SP) Around 1.246 GHz (SP)	1.561098 GHz (B1) 1.589742 GHz (B1-2) 1.20714 GHz (B2) 1.26852 GHz (B3)	1.164 - 1.215 GHz (E5a and E5b) 1.260 - 1.300 GHz (E6) 1.559 - 1.592 GHz (E2-L1-E11)
Status	Operational	Operational, CDMA in preparation	15 satellites operational	In preparation

1.1 Purpose of the dissertation

In order to develop an end-user GNSS-based localisation system the main blind spots in the current GNSS-based localisation systems research must be found and suitable solutions for those found issues must be proposed.
These blind spots are focused on the user side of the GNSS-based localisation system. According to the two main parts of the general architecture of the GNSS-based localisation system presented in Figure 1.1 the two most relevant perspectives are:

1. The GNSS-Receiver (GNSS-R) point of view, and
2. The Reference System (RS) point of view.

Some GNSS-based localisation systems focus on safety-relevant applications [12]. Therefore the RS must be typically an independent source of location information in order to validate the information provided by the GNSS-R [13]. The proposed intelligent system in this thesis develops a new approach from both the GNSS-R and the RS to be applied within a safety-relevant frame.
This thesis presents a new certification method for GNSS-Rs [9, 14, 15], focused on a new quality description based on a new accuracy-based evaluation of the deviation between the GNSS-R and the RS data by means of Mahalanobis Distance (MD), also referred as D^2 as developed in [16]. In combination with extended newly applied filter techniques [15], the resulting GNSS-based system can be referred as "intelligent" for being validated by means of artificial intelligence (AI) techniques, such as Artificial Neural Networks (ANN) models, as developed in [10].

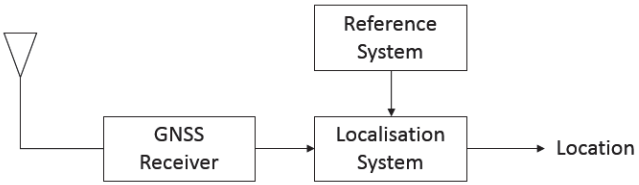

FIGURE 1.1: General architecture of GNSS-based localisation systems

1.2 Blind spots of localisation systems

Three main issues must be addressed regarding the current GNSS-based localisation system research field.

First, from the GNSS-R point of view, the lack of certification processes and quality control methodologies present two significant blind spots. Only certified GNSS-Rs can be part of localisation systems for safety-relevant applications. And also a continuous quality control procedure must be standarised. Both of these issues are grounded on the lack of an intelligent GNSS location data evaluation that would allow the means for GNSS-R certification and periodically quality control procedures.

Second, from the RS point of view, there is a significant blind spot regarding the location estimation used for reference behaviour purposes. Many filter theory approaches have been applied to estimate GNSS location data [17, 18], and particularly Particle Filter (PF) in [19–21], but no proper filtering approach has been yet developed to create a GNSS-Rs estimation usable as a reference for validation of an independent RS or as a hybrid GNSS-based RS. A standardised validation procedure of GNSS-based localisation systems must be conceived by means of proper GNSS location estimators for safety-relevant applications, as presented in this dissertation.

Finally, as an overall view of the GNSS-based localisation system depicted in Figure 1.1, the global blind spot is the lack of on-line quality evaluation for the provided location information. This quality description should be the result from the combination of the interpretation of the available accuracy of the system and its expected accuracy-based behaviour. This is presented in this thesis by means of AI-based validation tools.

1.3 Structure of the dissertation

All the issues described above exist nowadays in any GNSS-based localisation system and can be addressed by the implementation of this dissertation's methodologies, as presented in the development of the resulting Demonstrator-Tool. The achieved prototype of the so-called intelligent GNSS-based localisation system basic architecture can be seen in Figure 1.2.

Each part of the depicted system will be presented one by one in the following chapters, along with a detailed description of the correspondent theoretical ground.

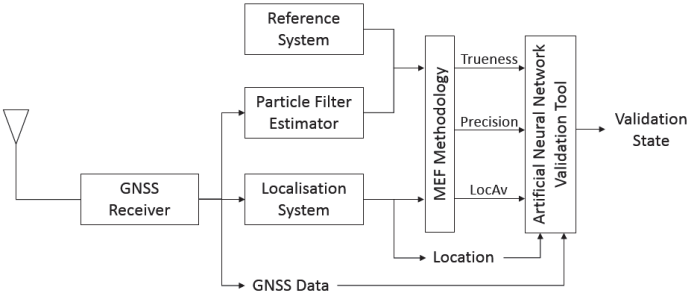

FIGURE 1.2: Graphical description of an intelligent GNSS-based localisation system.

The structure of this dissertation is constructed following the BMW principle proposed in [22]. In German "BMW-Prinzip" stands for In German BMW stands for *Beschreibungsmittel* (means of description), *Methode* (methods) and *Werkzeug* (tool).
The chapters in this dissertation are divided in three sections:

1. **Means of description** of the intelligent GNSS-based localisation system: Introducing the general concepts and presenting the state of the art of the applied technologies to be improved. (Chapter 1 and Chapter 2)

2. **Methods** for the intelligent GNSS-based localisation system: Describing in detail each part of the developed system depicted in Figure 1.2, as well as their theoretical bases. (Chapter 3, Chapter 4, Chapter 5, and Chapter 6)

3. **Demonstrator-Tool** of the intelligent GNSS-based localisation system: Describing an applied prototype of the developed methodologies, as well as presenting results of actual performed test runs. (Chapter 7)

A detailed description of all the chapters is presented as follows:

- **Chapter 1** has presented an overview of the purpose of this thesis, focusing on the problems to be solved to achieve a safety-relevant intelligent GNSS-based localisation system. Also the starting points for the respective solutions of the blind spots on current GNSS-based localisation systems have been set.

- **Chapter 2** presents the state of the art in research fields such as GNSS quality description, as well as its terminology and development of validation and certification processes for GNSS-Rs. Also the mathematical background for the new accuracy-based evaluation focused on MD, as well as the theories of PF and ANN to location estimation and validation. Finally an overall description of the contributions to those fields in this dissertation is shown, by means of a detailed graphical representations of the remaining chapters.

- **Chapter 3** presents a new GNSS-Rs certification approach, focused on validation processes, based on detailed GNSS quality evaluations. The proposed quality description is updated by means of a deeper explanation of its properties (Availability, Accuracy, Reliability and Integrity). Finally an approach for the gathering of the validations processes including AI-based evaluations are presented for final attestation.

- **Chapter 4** presents a new accuracy-based evaluation of GNSS data, based on MD. The newly developed Mahalanobis Ellipses Filter (MEF) methodology describes the accuracy of localisation system by its characteristics of trueness, precision and location availability, and also a new statistical quality control (SQC) methodology for GNSS-Rs inspired on the MEF methodology, as well as its comparison with classical SQC methodologies.

- **Chapter 5** presents newly developed Particle Filter (PF) approaches for GNSS-R behaviour estimation. Both static and dynamic measurement systems estimators are presented. And examples for both static and dynamic PF-Estimators and the impact of the application of PF-estimators as part of the newly accuracy-based SQC methodology are shown.

- **Chapter 6** presents a new ANN-based approach to develop intelligent validation tools for GNSS-based localisation system, based on accuracy estimation. Both quantitative and qualitative evaluations of the GNSS data by means of ANN models are described. And an exemplary case is presented for both quantitative and qualitative evaluation of GNSS-based localisation systems for safety-relevant applications.

- **Chapter 7** presents the Demonstrator-Tool with all new developed methodologies applied. Both software and hardware of the Demonstrator-Tool are briefly described, and actual results from performed test runs are presented in details.
- Finally **Chapter 8** presents conclusions for the overall content of this dissertation and potential further work on all participating research fields.

Figure 1.3 depicts the whole structure of this dissertation by means of a block diagram.

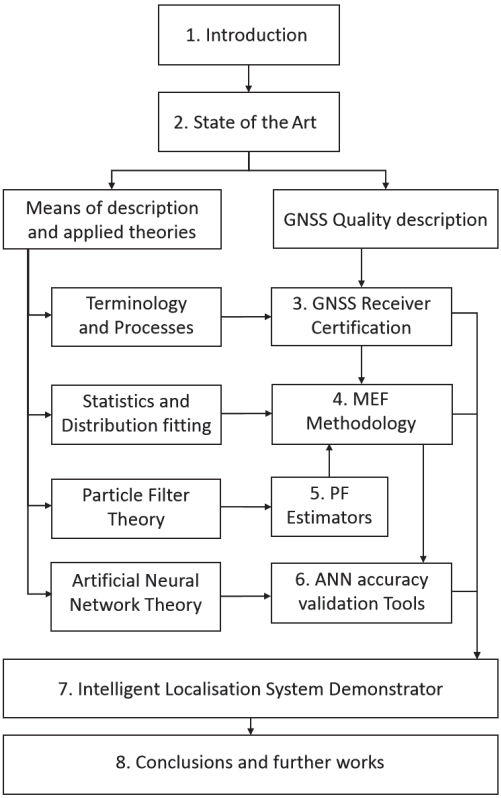

FIGURE 1.3: Structure of the Dissertation.

Chapter 2

State of the Art

"If I have seen further it is by standing on the shoulders of giants."

Isaac Newton

Before describing the newly developed intelligent GNSS-based localisation system and its intrinsic correspondent methodologies, six used methods are presented. Finally a general description of these dissertation's contributions are presented.

1. **Terminology:** where terms and definitions of concepts regarding the subjects and relationships in this dissertation are presented in detail.
2. **GNSS quality concept:** the current research in GNSS quality description is presented and useful concepts for the present dissertation are detailed.
3. **Validation and certification processes:** from the GNSS-Receiver perspective, detailed research about its validation and certification is presented.
4. **Dynamic measurement evaluation:** current dynamic measurement data research is presented, with a detailed description of the measurement evaluations and its blind spots are described.
5. **Filters techniques for position estimation:** filter applications for position estimation are presented, from Kalman Filter to Particle Filter.
6. **Artificial intelligence based estimation:** Artificial Neural Networks (ANN) approaches for quality estimation and intelligent calibration are described.

2.1 Terminology

The *iglos*-project (acronym for "intelligent glossary") aims at developing a means of modelling highly interconnected terminologies to overcome language barriers enabling transdisciplinary communication [23]. The *iglos*-project is based on a new trilateral sign model which constitutes the linguistic sign from its special language context, for optimising its scientific communication, intended to accelerate and facilitate a consistent, multilingual and unambiguous development of technical terminology [24]. The *iglos* sign model is trilateral and variety-based, describing lexemes as "abstract morphological units", which are concretised by their grammatical word forms [25].
A lexeme consists of three constituent sides:

- **Lemma:** actual denomination of the lexeme.
- **Definition:** description of the content of the lexeme.
- **Variety:** the context of the lexeme (technical language).

The detailed trilateral sign model understands the linguistic sign to be constituted by its special language context, and consistently models, as depicted in Figure 2.1 into variety(linguistic context), lemma (designation) and definition (concept).

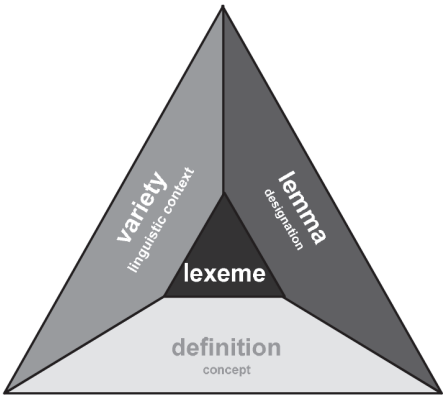

FIGURE 2.1: Trilateral and variety-based sign model [26]

The designation (signifier) is the concept's representation using linguistic (e.g. appellation) or other means, such as symbols or formulas. According to lexicography and lexicology the signifier [27] or designation is also called lemma [28, 29].
The actual 'concept' (signified): According to [30], terms are defined as "unit of knowledge formed by an amount of objects and determining their shared characteristics using abstraction". Then terms are used for identifying objects and gaining a common understanding about objects, as well as organizing objects mentally [31].
In the trilateral model of a linguistic sign, the meaning of a term is represented by its definition [32]. A variety is used for classifying concept and designation into a context of use [33], the respective language for special purposes. The variety is considered an essential constituent of the metalinguistic model of a linguistic sign [26].
Since technical terms are special lexemes, in order to relate lexemes with each other there must be relational lexemes (relation type) placed between the lexemes, as seen in Figure 2.2. By avoiding terminological haziness and creating and visualising concrete unobstructedly typable relations between terms in a systematic variety, the *iglos* sign model facilitates the specification of terminologies and avoids synonymy and ambiguity (disambiguation) of terms within the communication between different fields (multidisciplinarity) and different national languages (multilingualism) [34].

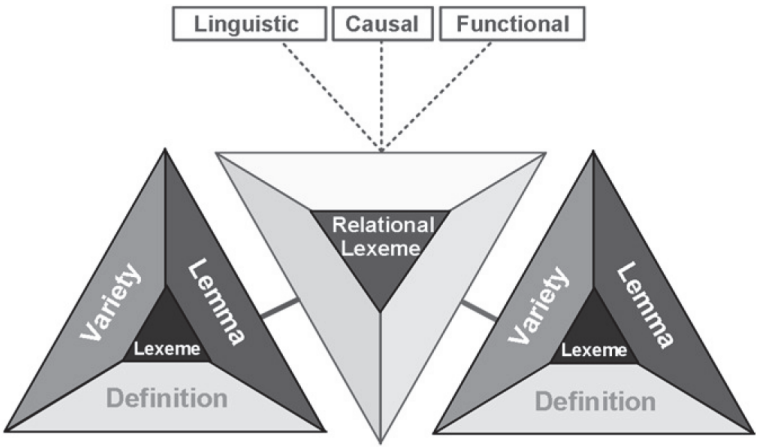

FIGURE 2.2: Interconnectivity between lexemes by relational lexeme [34]

2.1.1 Important Definitions

Based on [35, 36], the following definitions of terms must be taken into consideration, as part of the Traffic Engineering Terminology:

- **Position:** spacial state of an item given by a set of coordinates related to a well defined coordinate reference frame. [35]
- **Location:** a measured or determined position in terms of topological relations, e.g. movement of an item. [35]
- **Positioning:** process of obtaining a position. [35]
- **Localisation:** process of obtaining a location. [35]
- **Navigation:** combination of routing, route traversal and tracking. [36]

In [34] the visualisation of the relations between English navigation terms are presented in the *iglos* graph, as seen in Figure 2.3.
With this methodological approach of terminology modeling, the differences and relating navigation terms linguistic problems can be avoided, presenting the definition of terms connected with their correspondent variety and context, as well as with their definitions.

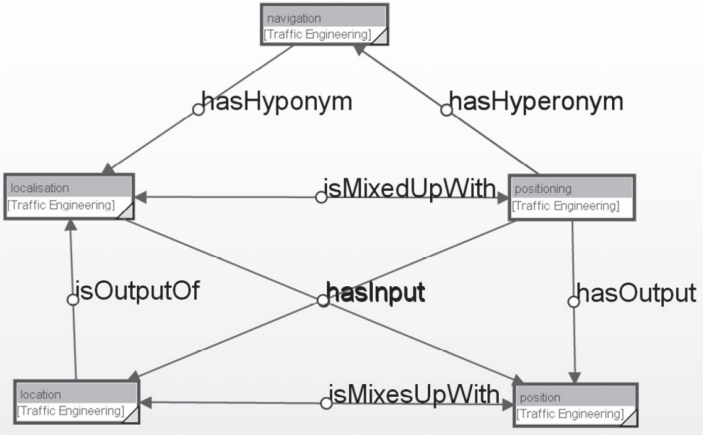

FIGURE 2.3: English Navigation Terms in Traffic Engineering Language [34]

To conclude this terminology sections, based on [4, 37–40] the following definitions are the terminological ground for this dissertation and the description of GNSS quality concept, detailed in the following section and specifically developed in Chapter 3[1]:

- **Accuracy:** the degree of conformance of that position with conventional true position of the craft (vehicle, aircraft, vessel) at the given time. [38]
- **Availability:** The ability of a product to be in a state to perform a required function under given conditions at a given instant of time or over a given time interval assuming that the required external resources are provided. [37]
- **Reliability:** the probability that a system will perform its function within defined performance limits for a specified period of time under given operating conditions. [39]
- **Integrity:** the likelihood of a system satisfactorily performing the required safety functions under all the stated conditions within a stated period of time. [37].

Also, in [40] **integrity** is defined as "the measure of the acceptance of the information supplied by the navigation system". And furthermore this acceptance is defined as "the worst case of accuracy for a certain service by confidence interval presented by the alarm limit that also includes the ability of the system to provide timely warnings to users when the system should not be used for navigation". This extended definition will be used as the basis of the integrity evaluation presented in Chapter 3.
The convergent point between terminology and the intelligent GNSS-based localisation system developed in the present dissertation is safety (defined as "Freedom from unacceptable risk of harm" in [37]). Especially for safety-related applications it is mandatory to ensure a clear understanding of terminology which shall enable for example certification process for GNSS receivers for satellite-based localisation systems [26]. During the rest of the present dissertation these terms and their correspondent definitions will be used as a semantic frame for the developed intelligent GNSS-based localisation system.

[1] In contrast to aircraft systems engineering, where dependability is a measure of a system's availability, reliability, and its maintainability.

2.2 GNSS Quality Concept

The description of GNSS quality is based on the generic structuring of objects properties from [41]. The chosen structure compatible with the German standards DIN 1319-1 [42] is described by attribute hierarchy:

- Concept
- Properties
- Characteristics
- Quantities
- Value-Unit

Figure 2.4 presents a translated version of the Unified Modeling Language (UML) representation of the quality of measurement proposed in [43], where the described concepts are coherent with the definitions in the Terminology section above.
All properties from the Measurement Quality in Figure 2.4 and their correspondent characteristics are detailed in [43], as well as all their correlations within the terminology.
Also the Safety-Of-Life (SoL) service description presented in [4] and displayed in detail in Table 2.1 provide the SoL service requirements, used for standarisation purposes [40]. The SoL Service are focused on safety critical users, for example maritime, aviation and trains, whose applications or operations require stringent performance levels [4], providing high-level performance globally to satisfy the user community needs and increasing safety especially in areas where services provided by traditional ground infrastructure are not available. This would increase the efficiency of companies operating in a global basis, e.g. airlines, transoceanic maritime companies. In Table 2.1 the summary of the service performances for the Galileo SoL Service depict the requested relationship between GNSS-R, its accuracy and integrity related to its continuity risk.
Considering the carriers section, the SoL Service signals are in the E5a+E5b and L1 bands, even though the level of performances indicated can be achieved by using only L1 and E5b frequencies. These performances of the service based on E5a+E5b and L1 frequencies are mentioned in [4] as under assessment.

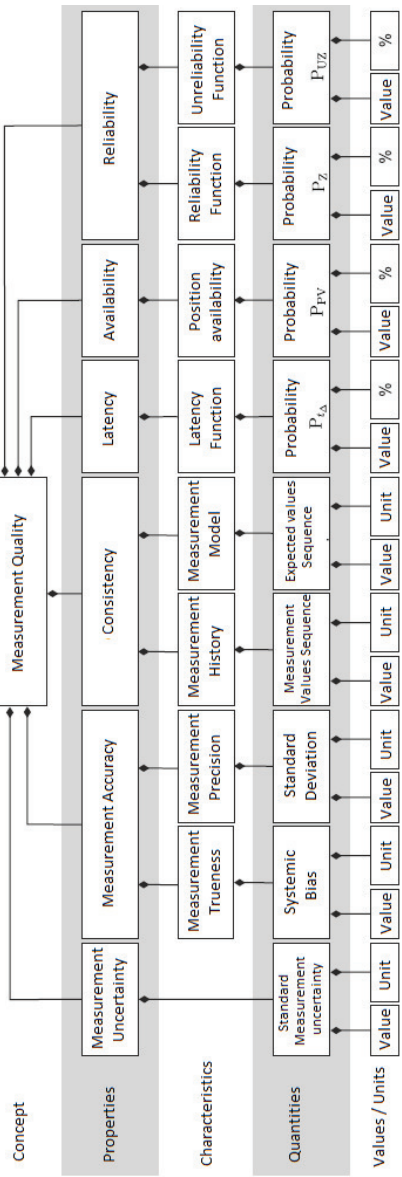

FIGURE 2.4: Constituents of the quality of measurement in UML notation [43]

TABLE 2.1: Service performances for the Safety of Life Service [4]

Safety-Of-Life Service			
Type of Receiver	*Carriers*	*Three Frequencies*	
	Computes Integrity	*Yes*	
	Ionospheric correction	*Based on dual-frequency measurements*	
Coverage		*Global*	
		Criticial level	**Non-critical level**
Accuracy (95 %)		H: 4 m V: 8 m	H: 220 m
Integrity	*Alarm Limit*	H: 12 m V: 20 m	H: 556 m
	Time-To-Alarm	6 seconds	10 seconds
	Integrity Risk	3.5 x 10^{-7} / 150 s	10^{-7} / hour
Continuity Risk		10^{-5} / 15 s	10^{-4} - 10^{-8} / hour
Certification / Liability		Yes	
Availability of integrity		99.5 %	
Availability of accuracy		99.8 %	

Also the actual value for Time-To-Alarm to be considered depends on the results of the feasibility phase.

And the provision of integrity information at global level is the main characteristic of this service.

These specifications include two levels to cover two conditions of risk exposure and are applicable to many applications in different transport domains, for example air, land, maritime, rail:

- The Critical level covers time critical operations for example, in the aviation domain approach operations with vertical guidance.
- The Non-Critical level covers extended operations that are less time critical, such as open sea navigation in the maritime domain.

The presented quality description for specific services provided to end users is the ground for the proposed GNSS quality description approach in the present dissertation. In Chapter 3 specific details are described for the certification process of GNSS-Rs, based on the developed quality description mainly focused on accuracy-based evaluation.

2.3 Validation and Certification Processes

Both validation and certification processes are based on [44], where a constructive approach to describe processes and taxonomy was carried out by way of example within normative documents.
To apply the method of structural modelling presented in [44] for new standards with the resulting formal model of certification of GNSS-Rs.
A detailed description of the certification process from [44] states: "The receiver must be evaluated regarding a quality criteria and the results must be analyzed to meet predetermined requirements". The resources for this process are illustrated in Figure 2.5, as used in the Institut für Verkehrssicherheit und Automatisierungstechnik.
In addition to the certification process for GNSS-Rs, the certification and accreditation of laboratories and certification bodies should also be modelled, to detail how would such organizations obtain authorization for the related activities, as seen in Figure 2.6, where a supervisory authority is recognized as the general organization that performs accreditation.
The processes for GNSS-Rs certification and accreditation for the necessary laboratories and certification bodies can be described as follows:
Figure 2.5 describes whether the reviewed GNSS-R meet the specified requirements, according to a specific quality criteria and its properties. The three properties for the quality criteria detailed here in [44] are:

- Time To First Fix (TTFF): refers to the time it takes for a GNSS-R until he makes his first valid position information.
- Static Accuracy: indicates the accuracy of the location information supplied by the GNSS-R, under static conditions.
- Dynamic Accuracy: indicates the accuracy of the location information supplied by the GNSS-R, under dynamic conditions.

For all three evaluation an independent reference provides location information that must be available to compare with the result from the GNSS-R to be tested.
Also for each evaluation an "accredited laboratory" must carry out the procedure, based on the analysis of the results regarding to the requirements for specific scenario conditions, which in turn depends of the desired applicability.

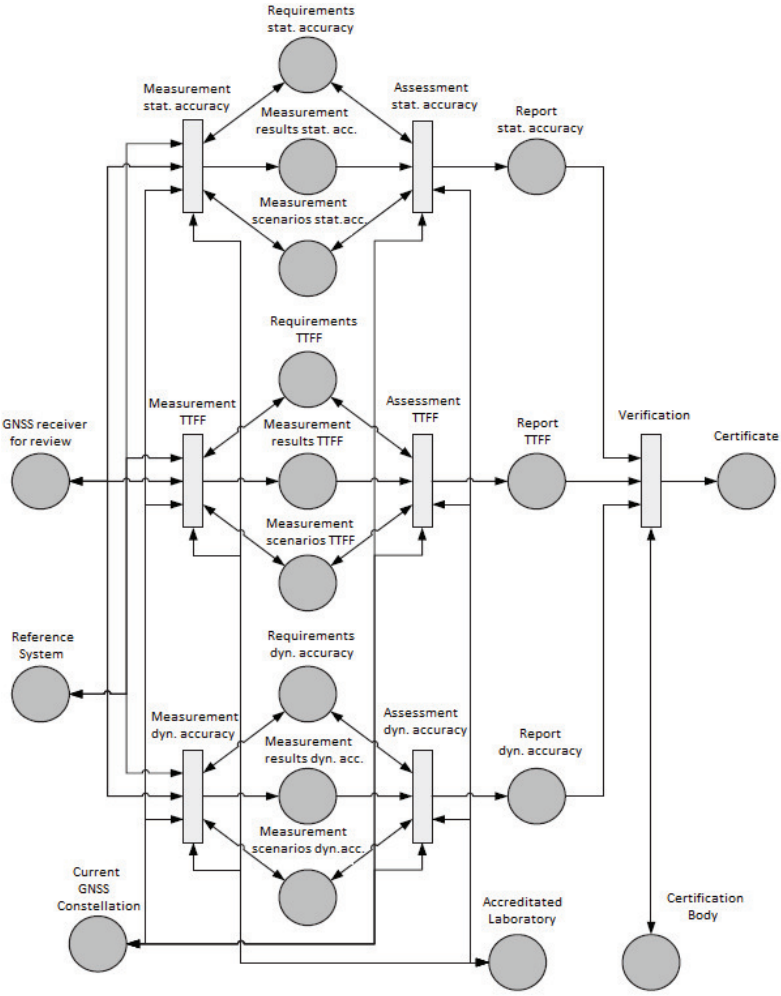

FIGURE 2.5: Certification Process for GNSS Receivers [44]

Finally it must be always taken into consideration the current position of the satellites (referred as "Current GNSS Constellation"), as well as the provided GNSS-R information. When all requirements are met, the three correspondent reports in Figure 2.5 are provided to be verified by the "Certification Body", in order to achieve the correspondent certification.

The accreditation for the certification bodies must be process as depicted in Figure 2.6. For a laboratory to receive an accreditation and thus to become an "accredited laboratory" first an audit is needed. And this procedure must be performed by a "supervisor authority". The supervisor checks the correspondent "requirements" for the laboratory (or the organization to be audit) and creates an audit results, as seen in Figure 2.6.

After the requirements are met the "supervisor authority" must assign the "accreditation" of laboratory or organization.

This accreditation process is simple, but still includes all the important steps [44]. Moreover, this, as well as the certification presented above are conceived regarding the basic process steps and the nomenclatures conform to the [45].

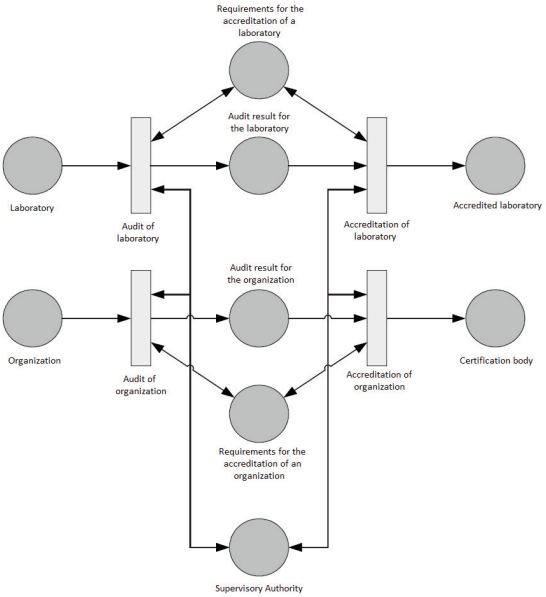

FIGURE 2.6: Accreditation Process for Laboratories and Certification Bodies [44]

2.4 Dynamic Measurement Systems Evaluations

A typical Dynamic Measurement System (DMS) is composed by the combination of the GNSS-R and an independent measurement system. Therefore the quality of a DMS can be separated into GNSS quality and RS quality.

Since all details regarding the GNSS quality and GNSS-Rs certification process have been presented in the sections above, the significant part of the localisation system that remains to be listed is the actual independent RS and the methods attached to the DMS evaluations.

Details from several projects focused on GNSS-quality and DMS reference data evaluations can be found in [46–51].

In publications related to the DemoOrt project [46], GNSS data analysis and DMS behaviour description for railway localisation system were made in [13, 52–56].

Also publications related to the QualiSaR project described in [47], regarding extensive GNSS data analysis and DMS behaviour description for automotive localisation system were made in [57–62].

For all the DMS mentioned above the treatment of the dynamic data must be a key factor. Current on-going work produced by Physikalisch-Technische Bundesanstalt (PTB) Working Group 8.42 ("Analysis of dynamic measurements") deals with this issue, as shown in [63].

The definition of the goal of any dynamic measurement is the "determination of a physical quantity whose value shows a time-dependence"[63].

A dynamic measurement system must be designed to have output signals proportional to the input signals, i.e. the time-dependent value of the measurand. However, this is possible in all occasions. In some cases an ideal behaviour is achieved only by input signals with a low-frequency spectrum. For input signals with large bandwidth, the output signal of the measurement system is no longer proportional to its input signal. And by taking the output signal of the measurement system as a time-dependent estimate of the value of the measurand, the so-called dynamic errors can be introduced.

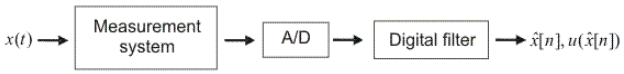

FIGURE 2.7: Schematic of dynamic measurement with subsequent compensation [63]

In order to compensate for the dynamic error, post-processing of the output of the measurement system is required for which digital filtering is an appropriate tool. Designing a compensation filter, the dynamic behaviour of the measurement system needs to be characterized, i.e. the measurement system has to be identified.

The determination of measurement uncertainty plays a key role in this particular branch of metrology. Since for a measurand with a constant value, agreed de-facto standards for the determination of measurement uncertainty are available, these tend to be based on a Bayesian point of view, allowing a consistent treatment of random and systematic influences.

However, these standards cannot be immediately applied to the case where the value of the measurand is time-dependent, and the concepts applied for the static case need to be extended [43].

The focus of the PTB working group in [63] is the development and application of methods for the following tasks:

- Identification of measurement systems.
- Design of digital compensation filters.
- Evaluation of dynamic measurement uncertainty.

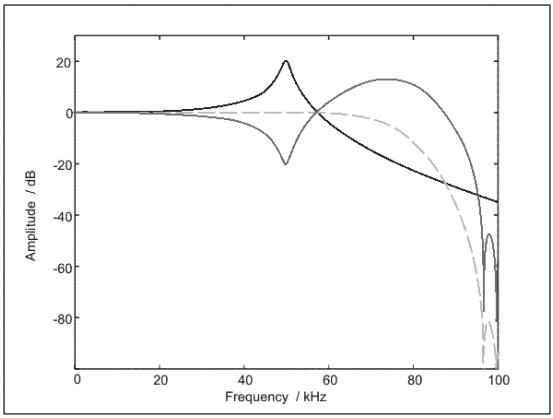

FIGURE 2.8: Magnitude plots of (1) frequency responses of a measurement system (black), (2) compensation filter (dark grey) and (3) compensated measurement system (light grey) [63]

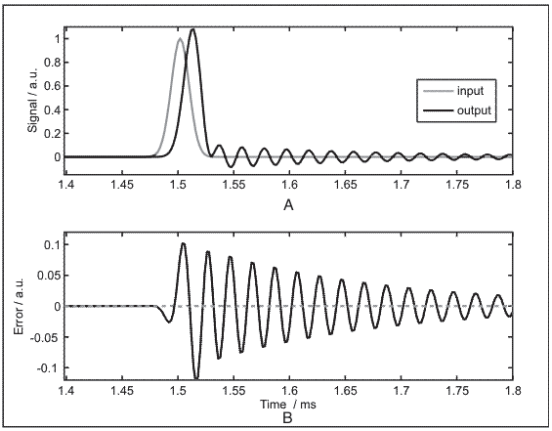

FIGURE 2.9: (A) Input and output signals of a measurement system. (B) Difference signal between the time-shifted output and the input with application of the digital compensation filter (light grey hidden line) and without it (black) [63]

In Figure 2.7 the DMS is shown schematically with a subsequent post-processing. The time-dependent value of the measurand passes through the measurement system and an analogue-to-digital (A/D) conversion. Then subsequent digital filtering compensates for the dynamic error and yields an estimate of the measurand, including the dynamic uncertainty associated with this estimate.

The compensation filter should have a frequency response which equals the inverse frequency response of the measurement system. However, this would also imply a strong amplification of high frequency noise components. Therefore, the design of a compensation filter requires some trade-off between sufficient noise suppression in the high frequency region and tolerable signal distortion due to non-ideal inverse filtering.

The Figure 2.8 shows the magnitude frequency response of such a compensation filter for a particular measurement system. The frequency response of the compensated measurement system is constant up to 60 kHz.

The need and benefit of applying a compensation filter to this measurement system is illustrated for a particular test signal in Figure 2.9 where the dynamic error is also shown if no compensation is applied.[2]

Finally Figure 2.10 also illustrates for the simulated data the comparison of an uncertainty evaluation based on a static analysis and based on a dynamic analysis, for the

[2]In the case of GNSS, due to delays a variable filter would be needed.

example presented above.

While the static analysis treats the output of the DMS as proportional to its input and ignores the dynamic behaviour, the dynamic analysis is based on a subsequent application of the compensation filter. Figure 2.10 shows the frequency with which 95% credibility intervals is determined by the analyses, covering the underlying true value of the measurand at the time of the input maximum of the signal. The results show that the bandwidth of the measurand increases while the coverage probability of 95% credibility intervals tends to zero for the static analysis, in contrast to the dynamic analysis. Therefore, in this case the reliable uncertainties can only be obtained by accounting for the dynamic behaviour of the sensor system.

The solution presented in [63] for the dynamic measurement data must be part of any application of any of the dynamic measurement localisation system mentioned above, as well as the developed system as part of the present dissertation.

Improvements in the dynamic model of [63] can be seen in [43, 64], by the enhancement of the Guide to the Expression of Uncertainty in Measurement (GUM) method to dynamical systems, as presented in [65]. Figure 2.11 depicts the trajectory of the input quantity X(k) of the low-pass filter with T = 1 s. A smaller input uncertainty is assumed at time k = 40 [64], to illustrate the output caused by the smaller magnitude.

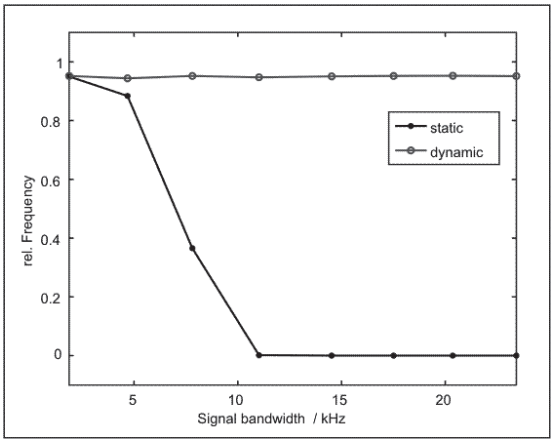

FIGURE 2.10: Estimated coverage probability for 95% credibility intervals obtained for the peaks of a Gaussian-like measurand using the static and dynamic approaches in the uncertainty analysis [63]

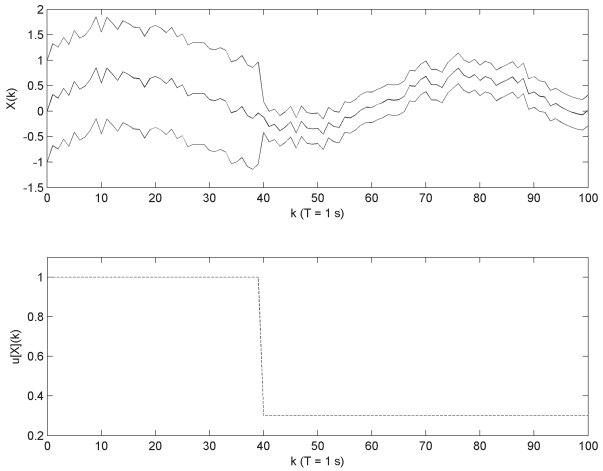

FIGURE 2.11: Trajectory of the input quantity to be filtered and its uncertainty [64]

The need and lack of a behaviour-oriented evaluation of the GNSS data for all dynamic systems presented above is already been considered in [13, 66], where the bases for further behaviour based GNSS data evaluation were presented.
In Chapter 4 the Mahalanobis Ellipses Filter (MEF) methodology developed in [16] and applied in [21, 66] is explained and extended for multidimensional deviation analysis.

2.5 Filter techniques approaches for GNSS position estimation

The usage of filter techniques for position estimation for safety-relevant purposes is an extensive field of research. State estimation by means of Kalman Filter (KF), as well as Extended Kalman Filter (EKF) and Particle Filter (PF) and others such as iterated Extended Kalman Filter (iEKF), Unscented Kalman filter (UKF), and iterated Unscented Kalman filter (iUKF) have been developed for several applications. This state of the art section introduces to filter techniques for position estimation presenting the essential concepts and mathematical background to comprehend the developed PF-based location estimators in Chapter 5.

2.5.1 Introduction to Bayesian filtering techniques for state estimation

In a state estimation problem, also called "non-stationary inverse problems", the available measured data is used together with prior knowledge about the physical phenomena to be described and the measuring devices, in order to sequentially produce estimates statistically the desired dynamic variables, by minimising the error [67].

State estimation problems deal with the combination of the model prediction combined with the uncertain measurements in order to obtain more accurate estimations of the system variables [68]. This kind of problems are typically solved by means of so-called Bayesian filters as developed in [67, 68]. In the Bayesian approach to statistics, an attempt is made to utilize all available information in order to reduce the amount of uncertainty present in an inferential or decision-making problem.

And as new information is obtained, it is also combined with previous information to form the basis for statistical procedures [69]. By using a formal method by means of Bayes' theorem the combination of the new collected information with the previously available information can be achieved [70].

The most widely known and used Bayesian filter method is the KF approach, as detailed and developed in [67, 68, 71–73]. However, the application of the KF is limited to linear models with additive Gaussian noises.

The EKF approach is a Bayesian filter method extended from KF approach, developed for less restrictive cases, by using linearization techniques as presented in [18, 74].

And also the so-called Monte Carlo Methods (MCM) have been developed in order to represent the posterior density in terms of random samples and associated weights. Theses methods are usually called Particle Filter methods and they do not require the restrictive hypotheses of the KF, making them better suited for specific applications, such as non-linear models with non-Gaussian errors [75, 76].

This following sections introduce in detailed the state estimation problem and its solutions by means of KF approach, EKF approach and also the Sampling Importance Resampling (SIR) algorithm, featured on PF approach.

2.5.2 State Estimation Problem

The definition of the state estimation problem is quoted from [69], where a model for the evolution of the vector x is considered, such as:

$$x_k = f_k(x_{k-1}, v_{k-1}) \tag{2.1}$$

where the subscript $k = 1, 2, \ldots$ denotes a time instant t_k in a dynamic problem.
The vector $x \in R^{n_x}$ is called the "state vector" and contains the variables to be dynamically estimated, advancing according to the state evolution model given by Equation 2.1, where f is, in the general case, a non-linear function of both the state variables x as well as the state noise vector $v \in R^{n_v}$, considering also that measurements $z_k \in R^{n_z}$ are already available at t_k, therefore when $k = 1, 2, \ldots$.

The measurements are related to the state variables x through the general, possibly non-linear, function h in the form:

$$z_k = h_k(x_k, n_k) \tag{2.2}$$

where $n \in R^{n_n}$ is the measurement noise. Equation 2.2 is called the "observation model".
The state estimation problem aims to obtain information about x_k, based on the state evolution model from Equation 2.1 and the measurements $z_{1:k} = \{z_i, i = 1, \ldots, k\}$ given by the observation model from Equation 2.2.
Then, the "evolution-observation model" given by Equations 2.1 and 2.2 is based on the following assumptions [70]:

1. The sequence x_k for $k = 1, 2, \ldots$, is a Markovian process:

$$\pi(x_k \mid x_0, x_1, \cdots, x_{k-1}) = \pi(x_k \mid x_{k-1})$$

2. The sequence z_k for $k = 1, 2, \ldots$, is a Markovian process from the history of x_k:

$$\pi(z_k \mid x_0, x_1, \cdots, x_k) = \pi(z_k \mid x_k)$$

3. The sequence x_k depends only on its own history past observations:

$$\pi(x_k \mid x_{k-1}, z_{1:k-1}) = \pi(x_k \mid x_{k-1})$$

For all assumptions $\pi(a \mid b)$ denotes the conditional probability of a when b is given. Additionally, for the "evolution-observation model" given by Equations 2.1 and 2.2 it is assumed that for $i \neq j$ the noise vectors v_i and v_j, and n_i and n_j, are mutually independent, as well as mutually independent of the initial state x_0. The vectors v_i and n_j are also mutually independent for all i and j.
Several problems can be solved by means of the "evolution-observation model" [67]:

1. **Prediction:** determining $\pi(x_k \mid z_{1:k-1})$.
2. **Filtering:** determining $\pi(x_k \mid z_{1:k})$.
3. **Fixed-lag smoothing:** determining $\pi(x_k \mid z_{1:k+p})$, where $p \geq 1$ is the fixed lag.
4. **Whole-domain smoothing:** determining $\pi(x_k \mid z_{1:K})$, where the complete sequence of measurements is $z_{1:K} = \{z_i, i = 1, \ldots, K\}$.

Since the present dissertation deals only with the filtering problem it is assumed that $\pi(x_0 \mid z_0) = \pi(x_0)$ is available and therefore the posterior probability density $\pi(x_k \mid z_{1:k})$ can be obtained with Bayesian filters in two steps illustrated in Figure 2.12:

1. **Prediction step:** where $\pi(x_k \mid z_{1:k-1})$ is determined given .
2. **Update step:** where $\pi(x_k \mid z_{1:k})$ is determined given .

The following sections deal with the solutions for the state estimation problem by means of the KF approach, the EKF approach and the Sampling Importance Resampling (SIR) algorithm featured on the PF approach.

2.5.3 Kalman Filter (KF)

In the KF approach it is assumed that the evolution and observation models given by Equations 2.1 and 2.2 are linear. Also, it is assumed that the noises in such models are additive Gaussian, with known means and covariances.
Therefore, the posterior density $\pi(x_k \mid z_{1:k})$ at $t_k, k = 1, 2, \ldots$ is also Gaussian and the KF results in the optimal solution to the state estimation problem [74]. This means that the posterior density is exactly calculated by the KF approach.

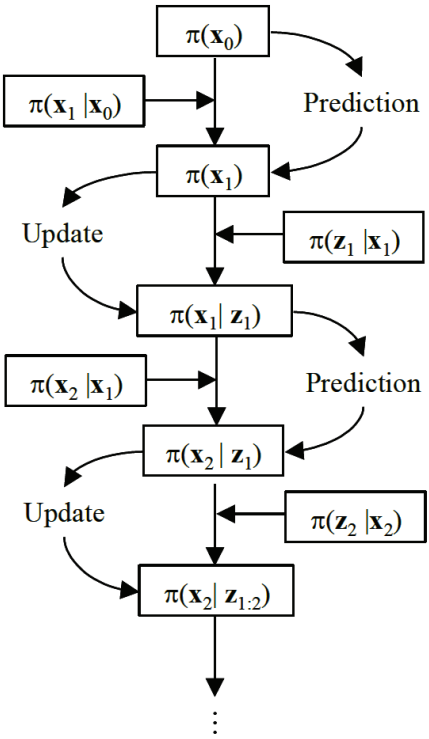

FIGURE 2.12: Prediction and update steps for the Bayesian filter [67]

Based on the foregoing hypotheses, the evolution and observation models can be written respectively as:

$$x_k = F_k x_{k-1} + s_k + v_{k-1} \tag{2.3}$$

$$z_k = H_k x_k + n_k \tag{2.4}$$

where F in Equation 2.3 and H in Equation 2.4 are known matrices for the linear evolutions of the state x as well as the observation z, respectively. Also s in Equation 2.3 is a known vector of inputs. By assuming that the noises v and n in both Equations 2.3 and 2.4 have zero as mean values and respectively covariance matrices Q and R, then the prediction and update steps of the KF approach can be given by:

Prediction:

$$x_k^- = F_k \hat{x}_{k-1} + s_k \tag{2.5}$$

$$P_k^- = F_k P_{k-1} F_k^T + Q_k \tag{2.6}$$

Update:

$$K_k = P_k^- H_k^T (H_k P_k^- H_k^T + R_k)^{-1} \tag{2.7}$$

$$\hat{x}_k = x_k^- + K_k(z_k - H_k x_k^-) \tag{2.8}$$

$$P_k = (I - K_k H_k) P_k^- \tag{2.9}$$

Where the matrix K is called Kalman's gain matrix. After predicting the state variable x and its covariance matrix P with Equations 2.5 and 2.6, a posteriori estimates for such quantities are obtained in the update step by means of Equations 2.7, 2.8 and 2.9 using the measurements z. The superscript "ˆ" above the state variable indicates that it is the "estimate" of the state vector.

For other cases in which the hypotheses of linear Gaussian evolution-observation models are not valid, the usage of the KF approach does not result in optimal solutions, since the posterior density is not analytic.

Applications of Monte Carlo techniques are the most general and robust approach to non-linear and/or non-Gaussian distributions, as developed in [75, 76]. This is despite the existence of the EKF approach and its variations, which generally involves a previous stage of linearisation of the problem.

2.5.4 Extended Kalman Filter (EKF)

Since the usage of KF is limited in practice by the ubiquitous non-linearity and non-Gaussianity of the physical world, numerous efforts have been devoted to the generic filtering problem, mostly within the KF framework. Pioneers in the subject, including [77, 78], have investigated the non-linear filtering problem since the fifties.

In general, the non-linear filtering problem per se consists in finding the conditional probability distribution (or density) of the state to be estimated, given the observations until the current instant in time [79], for time discrete applications.

In particular, the solution of non-linear filtering problem using the theory of conditional Markov processes can be very effective from a Bayesian perspective, having many advantages over the other methods, as presented in [80].

The recursive transformations of the posterior measures are characteristics of this theory. Strictly speaking, the number of variables replacing the density function is infinite, but not all of them are of equal importance, as detailed in [69]. One state is recalculated only in the updated version, improving the covariance. Therefore it is advisable to intelligently select the important ones and reject the remainder.

The solutions of non-linear filtering problem can be made by global and local method.

In the global approach, one attempts to solve a probability density equation (PDE) instead of an ordinary differential equation (ODE) into a linear case (e.g. Zakai equation, Kushner-Stratonovich equation), which are mostly analytically intractable. Then, numerical approximation techniques are needed to solve the equation. And in special scenarios (e.g. exponential family) with some assumptions, the non-linear filtering can admit the tractable solutions.

In the local approach, finite sum approximation (e.g. Gaussian sum filter) or linearisation techniques (i.e. EKF) are usually used.[3]

For the EKF approach the usage can be made by defining:[4]

$$\hat{F}_{n+1,n} = \left.\frac{df(x)}{dx}\right|_{x=\hat{x}_n}, \hat{H}_n = \left.\frac{dh(x)}{dx}\right|_{x=\hat{x}_{n|n-1}} \tag{2.10}$$

Equation 2.10 shows how is possible to linearised Equations 2.1 and 2.2 into Equations 2.3 and 2.4 to further employment in conventional KF technique.

Since EKF always approximates the posterior $p(x_n|y_{0:n})$ as a Gaussian, it works well for some types of non-linear problems, but it provides a poor performance when the true posterior is non-Gaussian (e.g. heavily skewed or multi-modal cases). The EKF approach estimation is usually biased[5], since in general $\mathbb{E}[f(x)] \neq f(\mathbb{E}[x])$ [81].

[3] In these cases the propagation of the covariance and the linearised update Equation 2.10 are relevant differences for the non linear states.

[4] The EKF uses the same equations with a statistical uncertainty approach.

[5] Since EKF is not included in the update stage, this can cause a linearisation in the wrong direction.

2.5.5 Particle Filter (PF)

The Sequential Monte Carlo (SMC) technique called Particle Filter (PF) for the solution of the state estimation problem (also known as "the bootstrap filter") consist on a condensation algorithm, interacting particle approximations and survival of the fittest [18], based on the representation of the required posterior density function by a set of random samples ("particles") with associated weights and the computation of the estimates based on these samples and weights. By making the number of samples very large, this SMC characterization becomes an equivalent representation of the posterior probability function and the solution approaches the optimal Bayesian estimate.

The Sequential Importance Sampling (SIS) algorithm for the PF approach includes a resampling step at each instant, described in detail in [74].

The SIS algorithm uses an importance density, defined as "density proposed to represent another one that cannot be exactly computed" making the samples be drawn from this density instead of the actual density.

Being $\left\{x^i_{0:k}, i = 0, \cdots, N\right\}$ the particles with associated weights $\{w^i_k, i = 0, \cdots, N\}$ and $x_{0:k} = \{x_j, j = 0, \cdots, k\}$ the set of all states up to t_k, where N is the number of particles. Weights are normalized so $\sum_{i=1}^{N} w^i_k = 1$. Then, the posterior density at t_k can be discretely approximated by mean of $\delta()$ (the Dirac delta function).

$$\pi(x_{0:k} \mid z_{1:k}) \approx \sum_{i=1}^{N} w^i_k \delta(x_{0:k} - x^i_{0:k}) \tag{2.11}$$

Taking into account the assumptions from [70] expressed above for the "evolution-observation model", the posterior density from Equation 2.11 can be written as:

$$\pi(x_k \mid z_{1:k}) \approx \sum_{i=1}^{N} w^i_k \delta(x_k - x^i_k) \tag{2.12}$$

By means of the PF approach the estimation of position for static GNSS-based localisation system studies were performed as part of the statistical quality control (SQC) presented in [21] and it is part of the SQC of GNSS-Receivers presented in Chapter 4 and Chapter 5.

In Chapter 5 PF-based estimators are developed by several approaches and analysed for its application as part of the intelligent GNSS-based localisation system from Chapter 7 in the present dissertation.

2.6 Artificial neural network approach for estimation

The usage of artificial neural network (ANN) models for estimators as validation tools for safety-relevant purposes in GNSS-based localisation systems is one of the new contributions of this dissertation.[6]

By means of ANN techniques the estimation of the accuracy-based GNSS quality and a subsequent AI-based estimation of the GNSS receiver's behaviour as part of the developed intelligent GNSS-based localisation system is presented in Chapter 6.

Tests within independent RMS to validate the developed intelligent estimators have proven to provide a sufficient frame for the validation of accuracy-based GNSS-Rs quality in [21]. In the following subsections a general overview of the existing ANN technologies applied in this dissertation are presented.

2.6.1 Artificial Neural Networks description

As described in [82] an ANN is composed of multiple simple processing units, called neurons, and weighted connections between those neurons. The general structure of an artificial neuron is presented in Figure 2.13, each neuron input is weighted with an appropriate w and the sum of the weighted inputs and the bias forms the input to the activation function f. Neurons can use any differentiable activation function f to generate their output.

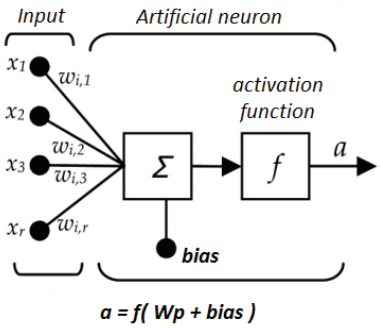

FIGURE 2.13: General structure of artificial neuron [82]

[6] In this context the further question of how can ANN be quantified is needed for validation and verification (certification) purposes.

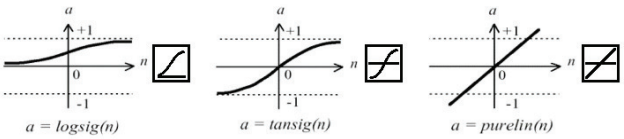

FIGURE 2.14: Activation functions [82]

The most commonly used activation functions are the log-sigmoid function, the tan-sigmoid function and the pure-linear function. Their standard symbols and curves are presented in Figure 2.14.

The artificial neurons in an ANN are interconnected following a structured topology. Many different topologies approaches can be defined, as presented in [83]. For the present dissertation a general description of the concept of ANN topology is presented and only detailed characteristics of the feed-forward topology are taken into consideration.

2.6.2 Artificial Neural Networks topologies

The simplest ANN topology is the single-layer perceptron, which consists of a single layer of output nodes. A single-layer perceptron is presented in Figure 2.15, where each shaded circle represents an artificial neuron.

The neurons can also be arranged into layers to obtain a better performing ANN. Such an arrangement is known as a multilayer network, where the results produced by one layer of neurons are used as inputs for other layers of networks.

The two main groups of multilayer networks can be identified as:

1. **Feed-forward neural network (FFNN):** class of ANN where connections between units do not form a directed cycle.

2. **Recurrent neural network (RNN):** class of ANN where connections between units form a directed cycle.

RNNs allow loops between different layers, where the output of one given layer can be used as an input to a previous layer. This type of networks can implement dynamic mappings, where the target functions depends on previous states of the input, although RNN may behave chaotically due to the presence of feedback loops.

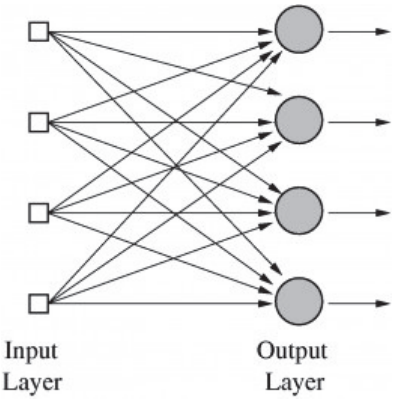

FIGURE 2.15: Representation of single layer ANN [82]

On the other hand FFNNs only allow direct feed between layers, where the output of one given layer can be used only as an input to the next layer. FFNNs are limited to static mappings, and no correlation between actual targets and previous targets can be properly modelled. However the simplicity of the FFNN allows more stable behaviours' estimations.

The feed-forward topology used in this dissertation is presented here in detail. Multilayer FFNNs include one or more hidden layers, which are layers of neurons that lay between the input and output layers and their output results can be used as input only to the next layer in the network, as seen in the one hidden layer example of Figure 2.16. The function of the hidden layers is to extract higher-order statistics while providing further neuronal connections as detailed in [84].

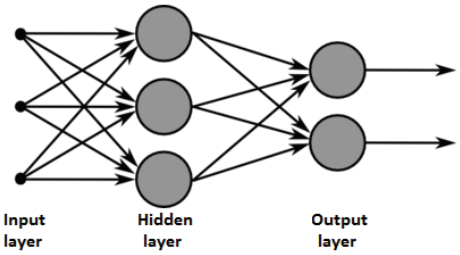

FIGURE 2.16: Feed-forward ANN topology [82]

Based on [82] the multilayer FFNN can be used as a general function approximator, which can approximate any function with a finite number of discontinuities arbitrarily well. Moreover, a FFNN with log-sigmoid activated hidden layer and a pure-linear activated output layer can be trained and analysed in order to find the relevance of each input to a given target function, as described in [85] and used in the quantitative estimation approach in Chapter 6. This topology is also used for the qualitative estimation approach for the accuracy-based evaluation of the GNSS-based localisation system.
More in depth studies in ANN topologies can be found in [83] and further development of ANN topologies can be found in [82], as well as potential evolutions on ANN topologies in [86, 87]. Some properly detailed exemplary ANN applications for spatial perception can be found in [88], as well as indoor-outdoor localisation systems in [89], where even the decision making algorithms are based on ANN models.

2.7 This dissertation contributions

The present dissertation's contributions can be seen in Figure 2.17. The marked sections in the depicted diagram block describe the specific chapters where the content of the part of the developed intelligent GNSS-based localisation system are presented in detail. The list of content for the following chapters is as follows:

- **Chapter 3:** Bases for GNSS quality description by means of Availability, Accuracy, Reliability and Integrity and GNSS-Receivers' certification process.
- **Chapter 4:** Newly developed Mahalanobis Ellipses Filter (MEF) methodology for accuracy-based evaluation of deviation datasets.
- **Chapter 5:** PF-based location estimator for independent reference validation and self-reference system development.
- **Chapter 6:** ANN-based validation tools for accuracy-based analysis of GNSS-based localisation systems.
- **Chapter 7:** Demonstrator-Tool of an intelligent GNSS-based localisation system, based on all previous developed technologies.

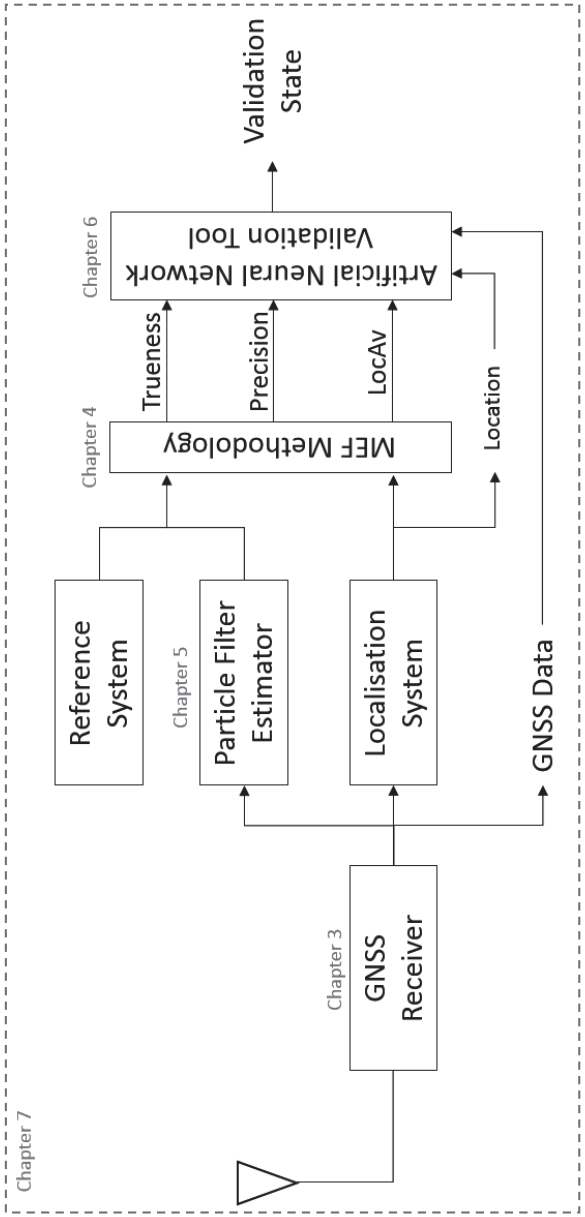

FIGURE 2.17: Graphical description of the contributions of the present dissertation.

Chapter 3

Evaluation Process for GNSS-receivers

"You can't fake quality any more than you can fake a good meal."

William Seward Burroughs

Based on the quality description from [43], this chapter presents a safety-relevant approach for GNSS quality description, as well as an adaptation of the certification process from [44]. The proposed process is composed by validation procedures based on the quality properties' evaluations. Finally a method to apply artificial intelligence based evaluation for validation and certification purposes is presented.

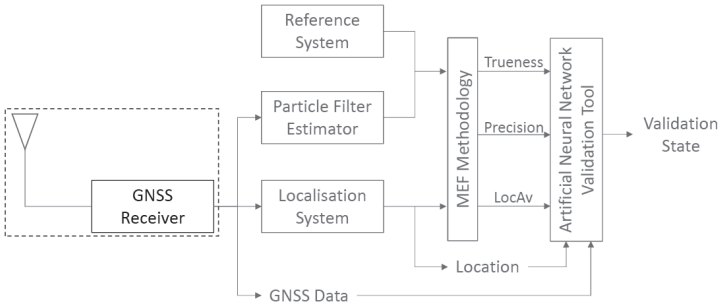

FIGURE 3.1: Graphical description of chapter 3: GNSS-Receivers Certification Process

GNSS-based localisation systems are the base for many future Intelligent Transport Systems (ITS). Therefore the need of previous evaluation of the generated location information by means of an independent reference measurement system results essential for all future implementations. Since all potential applications required previously certified receivers as the fundamental part of all localisation systems, a detailed enough description of the GNSS quality description is essential for all certification and validation purposes.

The proposed certification process from the present chapter is based on [44] detailed in Chapter 2 and it consists of a combined validation process of GNSS quality characteristics, constituted by four evaluations of the GNSS quality properties.

The GNSS receivers featured nowadays can provide a very wide spectrum of quality of service. Therefore the standardisation of a certification methodology based on GNSS receivers quality analysis will allow a better understanding of GNSS-based localisation system and an easier classification of receivers for different applications.

For this proposed certification process the receiver is considered a black box with several features to be assessed. Based on [9, 14, 15] a description in detailed of the hierarchical GNSS Quality presented in Chapter 2 can be shown by means of Availability-Accuracy-Reliability-Integrity (AARI) approach as basis for the GNSS-Receiver certification process for safety-relevant purposes.

3.1 GNSS-based System Quality Description

In [41] the attribute hierarchy (Concept/Properties/Characteristics/Values-unit) approach for quality based on [42] is applied to describe the GNSS quality description for safety-relevant applications, based on an Accuracy, Availability, Reliability and Integrity (AARI) approach.

The requirements for quality from [43] and the GNSS-based localisation systems' properties detailed in [40] allow the hierarchical description of quality presented in Figure 3.2, divided into all necessary characteristics and quantities.

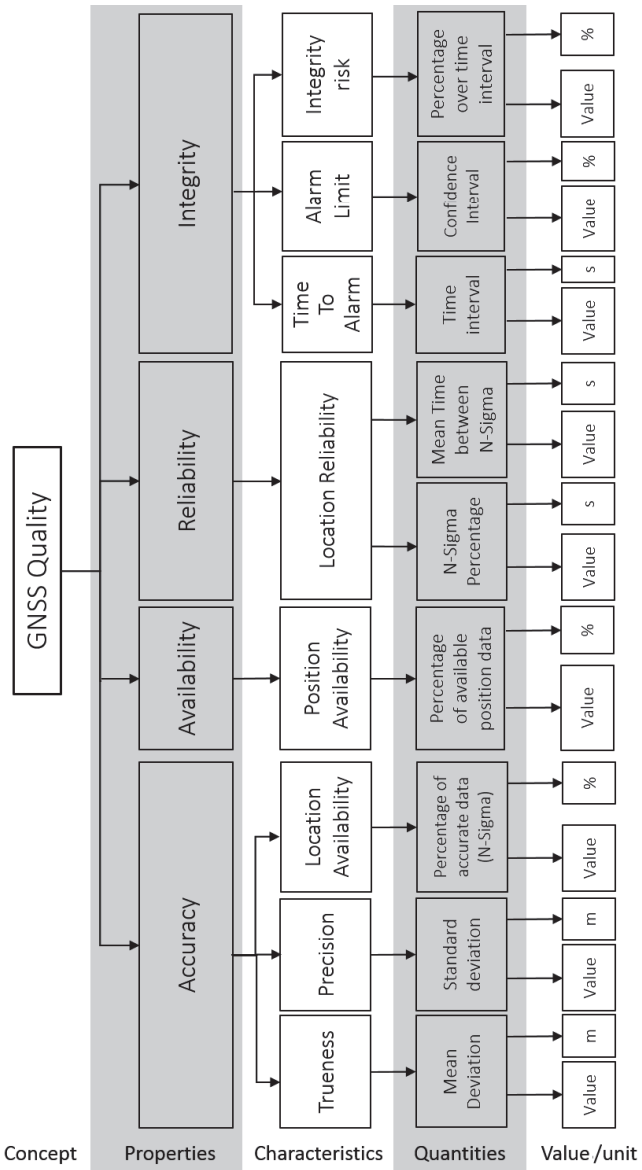

FIGURE 3.2: Graphical description of the GNSS quality by means of Availability, Accuracy, Reliability and Integrity.

In the terminology section of Chapter 2 the definitions of the AARI approach were presented. Figure 3.2 shows the decomposition from AARI into the characteristics to be assessed in the quality evaluation.

3.2 GNSS-Receivers' Certification Process

Since all generated location data by GNSS-based localisation systems must be assessed for safety-relevant applications, the GNSS-Receiver must be certified. The presented certification methodology is based on the GNSS quality properties' evaluation as shown in Figure 3.2.
The certification process depicted in Figure 3.3 can be divided into three levels. The first level is the certification process itself, where inputs are:

1. Reference System data,
2. GNSS-Receiver data, and
3. Current GNSS constellation information.[1]

And where the output is the Certificate provided by the attestation of the certification body, previously certified by the procedure depicted in Figure 2.6 in Chapter 2.
The second level is the validation process, where the inputs are the same as the certification process, but the output is the GNSS Quality report, provided by the accredited laboratory (also certified by means of procedure depicted in Figure 2.6).
Finally the third level is called the evaluation processes, where the measurements (inputs) are evaluated by means of the specific requirements within the significant scenarios, and the outputs are four quality reports, based on the four properties of GNSS-based quality.
The outputs of the AARI-based reports are combined into the GNSS Quality report that is the validation output to be attested in order to obtain the certification.

[1] Description of current GNSS constellation information include HDOP, SNR and number of satellites.

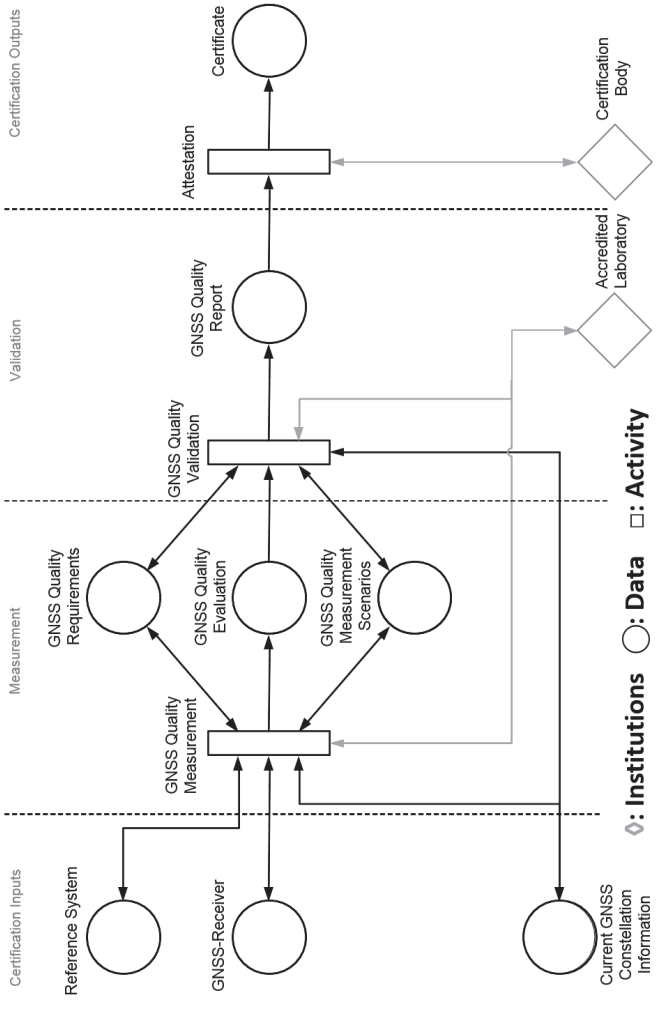

FIGURE 3.3: New certification process for GNSS-Receivers by quality assessment

3.3 Validations Processes Based on GNSS Quality

In Figure 3.3 the GNSS-Receivers certification occurs by means of measurement evaluation of the quality properties for further validation reports provided by an accredited laboratory to be assessed to conclude in a final certification by means of an accredited certification body. This procedure is proposed during the present dissertation based on the AARI-approach for GNSS quality description, depicted in Figure 3.2.
The model of the validation process based on GNSS quality is shown in Figure 3.4. The resulting AARI-based quality report of all four properties from the measurement must be framed into specific scenarios within their correspondent requirements.

3.3.1 AARI-based Quality Validation Process

The general description of the process in Figure 3.4 must be done separately for each one of the four quality properties. And the final combination of all four properties evaluations creates the GNSS Quality Report, output of the validation process and input for the certification stage in Figure 3.3.

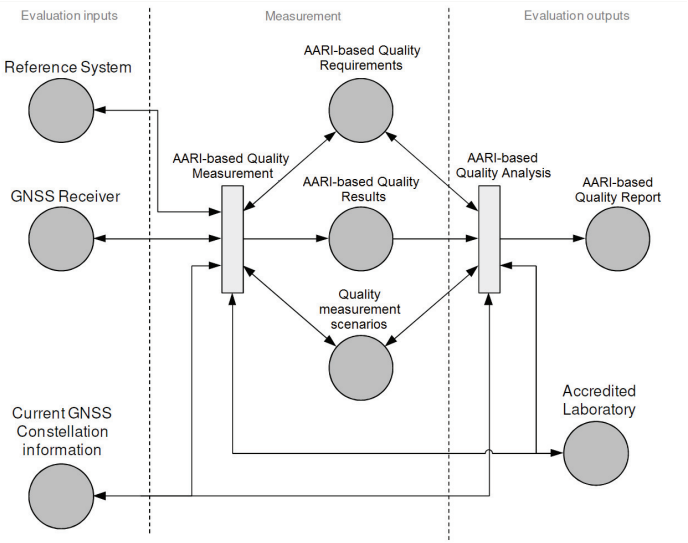

FIGURE 3.4: Evaluation Process for AARI-based Quality

3.3.2 Current GNSS Constellation Information

All evaluations that constitute the validation process are related to the "current GNSS constellation information" [9]. Therefore all AARI-based quality evaluations from GNSS-Receivers must be based on the current GNSS constellation information. For the National Marine Electronic Association interface standard NMEA 0183 the Global Positioning System Fix Data information (GPGGA) describes the essential current GNSS constellation fix data, which provides location and accuracy data from the GPS signal considered enough to describe the current GNSS constellation information [14]. An example table of a GPGGA sentence is presented in Table 3.1.
The general description of the current GNSS constellation for the all AARI-based GNSS quality validation process are based on the GPGGA information, for certification purposes of GNSS-Receivers.

Table 3.1: NMEA GPGGA sentence general description [90]

Field	***Value***	***Meaning***
1	*GGA*	*Global Positioning System Fix Data*
2	*123519*	*Fix taken at 12:35:19 UTC*
3	*4807.038*	*Latitude 48 deg 07.038'*
4	*N*	*Direction of Latitude (N-North;S-South)*
5	*01131.000*	*Longitude 11 deg 31.000'*
6	*E*	*Direction of longitude (E-East;W-West)*
7	*1*	*Fix quality:* *0 = invalid* *1 = GPS fix (SPS)* *2 = DGPS fix* *3 = PPS fix* *4 = Real Time Kinematic (RTK)* *5 = Float RTK* *6 = estimated (dead reckoning) (2.3 feature)* *7 = Manual input mode* *8 = Simulation mode*
8	*08*	*Number of satellites being tracked*
9	*0.9*	*Horizontal dilution of position*
10	*545.4*	*Altitude above mean sea level (MSL)*
11	*M*	*Unit of altitude (meters)*
12	*46.9*	*Height of geoid (MSL) above WGS84 ellipsoid*
13	*M*	*Unit of altitude (meters)*
14	*(empty field)*	*time in seconds since last DGPS update*
15	*(empty field)*	*DGPS station ID number*
16	**47*	*Checksum data, always begins with **

3.4 AARI-based Quality Evaluations

This section will detail all evaluations required for the proposed GNSS Quality properties (AARI approach) for Position Navigation and Timing (PNT) Systems, as proposed by the Federal Radionavigation Plan (FRP) in [91]. PNT is a combination of three distinct, constituent capabilities: [92]

- **Positioning**: the ability to accurately and precisely determine one's location and orientation two dimensionally (or three dimensionally when required) referenced to a standard geodetic system, such as [93].
- **Navigation**: the ability to determine current and desired position (relative or absolute) and apply corrections to course, orientation, and speed to attain a desired position anywhere around the world, from sub-surface to surface and from surface to space.
- **Timing**: the ability to acquire and maintain accurate and precise time from a standard Coordinated Universal Time (UTC) [94], anywhere in the world and within user-defined timeliness parameters.

3.4.1 Accuracy Evaluation

Accuracy was defined in Chapter 2 as the degree of conformance of that position with conventional true position of the craft at the given time [38], and in this chapter it was divided into the three characteristics:

1. **Trueness:** closeness of agreement between the expectation of a test result or a measurement result and a true value. [95]
2. **Precision:** closeness of agreement between independent test/measurement results obtained under stipulated conditions. [95]
3. **Location Availability:** the percentage of the the test/measurements results considered precise, after filtering with an nσ from a defined precision threshold. [9]

The difference between accuracy by trueness and precision is shown in Figure 3.5.

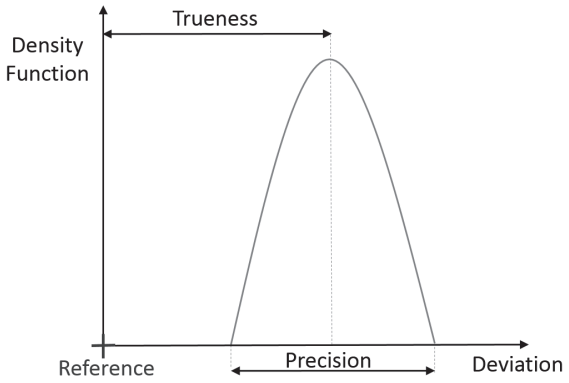

FIGURE 3.5: Graphical distinction between trueness and precision

Trueness[2] indicates proximity of measurement results to match the true value (calculated by means of absolute Euclidean distance between datum and reference) and Precision indicates the ability of measurement to be consistently reproduced (calculated by means of Mahalanobis distance between datum and all collected GNSS measurements).
In [91] accuracy of a PNT system depends on the quality of the pseudorange and carrier phase measurements as well as the broadcast navigation information.
Both the trueness and precision evaluation as part of the proposed AARI-approach certification process, two separated validation processes must be performed.
Each validation process is focused on the assessment of the GNSS receivers data, by means of an independent reference, within the information of the current constellation:

- The evaluation of the trueness and precision of static GNSS data.
- The evaluation of the trueness and precision of dynamic GNSS data.

The remaining evaluation is focused on the Location Availability characteristic. When specifying linear accuracy, or when the requirements are focused in terms of orthogonal axes (e.g., along-track or cross-track in railways applications), a 95% confidence level (2σ) is proposed to be used [40]. Also, when two-dimensional accuracy is required, the 2 Distance Root Mean Squared (drms) uncertainty estimate (twice the radial error drms) is proposed to be used, as proposed for the ergodic hypothesis.

[2]Trueness is day to day bias, so it is the combination of the most probable value plus an offset.

The radial error is defined as the root-mean-square value of the distances from the point of the location fixes to all collected GNSS measurements [40]. The distribution of the error is normally elliptical[3], as proposed in [96].
In [92] the specifications of PNT system accuracy refers the following types:

- **Predictable Accuracy:** here the accuracy of a PNT system's location solution with respect to the carted solution. Both the location solution and the chart must be based upon the same geodetic datum. [40]
- **Repeatable Accuracy:** here the accuracy of the PNT system's location is focused on the returning possibility of a user to a location whose coordinates has been measured at a previous time with the same PNT system. [40]
- **Relative Accuracy:** here the accuracy of the PNT system's location is focused on the possibility of a user to measure a location relative to a measurement by another user of the same kind of PNT system at the same time. [40]

Detailed representation of these accuracy evaluation results depend on the specific evaluations for trueness and precision. And for all accuracy-based evaluations, as well as the related reliability and integrity evaluations described in the following sections, both the GNSS location data and the independent reference system data must share a synchronised time frame with one common clock reference to make them valid inputs for the GNSS quality validation process. The bases for a proper accuracy evaluation is a correct deviation calculation.
A GNSS location datum at time t is represented as:

$$G_t = GNSS(t) = (x_{(t,G)}, y_{(t,G)})$$

While the independent reference system location datum at time t is represented as:

$$R_t = Reference(t) = (x_{(t,R)}, y_{(t,R)})$$

Then, the deviation between GNSS and reference at time t is calculated as drms:

$$\delta_t = \left|\overrightarrow{G_t R_t}\right| = \sqrt{(x_{(t,G)} - x_{(t,R)})^2 + (y_{(t,G)} - y_{(t,R)})^2} \tag{3.1}$$

[3]Typically specified as a circle, by circular error probable (CEP).

The deviation analysis performed by Equation 3.1 is the bases for both the accuracy-based evaluation, by means of MEF methodology (presented in detail in Chapter 4), and the subsequent reliability and integrity evaluations for the AARI-based GNSS quality report in Figure 3.4.

The combinations of the resulting evaluations outputs framed for the specific requirements and scenarios for actual applications must be incorporated into the validation output for later attested by an external certification body to conclude the certification process.

An accuracy evaluation can therefore result in one of the four depicted cases in Figure 3.6 regarding location estimation as presented in [97][4]:

1. HTHP - High Trueness, High Precision, when $\left(S \approx S'\right) \wedge \left(\delta \gg \delta'\right)$,
2. LTHP - Low Trueness, High Precision, when $\left(S \neq S'\right) \wedge \left(\delta \gg \delta'\right)$,
3. HTLP - High Trueness, Low Precision, when $\left(S \approx S'\right) \wedge \left(\delta \geqslant \delta'\right)$,
4. LTLP - Low Trueness, Low Precision, when $\left(S \neq S'\right) \wedge \left(\delta \geqslant \delta'\right)$.

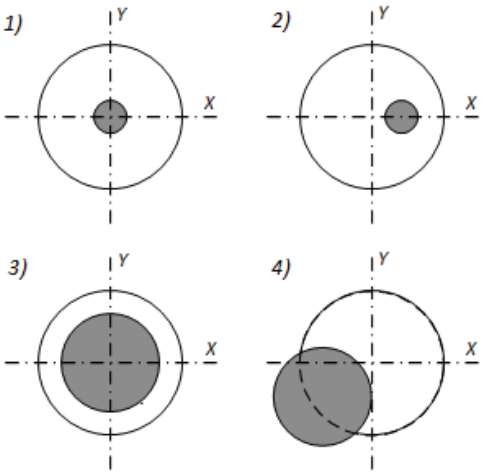

FIGURE 3.6: GNSS receiver's states of accuracy [97]

[4]In [97] the author concludes that the proposed CEP description is not the proper approach.

3.4.2 Availability Evaluation

The global availability of a PNT system is the percentage of time that the services of the system are usable [91]. The availability characteristic indicates the ability of the system to provide a usable navigation service within a specified coverage area. The availability function of both the physical characteristics of the environment and the technical capabilities of the transmitter facilities is defined as a percentage function:[40]

$$Availability = \frac{time\ service\ usable}{total\ time} \mid specified\ coverage\ area \tag{3.2}$$

Therefore, for the AARI-approach GNSS characteristics evaluation presented in 3.4 regarding availability evaluation the Equation 3.2 must be used. And the resulting availability-based evaluation output must be combined into the resulting GNSS quality report (validation output), for later attested by an external certification body to conclude the certification process.

3.4.3 Reliability Evaluation

The reliability[5] of a PNT system is a function of the frequency with which failures occur within the system [92]. It can be defined as the probability that a system will perform its function within defined performance limits for a specified period of time under given operation conditions. Formally the mathematical interpretation of the reliability characteristic of GNSS quality description can be presented in [40] as:

$$Reliability = 1 - P(system\ failure) \mid specified\ function\ and\ time \tag{3.3}$$

Therefore, for the AARI-based GNSS characteristics evaluation presented in Figure 3.4 regarding reliability evaluation the Equation 3.3 must be taken into consideration.
In [40] the proposed reliability evaluation of GNSS receiver is based on the appropriate precision levels of collected locations. The precision levels are determined through a throughout accuracy evaluation which provides the standard deviation (σ) of the locations in advance. Then reliability is assured by the comparison between nσ and the reliability requirements for corresponding applications and scenarios.
Three separated evaluations constitute the reliability-based process [14]:

[5] Another approach for reliability evaluations can be found in [98].

- Evaluation of the reliability for static GNSS receiver location data.
- Evaluation of the reliability for dynamic GNSS receiver location data.
- Evaluation of the receiver's time between nσ levels.

These three reliability-based evaluations compose the necessary process for GNSS receivers certification, based on the GNSS quality description depicted in Figure 3.4.
The used reliability evaluation methodology of GNSS receiver was previously established for train localisation purposes in [54, 55]. In the present dissertation this methodology is expanded and generalised into a universal approach for a wide range of certification purposes. Before the reliability-based evaluations take place, a previous accuracy-based evaluation must be performed. Therefore, the dataset description for the reliability-based evaluations must be correctly collected and synchronised. From the deviation analysis performed by Equation 3.1, the resulting deviations are fitted into suitable distributions with parameters of mean value μ, and variance σ^2.[6] These are the starting points for the reliability-based evaluations of the GNSS-Rs' certification process, by means of Equation 3.3.
As presented in Figure 3.4, GNSS measurements are synchronised with the correspondent reference system in addition to the current GNSS constellation information (certification inputs) that subsequently produce three reliability-based evaluation outcomes, related with their correspondent reliability levels requirements. The collected GNSS locations are firstly processed for accuracy quality evaluation, as presented in the accuracy-based evaluation section above and based on the accuracy evaluation results, the GNSS locations evaluated parameters (μ and σ) are used for three reliability evaluations:

1. **Static reliability:** The reliability from the collected static GNSS data is evaluated, related to its correspondent current GNSS constellation information.
2. **Dynamic reliability:** The reliability from the collected dynamic GNSS data is evaluated, related to its correspondent current GNSS constellation information.
3. **Reliability of times between nσ levels:** The reliability of the times between nσ levels from the collected GNSS signal data is evaluated, related to their correspondent current GNSS constellation information.

[6] Suitable distributions would be Normal (Gaussian), Rayleigh, Lognormal, or Gaussian Mixture, as proposed in [40].

The GNSS locations are analysed according to 1) nσ of the GNSS locations and 2) the mean time within nσ.

The GNSS receiver is specified for an application in the requirements of the GNSS receiver locations performance level into a certain number as α meters.

The mean value μ and the variance σ of the GNSS measurements have been calculated from accuracy evaluation, by means of Mahalanobis Ellipses Filter (MEF) methodology (in detail in Chapter 4). Mahalanobis distance (MD) provides an appropriate measurement for outliers' detection process in a bivariate deviation data [16]. Therefore the nσ determines the correct categories and percentage of each nσ.

The evaluations that constitute the validation process are all related to the current GNSS constellation information. The reliability-based validation process for GNSS receivers is based on three separated evaluations, focused on specific characteristics of the GNSS receiver. Figure 3.7 shows an exemplary measurement series, where the mean time of deviation smaller than the required nσ is settled as the characteristic of the reliability performance.

This presented evaluation is applicable for both static and dynamic GNSS measurements. The whole reliability-based analysis focuses on the comparison between the previously specified reliability requirement, based on the accuracy evaluation previously performed and the actual reliability analysis results. As described in Figure 3.4, all reliability-based evaluations are performed by accredited laboratory and the reliability part of the AARI-based validation process ends when the three evaluations are combined into the reliability-based quality report (output of the reliability-based analysis), related to the general behaviour of the GNSS constellation.

Finally the report is presented for attestation by a certification body after being combined into the resulting GNSS quality report (validation output).

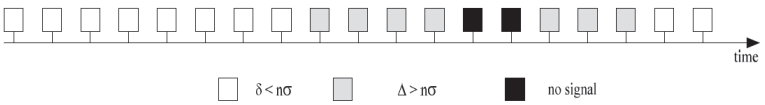

FIGURE 3.7: GNSS location measurenemt series nσ requirement representation [14]

3.4.4 Integrity Evaluation

The integrity of a PNT system is the measure of the trust that can be placed in the trueness of the information supplied by the system [92].
The characteristic of integrity of the GNSS quality description included its ability to provide timely warnings to users when the system should not be used for navigation purposes, depicted as Time-To-Alarm, Alarm Limit and Integrity risk in Figure 3.2.
For specific applications (e.g. in railway domain), the ambiguity between the terms reliability and continuity was dealt in [40]. Also in [91] all requirements for specific applications present a direct relationship between integrity and accuracy requirements.
For railway application, integrity is defined in [99] as "the capability of a system to detect performance anomalies and warn users whenever the system should not be used, relates to the trust that can be placed in the trueness of the functional components, i.e. train localisation system (TLS)".
In this exemplary application integrity is described by its three characteristics:

- **Time-to-alarm:** indicating the maximum allowable time interval between an alarm condition occurring and the alarm being present at the output. [99]
- **Alarm limit:** indicating the maximum allowable error in the determined position before an alarm is triggered. [99]
- **Integrity risk:** indicating the probability of an undetected failure, event or occurrence within a given time interval. [100]

Non-satisfaction of integrity, and therefore the corresponding triggered alarm, can be indicated by detectability of Location Error (LE), its correlation with Protection Level (PL), and Alarm Limit (AL) for specific applications, as presented in Figure 3.8.
The TLS example for integrity assessment can be summarized in two cases from the depicted integrity assessment of Figure 3.8. And the correspondent solution space of the relation identification is here based on [99].
In Figure 3.8 the train location is adopted in two-dimensional space, which has been proved more suitable and recommended for the GNSS-based train localisation in [101].[7]

[7]The newly presented elliptical approach should be considerate against the CEP approach in [99].

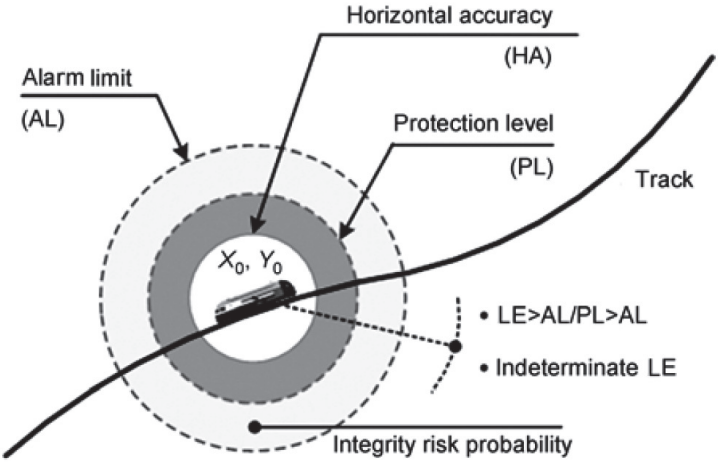

FIGURE 3.8: Integrity assessment in GNSS-based train localisation system. [99]

The described cases can be summarised as:

1. TLS cannot hold the position accurately. LE or PL is not within the bound of AL, and the AL-exceeding will trigger an alarm in the proposed time interval.

2. TLS loses capability of position determination. The absence of train localisation information means a terrible failure in localisation function of TLS.

The assurance of integrity begins with the detecting and relation identification among PE, PL and AL. The solution space can be described as listed in Table 3.2.
Using Autonomous Integrity Monitoring and Assurance (AIMA) this kind of integrity-based evaluation can be performed, as presented in [102, 103].

TABLE 3.2: States of integrity assessment in GNSS-based train localisation system [99]

		Integrity Status	
		Alarm ON	Alarm OFF
Location Accuracy	No fault	false alarm (safe failure)	Normal operation
	Fault	Correct detection	Missed detection
	Fault >AL	Correct detection	Hazard situation

The missed detection and hazard situation in Table 3.2 refer to the non-reaction of the TLS to failures that should have trigged the alarm, while the false alarm indicates incorrect reaction with non-existing faults, which may not cause damage to safety, but is harmful to the availability of the GNSS-based train localisation system.[8]

These three states are significant indicators of integrity level in a statistical sense, which have to be highly concerned. In general, with detecting and monitoring as major means, integrity assurance of the GNSS-based train localisation system is actually a substantiation of the detection-response mechanism [99].

The capability of detecting fault states is the foundation to assure and enhance the integrity property of a GNSS-based system. Processing (e.g. isolating and eliminating) of the detected fault and the following response (alarm or not) provide feedbacks to detection results [104]. Since the course of integrated localisation involves several different objects (e.g. the raw measurements, error estimates [105] and map matching techniques [106], there might be probable failures in every step, such as the "missed detection", "non-isolation", and the following response of "missed alarm".

FIGURE 3.9: Integrity related to operations in GNSS-based train integrated localisation system [99]

[8]In the scenario where the driver is not trusting the system (false alarm) maybe it's better to switch the whole system off.

Figure 3.9 shows the state space of the integrity related operations in the GNSS-based train integrated localisation system [99]. In the optimum decision perspective, high integrity suggests minimizing error rate in the detection and response procedures. As the state space shown in Figure 3.9, for integrity assurance, attention should be focused on the related performance indices, such as the detection missed rate (DMR), detection false rate (DFR), and fault non-isolation probability (FNP).

The integrity-based evaluation by means of Figure 3.4 also includes the integrity risk calculation, based on the probability of risk occurrence over time interval.

The combinations of the resulting integrity-based evaluations outputs framed for the specific requirements and scenarios for actual applications must be incorporated into the validation output for later attested by an external certification body to conclude the certification process.

3.5 Acquisition time evaluation

For all AARI-based GNSS quality validation presented in Figure 3.4 the requirements and scenarios must be set for specific application, as well as the nσ level of location availability and reliability. Only one parameter regarding specific scenarios must be always take into consideration: the acquisition time.

There are three start modes for all GNSS-Rs. Table 3.3 is a description based on the differences between the available information from the receivers for the three mentioned start modus: Cold start, warm start and hot start.

These three acquisition times are the mean durations (in seconds) that characterize the receivers' behaviour, related to the available information from GNSS-receivers and to the information regarding the scenarios and requirements. Table 3.3 is a description based on [107] of the differences between the available information from the receivers for each of the three mentioned start modes.

Table 3.3: Start modes of GNSS receivers [9]

Start modus	Available information of GNSS receivers			
	Estimated Position	Estimated Time	Current almanac Data	Current ephemeris Data
Cold start	No	No	No	No
Warm start	Yes	Yes	Yes	No
Hot start	Yes	Yes	Yes	Yes

Detailed definition for each of the three mentioned start modes can be found in [108]:

- **Cold start:** The receiver is missing, or has inaccurate estimates of, its position, velocity, the time, or the visibility of any of the GPS satellites. As such, the receiver must systematically search for all possible satellites. After acquiring a satellite signal, the receiver can begin to obtain approximate information on all the other satellites, called the almanac. This almanac is transmitted repeatedly over 12.5 minutes. Almanac data can be received from any of the GPS satellites and is considered valid for up to 180 days. Manufacturers typically claim the factory TTFF to be 15 minutes.

- **Warm start:** The receiver has estimates of the current time within 20 seconds, the current position within 100 kilometers, and its velocity within 25 m/s, and it has valid almanac data. It must acquire each satellite signal and obtain that satellite's detailed orbital information, called ephemeris data. Each satellite broadcasts its ephemeris data every 30 seconds, and is valid for up to four hours.

- **Hot start:** The receiver has valid time, position, almanac, and ephemeris data, enabling a rapid acquisition of satellite signals. The time required of a receiver in this state to calculate a position fix may also be termed Time To Subsequent Fix (TTSF).

This classification of three kinds of start modus for GNSS-Rs results in three acquisition time duration analyses.
As already mentioned these three acquisition times (cold acquisition time, warm acquisition time and hot acquisition time) are durations (in seconds) that characterize the receivers' behaviour, related to the available information from GNSS receivers.
The correspondent mean time acquisition evaluations must be complementary applied related to specific scenarios and applications, with the percentage of evaluated data within the nσ requirements (In this thesis typically n = 1).
Further statistical analyses of acquisition times for standarised test scenarios for GNSS-based localisation system applications must be performed to provide a future frame for this kind of evaluation.

3.6 Final Validation Report

After all validation procedures have been done for all four GNSS quality properties a technique for combination them into a final certification report must be done.
Since this dissertation presents artificial intelligence (AI) based validation tools, their validity statement should be conceived as one more expert validation.
The AI-based certification process consists on the development of AI-based decision-making machines as part of the accuracy-based evaluations of the GNSS-Rs certification process as "intelligent" validation tools that can provide certification results for dynamic localisation systems, learning by quantifiable measurements for GNSS-Rs and acquiring human experience related to the GNSS-Rs behaviour, as well as the accuracy-based GNSS quality description by MEF methodology.
Therefore, based on the methodology for AI-based systems validity evaluation [109, 110], based on Turing test [111] all information provided by the AI-based validation tool presented in Chapter 6 can be used as part of the certification process introduced in the present chapter.
Figure 3.10 shows the summary of the four steps of the Turing Test Methodology for incorporating AI-based evaluations as part of validation process of the GNSS-Rs' certification process.

1. Solving of the test case (AARI-based quality evaluations) by the expert validation panel (persons) as well as by the expert system (AI-based developed tools) to be validated.
2. Randomly mixing the test cases solutions (evaluations) removing their authorship.
3. Rating all (anonymous) test case solutions (evaluations).
4. Evaluation of the ratings.

Since the objective of this approach is to propose a validity statement based on the results of the AARI-based evaluations based on AI expert systems the need to have human experts in the accredited certification body is essential. A validity statement cannot be totally objective because it is based on human judgement. Nevertheless, this Turing-based methodology presented here makes the final attestation as objective as possible, regarding the expert system assessment.

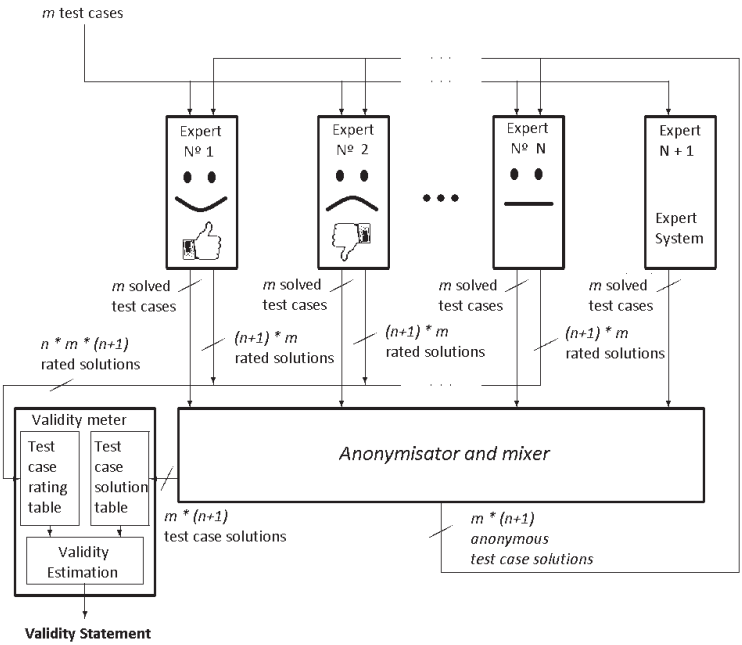

FIGURE 3.10: Survey of the Turing test to estimate an AI system's validity [109]

In [109] one way to improve the approach is proposed, by means of finding out the tendencies of the validating experts:

"Humans have the inherent property of being either more pessimistic or optimistic in nature. Therefore a good (poor) rating of a pessimist (an optimist) should have more influence on the validity statement than a good (poor) rating of an optimist (a pessimist)."

The AI-based evaluations by means of intelligent validation tools are focused on a more complex structured validity statement that can be:

1. Much more expressive (better description of the whole system behaviour) than a "flat" number.

2. A useful basis for certification process improvements.

3.7 GNSS-Receivers' Evaluation Process Summary

This chapter has presented the all new GNSS quality-based certification process, developed as part of the present dissertation focused on the newly developed AARI-based description of the GNSS quality description for safety-relevant applications.
The presented certification process is the necessary previous step for the usage of GNSS-Rs as part of intelligent GNSS-based localisation systems.
The PF-based location estimators created in Chapter 5, the AI-based validation tools developed in Chapter 6, and the Demonstrator-Tool designed and tested in Chapter 7 and Chapter 8 depend on the GNSS-R properly certified by means of quality-based evaluations.

Chapter 4

Mahalanobis Ellipses Filter Methodology

"Accuracy is the twin brother of honesty; inaccuracy, of dishonesty."

Nathaniel Hawthorne

The certification process presented in Chapter 3 depends on a proper accuracy-based analysis. This chapter focuses on the newly developed MEF methodology.

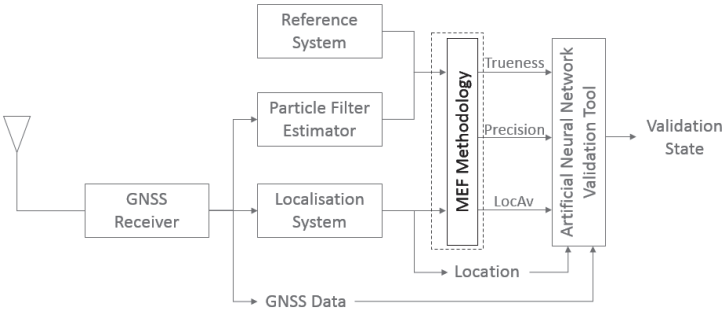

FIGURE 4.1: Graphical description of chapter 4: MEF Methodology

4.1 Accuracy Characteristics

Based on the GNSS quality description presented in Chapter 3, this chapter focuses on a new accuracy-based evaluation by means of trueness, precision and location availability, as presented in Figure 4.2. **Accuracy** was defined in Chapter 2 as "the degree of conformance of that position with conventional true position of the craft at the given time" [38], and the already mentioneed characteristics from [16] can be defined as:

1. **Trueness:** closeness of agreement between the expectation of a test result or a measurement result and a true value. [95]
2. **Precision:** closeness of agreement between independent test/measurement results obtained under stipulated conditions. [95]
3. **Location Availability:** the percentage of the test/measurements results considered precise, after filtering with an nσ from a defined precision threshold. [9]

The presented characteristics can be described by means of the following quantities:[1]

1. Mean Deviation [μ]
2. Standard deviation [σ]
3. Percentage of accurate data [LocAv]

The equation for the Mean Value, assuming ergodic hypothesis, can be described as:

$$\mu = \frac{\sum_{i=1}^{n} x_i}{n} \tag{4.1}$$

And the Standard Deviation can be described as, also assuming ergodic hypothesis:

$$\sigma = \sqrt{\frac{1}{n-1}\sum_{i=1}^{i=n}(x_i - \mu)^2} \tag{4.2}$$

[1] Provided that μ and σ are defining the density.

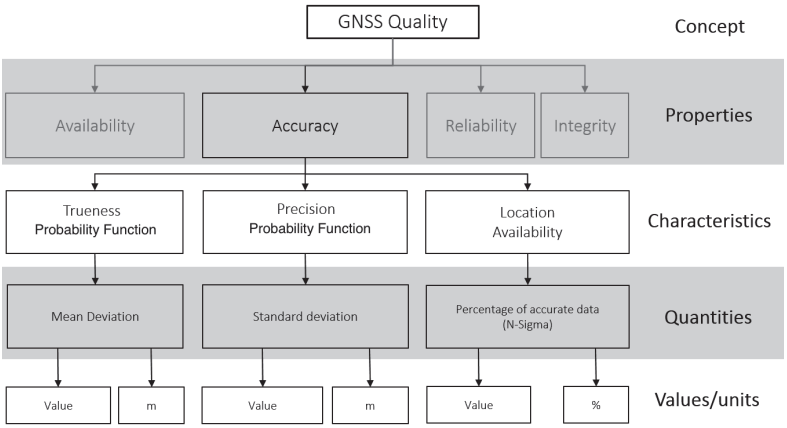

FIGURE 4.2: GNSS Quality description by means of accuracy characteristics

For explaining the Localisation availability concept the usage of Mahalanobis distance must be taken into consideration. The following sections describe the mathematical background for Mahalanobis distance and propose the bases for a standarisation of accuracy-based analysis within 1σ threshold.

4.2 Mahalanobis distance history

Prasanta Chandra Mahalanobis (29 June 1893 - 28 June 1972) was an Indian scientist and applied statistician (Figure 4.3).

During his 6-month stay (1926-1927) at Karl Pearson's laboratory at University College, London Mahalanobis undertook an extensive analysis of anthropometric data of various European population groups [112]. While examining the utility of coefficient of racial likeness (CRL) for measuring population relationships, Mahalanobis realised the statistical shortcomings of this method.

Mahalanobis's ideas on the problem of incorporating the observed correlations into the anthropometric measurements used to compute the distance took more concrete form in [113], where he introduced the concept of D^2 statistic.

The also called "Mahalanobis distance" (MD) can be defined as a distance measure developed in [114, 115] for the anthropometric measurements research in Biometry.

FIGURE 4.3: Prasanta Chandra Mahalanobis (29 June 1893 - 28 June 1972)

MD is based on the correlations between variables within one common dataset. This distance measurement allows the identification of different patterns within related datasets, by analysing the similarity of unknown samples from one dataset to a known one, as extensively presented in [115–117].
MD is nowadays used for several purposes, beyond its initial application in Biometry [118]. Significant fields such as pattern recognition [119] and outlier detection [120] and more complex examples applications such as General Packet Radio Service (GPRS) network user satisfaction estimation [121] and advanced face retrieval algorithms [122].

4.3 Mahalanobis distance calculation

In this section the MD calculation procedure is presented for the general multivariate dataset scenario. Considering m-dimensional multivariate datasets, each sample can be represented as a vector, such as:

$$Dataset = \{\overrightarrow{vec_1}, \overrightarrow{vec_2}, \cdots, \overrightarrow{vec_n}\}$$

Where each vector has m components, such as:

$$\overrightarrow{vec_i} = \left\{ x_i^{(1)}, x_i^{(2)}, \cdots, x_i^{(m)} \right\}$$

And each vector component itself belongs to an independent univariate subdataset:

$$\begin{gathered} x_i^{(1)} \in Subdataset\ x^{(1)} = \left\{ x_1^{(1)}, x_2^{(1)}, \cdots, x_n^{(1)} \right\} \\ x_i^{(2)} \in Subdataset\ x^{(2)} = \left\{ x_1^{(2)}, x_2^{(2)}, \cdots, x_n^{(2)} \right\} \\ \cdots \\ x_i^{(m)} \in Subdataset\ x^{(m)} = \left\{ x_1^{(m)}, x_2^{(m)}, \cdots, x_n^{(m)} \right\} \end{gathered}$$

Then, the calculation of the mean value (μ) for each subdataset is:

$$x_\mu^{(1)} = \frac{\sum_{i=1}^{n} x_i^{(1)}}{n}; x_\mu^{(2)} = \frac{\sum_{i=1}^{n} x_i^{(2)}}{n}; \cdots; x_\mu^{(m)} = \frac{\sum_{i=1}^{n} x_i^{(m)}}{n}$$

And the mean value of the complete multivariate dataset represented as a vector is:

$$\overrightarrow{vec_\mu} = (x_\mu^{(1)}, x_\mu^{(2)}, \cdots, x_\mu^{(m)})$$

From the dataset multivariate samples, the correlation matrix can be expressed as:

$$S = \frac{1}{n-1} \sum_{i=1}^{n} (\overrightarrow{vec_i} - \overrightarrow{vec_\mu})^T (\overrightarrow{vec_i} - \overrightarrow{vec_\mu}) \tag{4.3}$$

And the MD for any given sample vec_i can be calculated as:

$$D_M(\overrightarrow{vec_i}) = \sqrt{(\overrightarrow{vec_i} - \overrightarrow{vec_\mu}) S^{-1} (\overrightarrow{vec_i} - \overrightarrow{vec_\mu})^T} \tag{4.4}$$

This set of equations constitutes the necessary mathematical background for the presented accuracy-based evaluation, by means of MD and covariance calculation.

When there is no correlation between the vector components of the multivariate dataset, the covariance matrix S presented in Equation 4.3 is a diagonal matrix.

Additionally, when the vector components have a unity scale of σ the S matrix is the identity matrix. In this case, the MD from Equation 4.4 is equivalent to the Euclidean Distance (ED) between a given sample and the centre of the dataset.

When the covariance matrix is not the identity matrix the ED and the MD are not equivalent, as only the latter takes into account the correlations of the entire dataset.

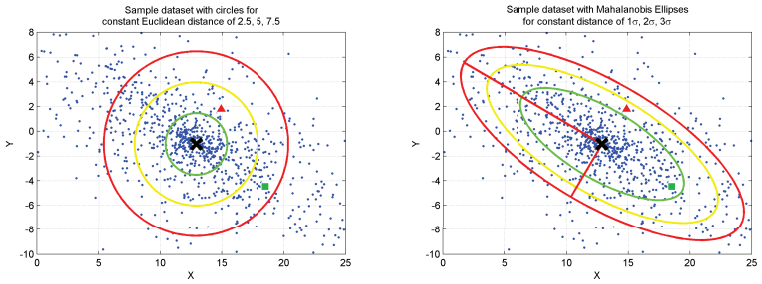

FIGURE 4.4: (A) Sample dataset with constant Euclidean Distance circles. (B) Sample dataset with constant Mahalanobis distance ellipses

This makes the MD a multivariate effect size distance. As the MD increases, the probability density decreases for a multivariate normal distribution. Due to this property the MD is a very useful tool for detection of multivariate outliers.

Advantages of the MD over ED for outliers' detection evaluation and behaviour description of deviation dataset are presented by a bivariate dataset in Figure 4.4.

The coloured circles in Figure 4.4A represent constant ED from the centre of the dataset, while the coloured ellipses in Figure 4.4B correspond to constant MD of 1σ, 2σ and 3σ, helping to visualise the MD application for multivariate dataset evaluation.

There are two marked observations from the dataset to illustrate significant advantages. One observation is marked with a red triangle and the other is marked with a green square. The listed remarks about Figure 4.4 are:

- Considering Figure 4.4A the comparison of marked measurements to the constant ED circles it seems clear that the red triangle is closer to the dataset centre.
- Considering Figure 4.4A an outliers' detection evaluation would present the green square to be a further away measurement from the dataset centre.
- In contrast, considering Figure 4.4B, an opposite interpretation can be achieved. The comparison of the marked measurements using the traced MD ellipses concludes that the red triangle has a bigger MD than the green square. Therefore, considering outliers' detection evaluation the red triangle represents a less probable observation than the green square, making it a more plausible outlier candidate.

The difference in results between the ED and MD is consequence of the ED's lack of consideration of the scale and correlations within the measurements from the dataset. This makes ED not an appropriate statistical measure for outliers' detection evaluation. On the other hand, MD proves to provide an appropriate statistical measure for outliers' detection evaluation within this kind of bivariate deviation data.

This approach also provides additional information of behaviour of the deviation dataset. For example, the angle between the axes of the formed ellipses describe the direct correlation between the rotated axes from the dataset. For both static and dynamic GNSS measurement evaluations this information helps to comprehend the way the GNSS-Receiver behaves. Therefore the constant MD ellipses are a straightforward representation of the nσ level of the Location Availability characteristic of the deviation dataset. This provides the bases for the Mahalanobis Ellipses Filter (MEF) methodology, explained in the next section. Examples of the MEF methodology for quality control of GNSS-Receivers by means of accuracy-based evaluations are shown in the following sections.

4.4 Mahalanobis Ellipses Filters concept

Based on the True Score Theory (TST) model from [123], GNSS quality by means of accuracy can be presented from a user side depicted in Figure 4.5 as a trueness and precision evaluation of the GNSS-Receiver based on deviation analysis. To present this as the bases for the MEF concept to calculate the LocAv of the reviewed receiver a short description of deviation by means of error analysis is presented.

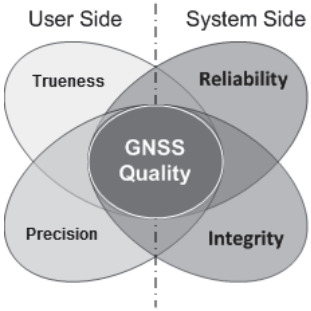

FIGURE 4.5: GNSS quality, user side and system side [21].

It can be stated the location provided by a GNSS receiver is:

$$Location = Reference + Error$$

Deviation can be defined as "the error between the actual reference and the provided location". And from the numerical analysis basis presented in [124] the deviation can also be divided into two significant components:

$$error = deterministic\ error + stochastic\ error$$

Where deterministic error can be defined as "the intrinsic error of the receiver's behaviour" while the stochastic error (also called non-deterministic error) can be defined as "the randomly added error to the receiver's behaviour".[2]

In addition to the trueness and precision analysis to describe the GNSS quality by means of accuracy, this dissertation has presented the concept of **location availability**, defined as the percentage of the GNSS data provided by the system that is considered precise, after filtering with an Nσ from a defined precision threshold. This characteristic can be mathematically defined as:

$$LocAv_{N\sigma} = \frac{N\sigma\ filtered\ number\ of\ samples}{Total\ number\ of\ samples} * 100\% \tag{4.5}$$

Since the measurement calculated to analyse accuracy of a GNSS-based system is deviation over time, Figure 4.6 shows a graphical description of the deviation analysis, presenting the deviation by means of its components.

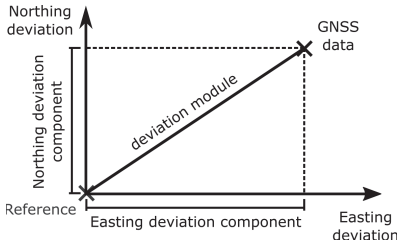

FIGURE 4.6: Deviation description [21]

[2]This deterministic error is the sum of an offset and a random value.

Deviation is the distance between a GNSS datum (location) and its correspondent reference system datum. As seen in Figure 4.6. the vector of the deviation can be also decomposed in easting and northing deviation. Therefore, depending on the approach, a univariate dataset (composed by the deviation module over time) or a bivariate dataset (composed by easting and northing deviation over time) can be processed.

In order to calculate deviation, both GNSS datum and the reference system datum must be represented over the same period time, in perfect synchronisation, allowing a valid time framed comparison. This deviation analysis and its decomposition have been presented as the the base for finding reliability margins of accuracy [13]. But since deviation is the measurement of interest,taking into account the location provided by the GNSS data as well as the reference system, allowing a good description of the whole localisation system's behaviour, for example the intelligent GNSS-based localisation system developed in the present dissertation. Therefore a properly established deviation analysis is the basis of all accuracy-based evaluations.

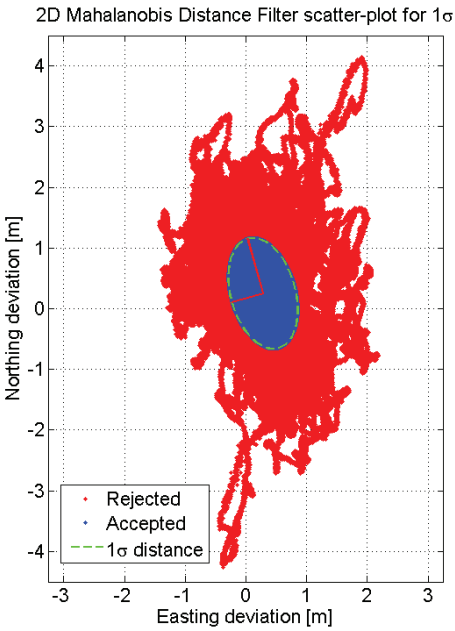

FIGURE 4.7: Scatter-plot for 1σ MEF filter [16].

Typically an accuracy evaluation is performed as the statistical analysis of the deviation, where a suitable distribution is fitted to the deviation data in order to characterise the behaviour of the GNSS receiver [13]. In this context accuracy is described by quantitative values of trueness and precision of the GNSS; typically provided by μ and σ of the normal distributed fitted dataset, while the LovAv is described as the percentage of the total received data that can be considered precise under Nσ boundaries; where N is the level of requested precision for specific applications.

Several statistical approaches based on the fitted distributions were developed and analysed in [16, 21]. Filtering based on the lognormal distribution for the deviation module was analysed, as well as filtering independently by easting and northing deviation component, but both approaches have proven to be limited, provided an incomplete description of the GNSS receiver behaviour, since the possible correlation between deviation components is not taken into consideration [21]. Mahalanobis Ellipses Filter (MEF) approach developed in [16] has proved to be the best filter technique for GNSS-Receiver's deviation datasets, according to receiver's behaviour description and coinciding with the theorised deviation ellipses described in [96] for bivariate GNSS data deviation.

An exemplary result of the MEF methdology can be seen in Figure 4.7, providing a general description of the description of GNSS-Receiver behaviour achieved by this methodology. Also, the present mathematical bases can be apply to multivariate filter, where all data can be filtered with the calculated MD of the multivariate deviation samples, regarding the whole deviation dataset. The Nσ filtering performed in this approach discriminates samples based on an elliptic boundary with MD of magnitude N, as visually represented by means of 1σ filtering in Figure 4.7.

The correspondent results of this MEF deviation analysis are presented in Table 4.1, where the **Ellipses center** describes the **trueness** part of the evaluation; the **Semi-radii** describes the quantitative **precision** part of the evaluation; and finally the **Rotation** and **MEF(1σ)** values describe the **LocAv(1σ)** part of the evaluation.

TABLE 4.1: MEF deviation analysis 1σ

Ellipses Center [m]	*Easting*	0.2831
	Northing	0.2533
Semi-radii [m]	*A*	0.529
	B	0.9316
Rotation [^{o}]	*Degrees*	15.497
LocAv [%]	*1σ*	42.2172

The MEF approach is homogenous despite the number of variables and takes into consideration the correlation between deviation components.
The MEF methodology presents additional characteristics of the GNSS behaviour, by means of ellipses semi-radii lengths and angles. The following section analyses these characteristics and presents graphic examples of the MEF approach as applied to multivariate datasets.

4.5 MEF applied for multivariate deviation datasets

The MEF methodology is general and can be applied homogeneously in either univariate or multivariate datasets. In the case of a univariate dataset, MEF presents a one-dimensional filtering interval, equivalent to univariate normal distribution based filtering. Figure 4.8 presents the results of univariate data filtering for a empiric dataset. The Nσ parameter in this case is set to 1σ.

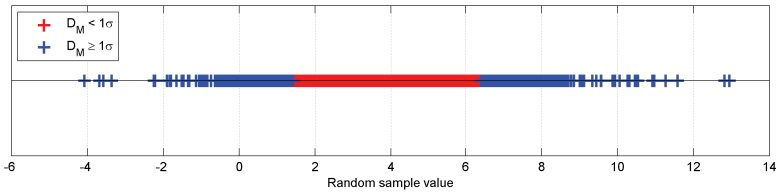

FIGURE 4.8: Univariate Gaussian distributed random samples classified by MD

Table 4.2 presents the description of the accuracy property by means of characteristics of the sample univariate dataset as provided by the MEF analysis depicted in Figure 4.8. LocAv for the univariate 1σ filter approaches the theoretical 68% when the deviation is normal distributed.

TABLE 4.2: MEF analysis of the univariate sample dataset

Characteristic	**Quantity**	**Value**	**Unit**
Trueness (Interval center)	Mean Value (μ)	3.92	m
Precision (Interval radius)	Standard Deviation (σ)	2.5	m
Location Availability	MEF (1σ)	69.10	%

For GNSS-based horizontal localisation system the deviation datasets are usually bivariate. In this case MEF leads to a Mahalanobis ellipse with constant distance Nσ that defined the boundary between reliable and unreliable measurements. Figure 4.9 shows a graphical representation of this kind of MEF applied to a bivariate deviation dataset. The additional descriptive provided by the MEF approach indicates for bivariate datasets, given by the centre, rotation angle and semi-radii of the ellipse.

In Figure 4.9 the centre of the ellipse represent the mean value of the deviation in both components, so its distance from the origin is the **trueness** of the dataset. The rotation angle in Figure 4.9 describes the direction of uncorrelated deviation error, and the semi-radii lengths are equivalent to the deviation root mean square (drms) in the two main perpendicular uncorrelated directions, describing the **precision** of the dataset.

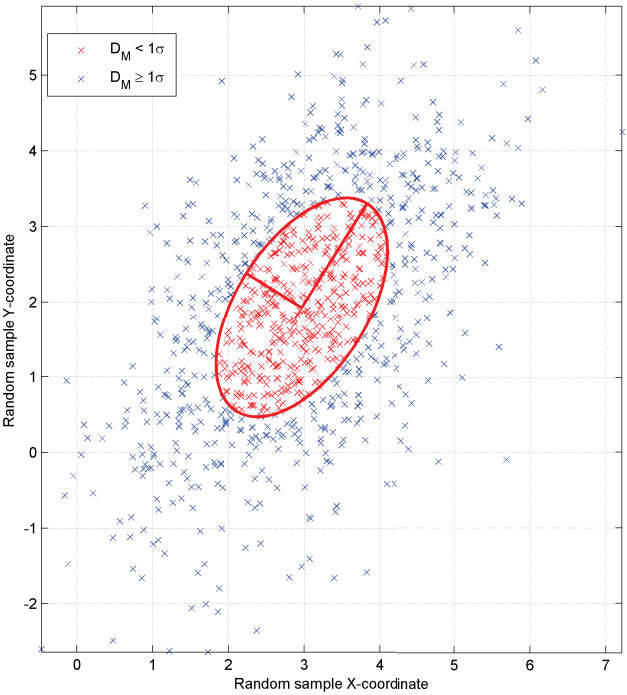

FIGURE 4.9: Bivariate Gaussian distributed random samples classified by MD

TABLE 4.3: MEF analysis of the bivariate sample dataset

Characteristic	**Quantity**	**Value**	**Unit**
Trueness (distance to center)	Mean Value (μ)	3.54	m
Trueness (X-coordinate)	Mean Value (X)(μ)	2.97	m
Trueness (Y-coordinate)	Mean Value (Y) (μ)	1.92	m
Precision (Semi-radius A)	Standard Deviation (A) (σ)	1.62	m
Precision (Semi-radius B)	Standard Deviation (B) (σ)	0.86	m
Inclination between semi-axis	Rotation angle	-32	^{o}
Location Availability	MEF (1σ)	40.80	%

Table 4.3 presents the summary description of the accuracy property by means of characteristics of the sample bivariate dataset as provided by the bivariate MEF analysis. LocAv for the bivariate 1σ filter approaches the theoretical 39% when the bivariate deviation is normal distributed.

Finally, when the height coordinate (Z-coordinate) is taken into consideration a three-dimensional localisation system can be achieved, resulting in trivariate datasets, where MEF approach leads to a 3-D Mahalanobis ellipsoid.

Figure 4.10 shows a graphical representation of the MEF approach behaviour applied to a trivariate deviation dataset. For trivariate datasets the MEF analysis results in the ellipsoid centre, two perpendicular main directions and three semi-radii lengths characterising the ellipsoid. Table 4.4 presents the main characteristics of the sample trivariate dataset as provided by the MEF analysis. **LocAv** for the trivariate 1σ filter approaches the theoretical 19% when the trivariate deviation is normal distributed.

TABLE 4.4: MEF analysis of the trivariate sample dataset

Characteristic	**Quantity**	**Value**	**Unit**
Trueness (distance to center)	Mean Value (μ)	3.57	m
Trueness (X-coordinate)	Mean Value (X)(μ)	2.94	m
Trueness (Y-coordinate)	Mean Value (Y) (μ)	1.82	m
Trueness (Z-coordinate)	Mean Value (Z) (μ)	0.86	m
Precision (Semi-radius A)	Standard Deviation (A) (σ)	0.95	m
Precision (Semi-radius B)	Standard Deviation (B) (σ)	1.73	m
Precision (Semi-radius C)	Standard Deviation (C) (σ)	3.71	m
Azimuth (first main direction)	Rotation angle	-20.55	^{o}
Inclination (first main direction)	Rotation angle	1.72	^{o}
Azimuth (second main direction)	Rotation angle	68.24	^{o}
Inclination (second main direction)	Rotation angle	-35.20	^{o}
Location Availability	MEF (1σ)	18.90	%

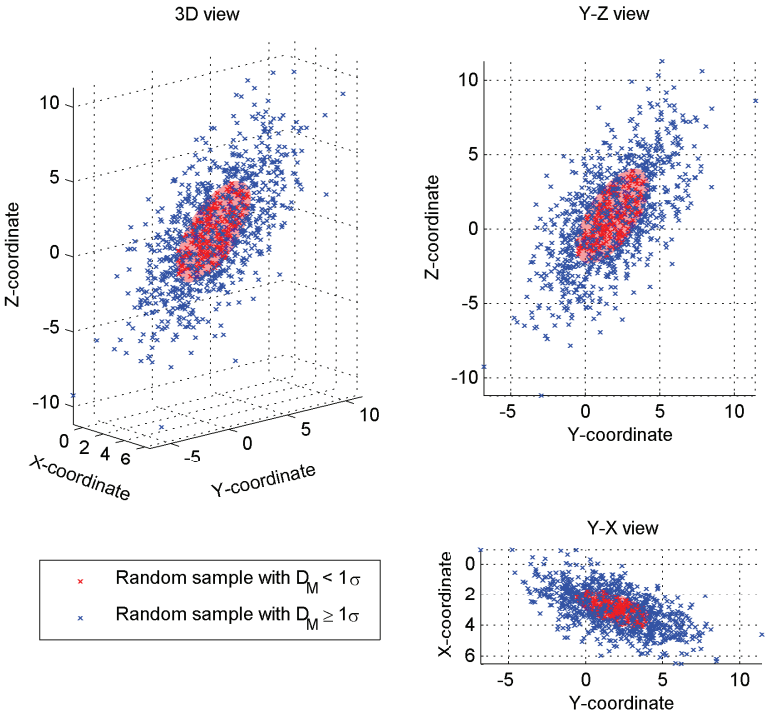

FIGURE 4.10: Trivariate Gaussian distributed random samples classified by DM

4.6 MEF for Statistical Quality Control

The statistical quality control (SCQ) methodology based on the developed MEF methodology by means of deviation evaluation is presented in this section.
Before presenting the results for the proposed MEF-SQC a revision of the classical SQC is presented and applied to static GNSS collected data, as follows:

1. SQC methodology by means of module deviation.
2. SQC methodology by means of easting-northing deviation.
3. MEF-based SQC methodology.

4.6.1 SQC Methodology with Module Deviation

In a first approach, a filter based in the lognormal distribution for the deviation module was analysed. The Upper Control Limit (UCL) and Lower Control Limit (LCL) for this approach are defined as:

$$UCL_M = e^{\mu_M + n\sigma * \sigma_M}$$
$$LCL_M = 0$$

where μ_M and σ_M are the parameters of the fitted lognormal distribution. From the static position measurement dataset presented in Chapter 5 for the Particle Filter Static Estimator, described in detail in [13] a fitting analysis for deviation data was performed, its results presented in Figure 4.11, where the lognormal distribution was identified as a suitable distribution for deviation module analysis, and the normal distribution was identified as a suitable distribution for separate easting and northing analysis.
The results of this approach are presented by means of a Quality Control Chart (QCC) and a Scatter-plot in Figure 4.12. The deviation module filtering approach provides limited description of the receiver behaviour, since the deviation direction is ignored.[3]

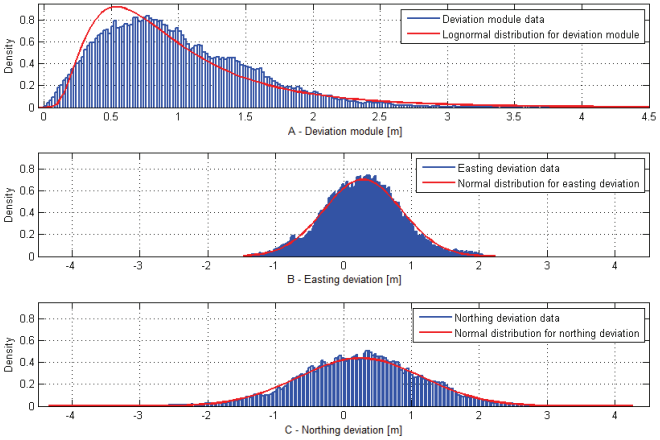

FIGURE 4.11: Fitted distributions for deviation analysis [16].

[3]Problems with lognormal fitting are presented in [40].

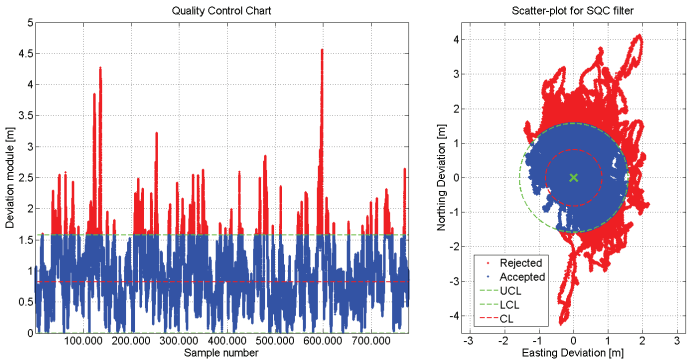

FIGURE 4.12: QCC and Scatter-plot for 1σ filter based deviation module [16].

Focused on the lognormal distribution fitting for the deviation module and the normal distribution fitting for the easting and northing deviations classical SQC approaches are presented in the following sections. Moreover, several filtering approaches based on the fitted distributions were analysed in [16, 21].

4.6.2 SQC methodology with easting-northing deviation

In a second approach, a filter based in the normal distribution for easting and northing deviation was analysed. This filtering approach consists of two passes, in each pass data from the deviation dataset is filtered out independently based in either the easting or northing deviation component. The UCL and LCL for either pass of this approach are:

$$UCL_E = \mu_E + n\sigma * \sigma_E$$
$$LCL_E = \mu_E - n\sigma * \sigma_E$$
$$UCL_N = \mu_N + n\sigma * \sigma_N$$
$$LCL_N = \mu_N - n\sigma * \sigma_N$$

where μ_E and σ_E are the parameters of the normal distribution fitted to the easting deviation component and μ_N and σ_N are the parameters of the normal distribution fitted to the northing deviation component.

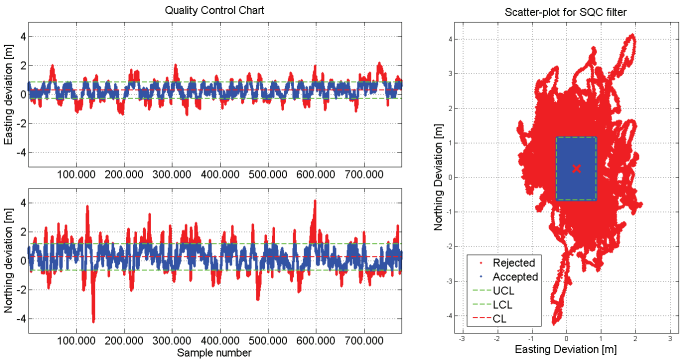

FIGURE 4.13: QCC and Scatter-plot for 1σ filter based on easting and northing [16].

The results of this approach are presented in Figure 4.13.

The independent easting-northing component filtering approach provides limited description of the GNSS receiver behaviour as the correlation between deviation components is not taken into consideration. On the other hand the Mahalanobis Ellipses Filter (MEF) approach developed in [16] proves to be the best filter for the receivers deviation datasets, according to the receivers behaviour and coinciding with the theorised ellipse, described in [96].

4.6.3 MEF-SQC methodology

The MEF approach provides a general approach to multivariate filter, where data is filtered based on the Mahalanobis distance of deviation samples with respect to the whole deviation dataset. The nσ filtering performed in this approach discriminates samples based on an elliptic boundary with Mahalanobis distance of magnitude n. The results of this approach are presented in Figure 4.14.

The MEF approach is homogenous despite the number of variables and takes into consideration the correlation between deviation components.

The Table 4.5 presents the results for the MEF-SQC deviation analysis. An exemplary 1σ LocAv is shown, and both A and B semi-radii are expressed in meters for easier understanding.

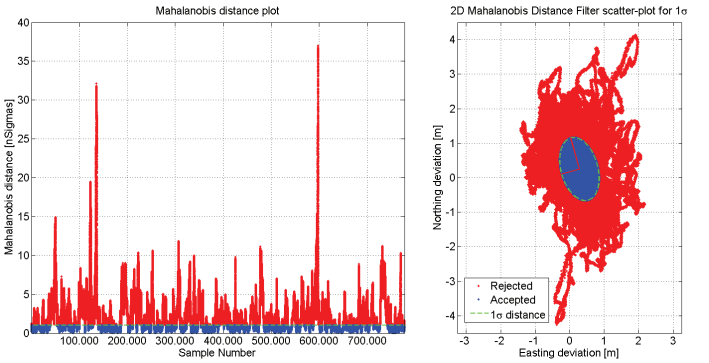

FIGURE 4.14: Mahalanobis distance plot and Scatter-plot for 1σ MEF filter [16].

4.6.4 Comparison of Results

Table 4.6 present the results of the comparison between the three analysed quality control trails for both SQC and MEF methodologies, and the effect of the application of the static PF-Estimator presented in Chapter 5.

SQC Module, SQC E/N and MEF results are presented by percentages values of the 1-σ outlier detection function, with and without PF-Estimator as reference.

The SQC Module filter test considers only the module of the deviation. It does not discriminate the deviation direction of the location samples, resulting in a high LocAv1σ that does not describe accurately the behaviour of the receiver.[4]

The SQC E/N filter test considers an independent evaluation of easting and northing deviations. It discriminates between two main deviation direction components, resulting in a lower LocAv1σ that seems to be a better representation of the receivers behaviour when there is a low correlation between easting and northing deviation.

TABLE 4.5: MEF-SQC deviation analysis

Ellipses Center [m]	**Easting**	0.2831
	Northing	0.2533
Semi-radii [m]	σ_A	0.529
	σ_B	0.9316
Rotation	[deg]	15.497
LocAv 1σ	[%]	**42.2172**

[4]Further distribution fittings should be tested.

TABLE 4.6: Summary of SQC approaches

SQC Module	**LocAv 1σ (with PF)**	***85.7486***
	LocAv 1σ (without PF)	86.0739
SQC E/N	**LocAv 1σ (with PF)**	***50.9816***
	LocAv 1σ (without PF)	49.452
MEF	**LocAv 1σ (with PF)**	***44.0213***
	LocAv 1σ (without PF)	42.2172

Finally the MEF test performs a simultaneous evaluation of easting and northing deviations, taking into account the deviation correlation. The MEF approach also works considering all possible deviation directions by means of the normalised Mahalanobis distance; resulting in a lower LocAv1σ that represents better than the SQC E/N filter the receivers behaviour.

For certification purposes a robust analysis of all involved tools should be presented. Since the MEF methodology is a promising new accuracy-based evaluation for a better representation of receivers' behaviour, more analyses based on robustness of this methodology should be studied.

4.7 MEF Methodology Summary

This chapter has presented the all new MEF methodology for deviation evaluation of GNSS data, developed as part of the present dissertation.

In this chapter the MEF approach has been evaluated based on an easting-northing coordinate system for static position measurements.

The described MEF approach can be also applied to a Tangential-Perpendicular coordinate system for dynamic position measurements, presenting significant advantages for deviation interpretation.

This methodology will be used in Chapter 6 for part of the learning stage of the AI-based tool for GNSS accuracy validation, as well as in the prototype constructed and tested in Chapter 7 and Chapter 8.

Chapter 5

Particle Filter Estimator for GNSS-Receivers

"Satellite, I'm watching you. I'm one step ahead."

Trent Reznor

The usage of PF-based techniques for location estimation presented in this chapter are an important part of the developed intelligent GNSS-based localisation system.

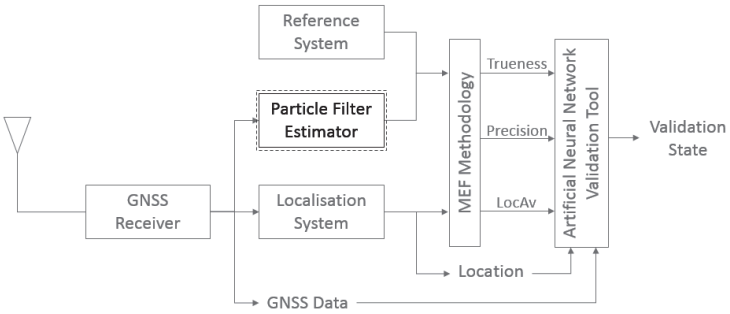

FIGURE 5.1: Graphical description of chapter 5: Particle Filter Estimator

5.1 Particle Filter application introduction

As presented in Chapter 2, Section 2.5.5, the Particle Filter (PF) Method is a sequential Monte Carlo (SMC) technique for the solution of the state estimation problem.[1]
The so-called Sequential Importance Sampling (SIS) algorithm for PF includes a resampling step at each instant, as described in detail in references [74]. The SIS algorithm makes use of an importance density, which is a density proposed to represent another one that cannot be exactly computed. Then, samples are drawn from the importance density instead of the actual density. Let $\left\{x_{0:k}^{i}, i = 0, \cdots, N\right\}$ be the particles with associated weights $\{w_k^i, i = 0, \cdots, N\}$ and $x_{0:k} = \{x_j, j = 0, \cdots, k\}$ be the set of all states up to t_k, where $k < N$ and N is the number of particles. The weights are normalized so that $\sum_{i=1}^{N} w_k^i = 1$. Then, the posterior density at t_k can be discretely approximated by:

$$\pi(x_{0:k} \mid z_{1:k}) \approx \sum_{i=1}^{N} w_k^i \delta(x_{0:k} - x_{0:k}^i) \tag{5.1}$$

where $\delta()$ is the Dirac delta function.
Also, taking into consideration the assumptions from [70] expressed for the "evolution-observation model" from Chapter 2:

1. The sequence x_k for $k = 1, 2, \ldots$, is a Markovian process:

$$\pi(x_k \mid x_0, x_1, \cdots, x_{k-1}) = \pi(x_k \mid x_{k-1}) \tag{5.2}$$

2. The sequence z_k for $k = 1, 2, \ldots$, is a Markovian process from the history of x_k:

$$\pi(z_k \mid x_0, x_1, \cdots, x_k) = \pi(z_k \mid x_k) \tag{5.3}$$

3. The sequence x_k depends only on its own history past observations:

$$\pi(x_k \mid x_{k-1}, z_{1:k-1}) = \pi(x_k \mid x_{k-1}) \tag{5.4}$$

where $\pi(a \mid b)$ denotes the conditional probability of a when b is given.

[1] Since results always depend on the dataset, for certification purposes reproducibility must be achieved.

Using the hypotheses from Equations 5.2 and 5.4, the posterior density from Equation 5.1 can be written as:

$$\pi(x_k \mid z_{1:k}) \approx \sum_{i=1}^{N} w_k^i \delta(x_k - x_k^i) \tag{5.5}$$

A common problem with the SIS Particle Filter is the degeneracy phenomenon, where after a few states all but one particle will have negligible weight [75].

This degeneracy implies that a large computational effort is devoted to updating particles whose contribution to the approximation of the posterior density function is almost zero.

This problem can be overcome by tuning the number of particles, or more efficiently by appropriately selecting the importance density as the prior density $\pi(x_k \mid x_{k-1}^i)$. In addition, the use of the resampling technique is recommended to avoid the degeneracy of the particles [125].

Resampling involves a mapping of the random measure $\left\{x_k^i, w_k^i\right\}$ into a random measure $\left\{x_k^{i*}, N^{-1}\right\}$ with uniform weights.

It can be performed if the number of effective particles with large weights falls below a certain threshold number.

Alternatively, resampling can also be applied indistinctively at every instant t_k, as in the Sampling Importance Resampling (SIR) algorithm described in [74] and illustrated by Figure 5.2.

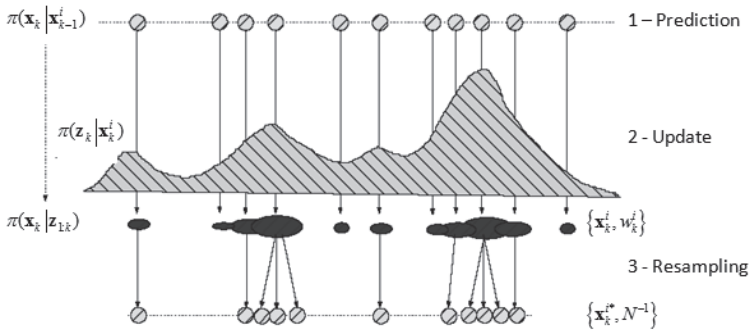

FIGURE 5.2: Representation of the Sampling Importance Resampling (SIR) algorithm of the Particle filter [69]

Such algorithm can be summarized in the following steps, as applied to the system evolution from t_{k-1} to t_k [18]:

Step 1. For $i = 1, \ldots, N$ draw new particles x_k^i from the prior density $\pi(x_k \mid x_{k-1}^i)$ and then use the likelihood density to calculate the correspondent weights $w_k^i = \pi(z_k \mid x_k^i)$.

Step 2. Calculate the total weight $T_w = \sum_{i=1}^{N} w_k^i$ and then normalise the particle weights, that is, for $i = 1, \ldots, N$ let $w_k^i = T_w^{-1} w_k^i$.

Step 3. Resample the particles as follows:

Step 3.1. Construct the Cumulative Sum of Weights (CSW) by computing $c_i = c_{i-1} + w_k^i$ for $i = 1, \ldots, N$, with $c_0 = 0$.

Step 3.2. Let $i = 1$ and draw a starting point u_1 from the uniform distribution $U[0, N^{-1}]$.

Step 3.3. For $j = 1, \ldots, N$

- Move along the CSW by making $u_j = u_1 + N^{-1}(j-1)$.
- While $u_j > c_i$ make $i = i + 1$.
- Assign samples $x_k^j = x_k^i$.
- Assign weights $w_k^j = N^{-1}$.

This resampling step reduces the effects of the degeneracy problem, but it may lead to a loss of diversity, making the resulting sample contain many repeated particles. The problem known as "sample impoverishment" can be severe in the case of small process noise, where all particles collapse to a single particle within few instants t_k [67].
Another significant disadvantage of the PF approach is related to the large computational cost due to the SMC methods, which may not allow its application to complex physical problems.
More involved algorithms have been developed, resulting in reductions of the number of particles required for appropriate representation of the posterior density, as well as resulting in the reduction of associated computational times. Algorithms capable of simultaneously estimating state variables and parameters have been developed in [74, 75].

5.1.1 Particle filter based map matching techniques

Map-matching algorithms integrate the localisation data provided by GNSS with spatial road network data (also called "digital map[2]") to identify the correct link (or track) on which a vehicle is traveling and to determine the location of a vehicle within the link (or track). In the railway domain the same integration can be performed by means of a "digital trap map" to identify the location within the tracks.
A map-matching algorithm can be the key component of the data fusion to improve the performance of a localisation systems that support the navigation function of intelligent transport systems (ITS).
The required horizontal positioning "accuracy" of such ITS applications is in the range of 1 m to 40 m (95%) with relatively stringent requirements placed on system availability, reliability and integrity (as the AARI-based approach presented in Chapter 3).
A number of map-matching algorithms have been developed using different techniques such as topological analysis of spatial road network data [126], probabilistic theory [127], Bayesian filtering [128], Fuzzy Logic (FL) [129], and Belief Theory (BT) [130].
The goal of map-matching techniques is to exploit prior information contained in road or railway networks.
However, incorporating digital map information within the conventional KF framework is not easy, because this constraint leads to highly non-Gaussian posterior densities that are difficult to represent accurately using conventional techniques.
In [131] a numerical approach based on PF was proposed, since the PF approach presents no restrictions regarding non-linearity of models and noise distribution the velocity and heading measurement errors can be accurately modelled.
The advantages of the PF approach for map-matching application are:

- PF approach provides a natural way for road map information to be incorporated into vehicle position estimation.
- PF approach is capable of capturing multi-modal distributions.

The PF approach proposed in [131] recursively estimates the position of the vehicle given a set of measurements.

[2]Road/track matching by the perpendicularity of the road/track to match presents a permanent error due to the precision of the digital map

There the state vector of the model consists on the vehicle's Northing and Easting coordinates: $x_k = [P_k^N \ P_k^E]^T$, with the subscript k corresponding to the time instant t_k. Also it is assumed that the vehicle is moving on known roads (or railway track), being part a known digital map database.

As proposed in [132] a general description of the roads (or tracks) by an implicit non-linear function $\rho^h(x)$ can be:

$$R^h = \left\{ x : \rho^h(x) = 0 \right\}, h = 1, M \tag{5.6}$$

For the purpose of map-aided estimation, the road or railway network must be approximated by a set of road segments $R_{k,k+1}$, each of which is a straight line between the nodes ξ_k, ξ_{k+1} that satisfy the Equation 5.6.

It is also assumed that the state can be described by partially observable discrete-time Markov chains. And furthermore, it is assumed that the state x_k depends on the previous state x_{k-1} according to the probabilistic law $\pi(x_k|x_{k-1})$.

This problem can be stated as estimation of the sequence of states $x_{0:k} = \{x_0, \ldots, x_k\}$ given the series of observation $z_{1:k} = \{z_1, \ldots, z_k\}$ subject to the motion model $\pi(x_k|x_{k-1})$, within the measurement model $\pi(z_k|x_k)$ and the constraints on the state vector given in form of the road or railway network.

The prior probability at t_0, $\pi(x_0)$ is assumed to be known and the goal is to find the "best" trajectory in terms of minimum mean-square error (MMSE) criteria.

This problem can be solved within the framework of Bayesian estimation theory from [132]. Although the resulting recursion cannot be analytically computed, it can be calculated using the SMC approximation.

The proposed transitional prior is based on the dead-reckoning Equations:

$$x_{k+1} = \begin{bmatrix} P_{k+1}^N \\ P_{k+1}^E \end{bmatrix} = X_k + V_k T_k \begin{bmatrix} cos\psi_k \\ sin\psi_k \end{bmatrix} \tag{5.7}$$

where V_k is the vehicle speed, ψ_k is the vehicle heading and T_k is the sampling period for the instant t_k.

The speed and heading measurement in Equation 5.7 can be obtained from on board sensors, whose characteristic measurement error distribution is taken into consideration during the sequential Monte Carlo simulation.

The proposed map-matching technique has two operational modes:

1. When the vehicle is moving along a given line (or track) in the road/track map.
2. When the vehicle is turning and it can be located by the system between two adjacent lines (or track) in the road/track map.

Switching between these two modes is performed based on the analysis of the vehicle's heading rate data from the sensors.
During the first operation mode the particles are propagated using only speed information from the on board speed sensors (odometer, GNSS-Receiver) and independent sensor (Doppler sensor).
The $i-th$ particle heading is assumed to be the same as the heading of the road segment where this particle is located, which is a known part from the map:

$$\psi_k^{(i)} = \psi_{seg}^{(i)} \tag{5.8}$$

This propagation model can guarantee that the particles will always stay on the road. However, different particles can move on different road segments. The road segment with the highest probability (with more particles on it) is selected as the most likely road segment where vehicle is located.
If the particles are moving on the correct road segment then estimated position cross-track error can be reduced substantially by applying a simple perpendicular projection of the position fixes onto the selected line.
The estimated vehicle location can also be calculated as the weighted average of all the particle coordinates from this segment.
During the second operational mode when the vehicle is turning, its heading and speed are required; the propagation model can be described by the dead-reckoning Equations 5.7, where the vehicle heading ψ_k can be measured by a gyroscope, a GNSS-Receiver, or a differential heading odometer.
The road (or track) segment identification (map-matching technique) is not performed at this step. Only a suitable line (or track) is selected to be processed in the first operation mode. Figure 5.3 presents the characteristic particle trajectories during a vehicle turn for the second operational mode, as presented in [131].

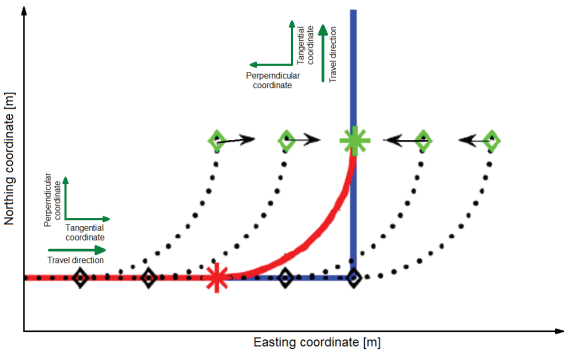

FIGURE 5.3: Characteristic particle trajectories during a vehicle turn [131]

There are some important features of these trajectories that help to reduce the along-track error of vehicle location estimation after the turn:

- The vehicle and the particles start turning at the same time since the turn is sensed by some heading-rate measuring device (e.g., gyroscope).
- The vehicle and the particles stop turning at the same time.
- If the gyroscope and odometer are used as dead-reckoning sensors the accumulation of position errors during the turn is small. Therefore all these trajectories are nearly parallel and can be obtained by parallel translation of the true trajectory along the horizontal road line or railway track.
- In ideal case, when propagation of particles during the turn is error free, the particles at the end of the turn will be on the same line, parallel to the road line (or railway track) where they started the turn. Applying perpendicular projection of the particles position fixes onto the selected line (or track) will eliminate the along-track error of the estimated vehicle position accumulated before the turn.

This approach for reducing the along-track error is also valid in the case when the turn angle is different from ninety degrees. Therefore, it works for all kinds of curved roads, as well as railway track curves.
However, due to the position errors accumulated during the turn, there will be some residual along-track error in the estimated vehicle location after the turn.

The magnitude of this error depends on the quality of dead-reckoning sensors and curvature of the turn. For road with small curvature, the reduction of along-track error is negligible.

5.2 Particle Filter Static Estimator

The first proposed approach to position filtering is based on a particle filter that takes into consideration a static evolution model, the vehicle in this model is considered to be motionless. In this approach Easting and Nothing components of the position are treated and filtered independently, leading to two filters each one with the following position evolution equation:

$$x_{k+1} = E_{k+1} = x_k + v_k \tag{5.9}$$

where E represents the evolution model estimated position.
The v_k term in Equation 5.9 is the noise component for the position evolution, this noise component models a random walk process [133] that allows for small changes of the vehicle position to be accounted in the evolution model.

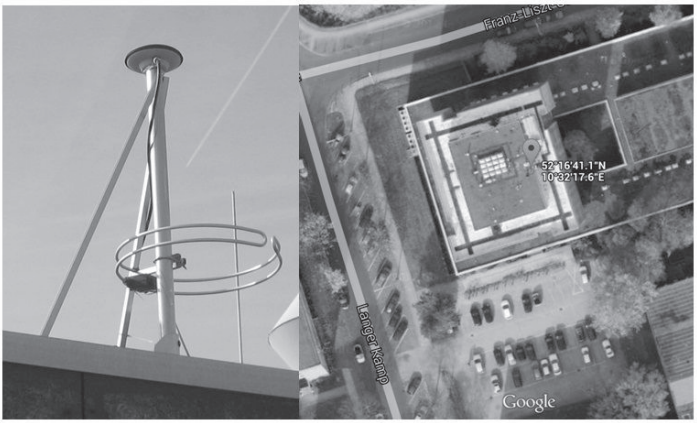

FIGURE 5.4: Installed equipment and Google view reference. [21]

The observation model for this approach is based on either the Easting or Northing position component as measured by the GNSS-R. The observation is modeled using the following equation:

$$z_k = O_{k+1} = x_k + n_k \tag{5.10}$$

where O represents the observed position. The n_k term in Equation 5.10 is the noise component for the observation and is based on the static accuracy of the GNSS-R.

The performance of this proposed filter was evaluated based on the static position measurement from 10 days, collected with a 1 Hz frequency in the period between 19.05.2011 and 01.06.2011, each resulting in dataset of 86400 locations, as presented in [21].

The positions were measured with a receiver u-blox EVU-6H with EGNOS turn on, assembled with the antenna Novatel GPS-702-GG and the location reference was determined geodetically on the roof of the Institut für Verkehrssicherheit und Automatisierungstechnik in Langer Kamp 8, Braunschweig, Germany. Figure 5.4 presents the picture of the installed equipment and the Google Maps reference.

All 10 datasets present similar characteristics: Each one has 86400 samples over a period of 24 hours, with a number of visible satellites between 7 and 12 (average of 10) and a Horizontal Dilution of Precision (HDOP) value between 0.69 and 1.51 (average of 0.91). According to [134], these characteristics describe the scenario as ideal. Table 5.1 shows the statistical analysis for the 10 datasets deviation analysis, referred to the PF-Estimator reference. The tenth dataset is a global dataset composed from the other 9 datasets and 19.05.2011, used for PF adaptation period, is not considerate for the rest of the analysis.

Table 5.1: Statistical analysis of the collected GNSS static datasets

Dataset date	**Trueness Module [cm]**	**Deviation Module Lognormal Fitting**		**Easting Deviation Normal Fitting**		**Northing Deviation Normal Fitting**	
		μ_M	σ_M	μ_E **[m]**	σ_E **[m]**	μ_N **[m]**	σ_N **[m]**
23.05	51.1417	-0.1591	0.6491	0.3124	0.5140	0.4049	0.8691
24.05	37.4525	-0.0512	0.6771	0.0763	0.5310	0.3667	1.1880
25.05	44.5379	-0.1277	0.6587	0.1331	0.6841	0.4250	0.8676
26.05	51.8165	-0.1668	0.5992	0.2969	0.5940	0.4247	0.7660
28.05	41.5153	-0.2046	0.6285	0.1621	0.4599	0.3822	0.8786
29.05	30.8001	-0.2979	0.6666	0.3069	0.4852	0.0256	0.9118
30.05	31.3785	-0.2955	0.7471	0.2811	0.5390	0.0256	1.0128
31.05	33.0559	-0.3721	0.5855	0.2459	0.4700	0.2210	0.6875
01.06	74.1256	-0.0919	0.5743	0.7331	0.5342	-0.1099	0.7181
Global	***37.9860***	***-0.1963***	***0.6526***	***0.2831***	***0.5673***	***0.2533***	***0.9088***

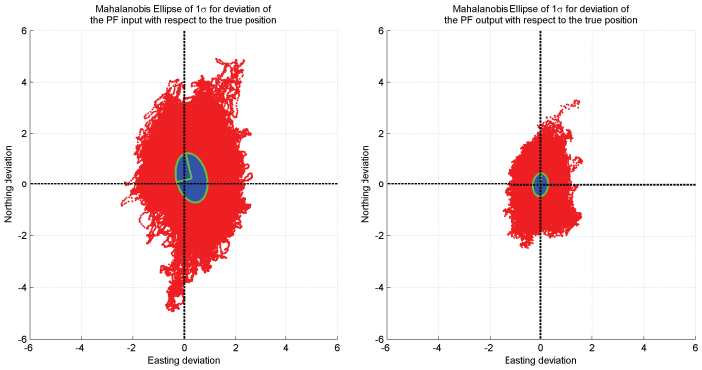

FIGURE 5.5: MEF of PF input and output for static sample

The developed PF aims to the position estimation of the receiver. In order to provide the PF a probability distribution, the measurements from the first day dataset were used to find the a stable weight distribution for the particles in the PF. Further analysis is performed by means of the MEF filter.

Figure 5.5 presents sample deviation clouds with 1σ Mahalanobis ellipses for both the filter input and the output estimated positions. Table 5.2 compares the resulting MEF parameters for both cases. From the results presented in Table 5.2 it is concluded that the filtering process provides both improved precision and accuracy for the estimated positions, as the semi-radii from the MEF analysis are smaller and the center of the ellipses is nearer to the origin for the filter output. This approach is a feasible solution for position estimation when the GNSS receiver does not move or moves at a very slow speed. A more general approach with better adaptation for dynamic positioning scenarios is presented in the next section.

TABLE 5.2: MEF parameters for deviation results of the input and filtered data

Parameter		**PF input**	**PF output**
Ellipses Center [m]	Easting	0.2830	0
	Northing	0.2533	0
Semi-radii [m]	σ_A	0.5950	0.2933
	σ_B	0.9976	0.4488
Rotation	[deg]	12.93	-5.55
LocAv 1σ	[%]	42.22%	44.56%

5.3 Particle Filter Dynamic Estimator

The second proposed approach to position filtering is based on a particle filter that takes into consideration a dynamic evolution model, with speed and heading control inputs. In this model the Easting and Nothing components of the position are processed simultaneously, leading to a bi-dimensional state variable with following position time-discrete evolution equation:

$$x_{k+1} = \begin{bmatrix} E^N_{k+1} \\ E^E_{k+1} \end{bmatrix} = x_k + \begin{bmatrix} cos\psi_k \\ sin\psi_k \end{bmatrix} vel_k \Delta T + v_k \tag{5.11}$$

where E is the evolution model estimated position and ΔT its sampling period.
In Equation 5.11 the vel_k term represent the measured speed of the vehicle and the ψ_k term represents the measured heading of the vehicle, both considered unpredictable control inputs. The v_k term in Equation 5.11 is the noise component for the position evolution, and represents the error in the position model caused by the uncertainties in the measurement of speed and heading.
The observation model for this approach is based on the horizontal position measured by the GNSS receiver. The observation is modeled using the following equation:

$$z_k = \begin{bmatrix} O^N_{k+1} \\ O^E_{k+1} \end{bmatrix} = x_k + n_k \tag{5.12}$$

where O represents the observed position.
The n_k term in Equation 5.12 is the noise component for the observation and is based on the static accuracy of the GNSS-R.
The performance of this proposed filter was evaluated based on simulated dynamic position measurements of a vehicle traveling along a defined path. The simulation dataset is composed of 1367 samples with a sampling rate of 1 Hz , and includes simulated values for position, speed, and heading. Additionally, simulated measurements with a defined level of noise are included in the dataset. In this simulation the vehicle follows a realistic path based on the scheduled route of Brunswick City tram line M3, in the segment between the stations Donaustraße and Bindestraße. Figure 5.6 shows the traveling path of the simulated vehicle.

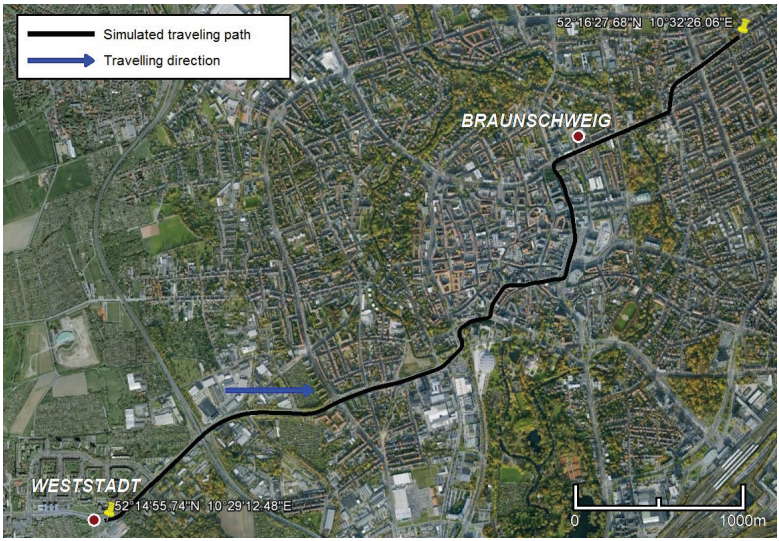

FIGURE 5.6: Google view of the simulated traveling path

An additive white Gaussian noise (AWGN) component is added to the simulated position measurement, taking into consideration 10 meters dynamic precision within a 95% confidence level, as presented by the US Navy in [135].

Moreover, another AWGN component is added to the simulated speed and heading measurements based on measurement error specifications for a u-blox NEO-6 GPS module presented in [136].

The simulated measurements from the described dataset are used as inputs for the proposed filter in order to calculate an estimate for the true position.

Figure 5.7 presents plots for significant segments of the simulation path, including the true position, the simulated position measurements and the position estimated by the proposed filter.

Figure 5.8 compares northing and easting deviation components of both the simulated measurement and the filter estimate regarding the true position.

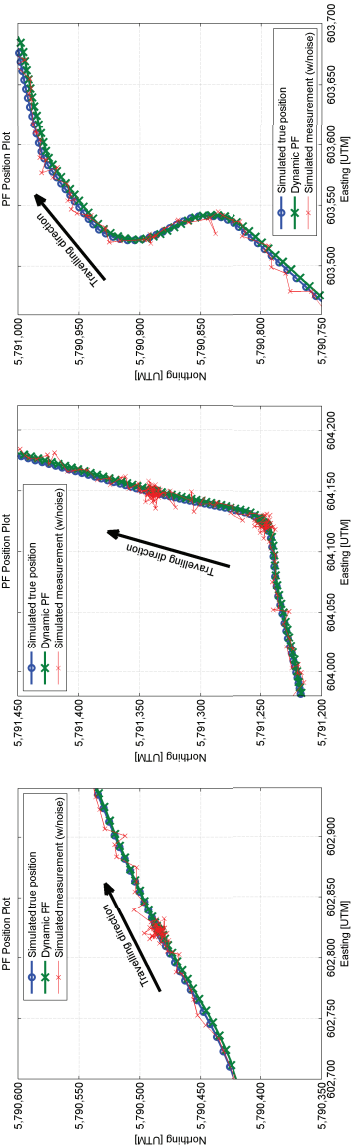

FIGURE 5.7: Position plot of the filter's input and output data

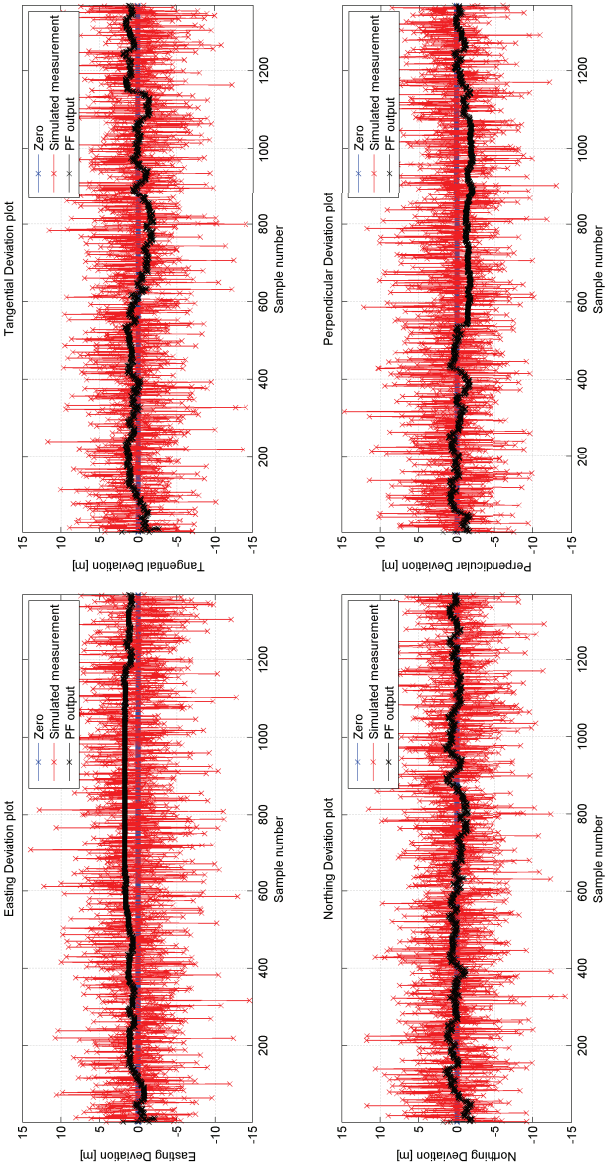

FIGURE 5.8: Deviation plot of the filter's input and output data

TABLE 5.3: MEF parameters for deviation results of the input and filtered data

Parameter		**PF input**	**PF output**
Ellipses Center [m]	Easting	0.0637	1.1937
	Northing	0.0039	0.1101
Semi-radii [m]	σ_A	4.1419	0.6550
	σ_B	4.1836	0.6824
Rotation	[deg]	-80.91	-31.97
LocAv 1σ	[%]	40.60%	47.70%

Further analysis is performed by means of the MEF filter. Table 5.3 compares the resulting MEF parameters for both cases.

From the results presented in Table 5.3 it is concluded that the filtering process provides improved precision for the estimated positions, as the semi-radii from the MEF analysis are smaller for the filter output. However the accuracy of the estimated positions deteriorates, as the ellipses center is farther from the origin.[3]

Figure 5.11 presents sample deviation clouds with 1σ Mahalanobis ellipses for the filter input, the output estimated positions, and the output aided by map-matching technique.

5.4 Particle Filter Dynamic Estimator with Map-matching

The third proposed approach to position filtering is based on a particle filter that takes into consideration a dynamic evolution model with speed control input and a constraining digital map.

The evolution model has been optimized for the case of a single-direction path where no branching is possible. The model assumes that the vehicle can only be located over the digital map. In this simplified model the position of the vehicle is described by a one-dimensional state variable, which is predicted with the following time-discrete evolution equation:

$$x_{k+1} = E_{k+1} = x_k + vel_k \Delta T + v_k \tag{5.13}$$

where E represents the evolution model estimated position and measures the distance along the digital map, from its starting point to the vehicle's position.

In Equation 5.13 the vel_k term represents the measured speed of the vehicle considered an unpredictable control input.

[3]This is due to the speed noise addition, producing a bias for the impossibility of negative speed values.

The v_k term in Equation 5.13 is the noise component for the position evolution, and represents the error in the position model caused by the uncertainties in the measurement of speed.

The observation model for this approach is based on the horizontal position measured by the GNSS receiver. The observation is modeled using the following equation:

$$z_k = \begin{bmatrix} O^N_{k+1} \\ O^E_{k+1} \end{bmatrix} = h(x_k) + n_k \tag{5.14}$$

where O represents the observed horizontal position.

The h function in Equation 5.14 is a time-independent non-linear function that relates the one-dimensional vehicle's position along the digital map with a bidimensional horizontal position in the GNSS coordinate system.

Also the n_k term in Equation 5.14 represents the noise component for the observation and is based on the static accuracy of the GNSS-R.

The evolution and observation models used in this approach do not take into consideration measured heading, as the heading is inferred from the digital map geometry.

A possible improvement for this approach could take into consideration the observed heading to achieve a better position estimation, or to enable the possibility of using digital maps with branching paths. The latter possible improvement has been analysed in [131].

The performance of this proposed filter was evaluated based on the simulated dynamic position measurements presented in the previous section.

Figure 5.9 presents plots significant segments of the simulation path, including the true position, the simulated position measurements and the position estimated by the proposed filter.

Figure 5.10 compares northing and easting deviation components of both the simulated measurement and the filter estimate with respect to the true position.

Further analysis is performed by means of the MEF filter.

Figure 5.11 presents sample deviation clouds with 1σ Mahalanobis ellipses for both the filter input and the output estimated positions.

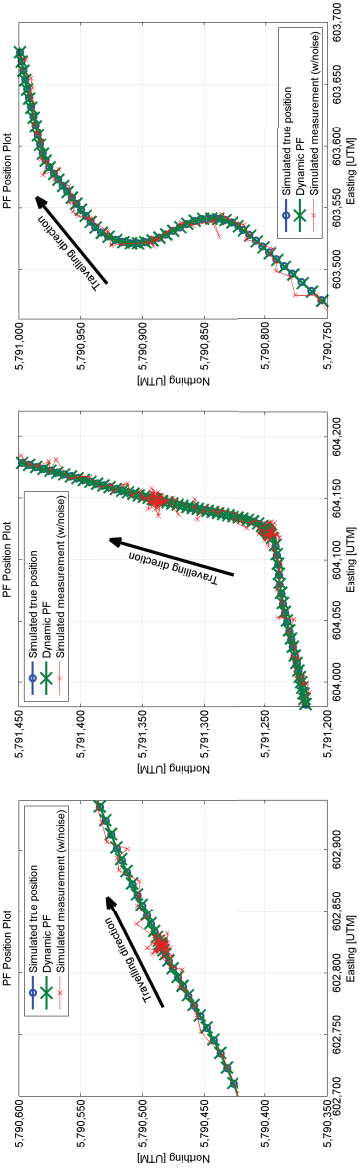

FIGURE 5.9: Position plot of the filter's input and output data

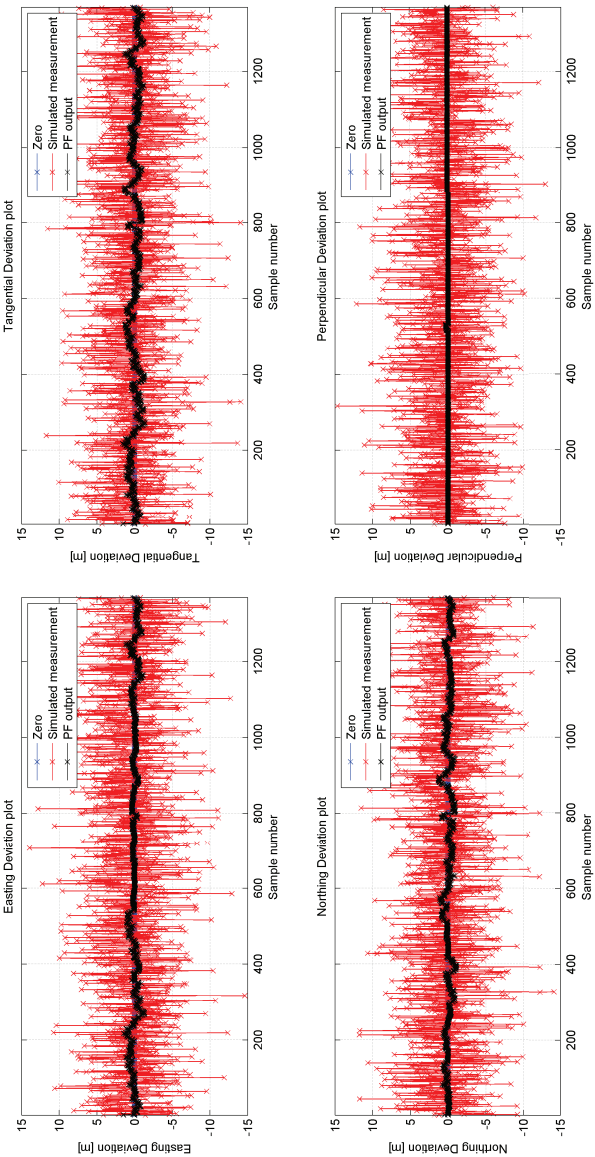

FIGURE 5.10: Deviation plot of the filter's input and output data

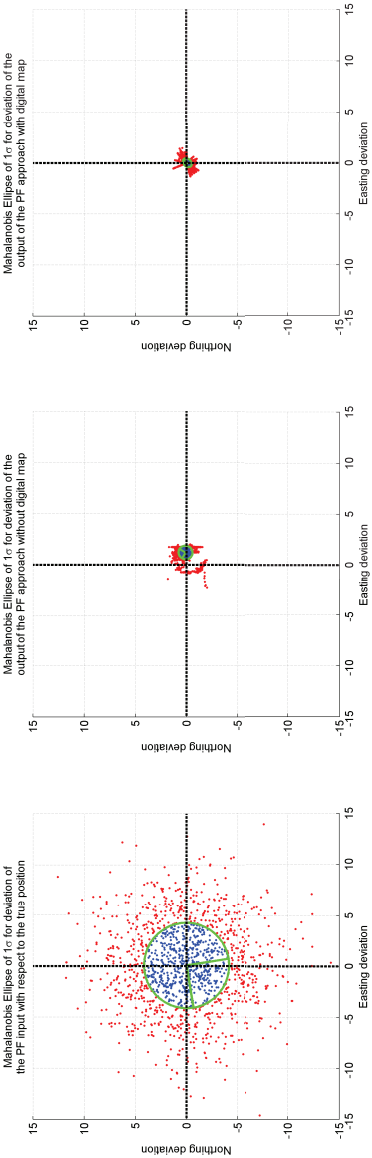

FIGURE 5.11: MEF plot of the filter's input and output data

TABLE 5.4: MEF parameters for deviation results of the input and filtered data

Parameter		**PF input**	**PF output**
Ellipses Center [m]	Easting	0.0637	0.0331
	Northing	0.0039	-0.0625
Semi-radii [m]	σ_A	4.1419	0.3554
	σ_B	4.1836	0.4867
Rotation	[deg]	-80.91	-44.09
LocAv 1σ	[%]	40.60%	44.99%

Table 5.4 compares the resulting MEF parameters for both cases.

From the results presented in Table 5.4 it is concluded that the filtering process provides both improved trueness and precision (general improvement of the accuracy) for the estimated positions, as the semi-radii from the MEF analysis are smaller and the center of the ellipses is nearer to the origin for the filter output. Figure 5.12 presents MEF plots comparing the results of the dynamic filtering approach without digital map[4], and the dynamic filtering approach with digital map[5].

5.5 Particle Filter Estimator summary

This chapter has presented the PF-based applications for location estimation.

Theoretical background as well as static and dynamic applications for PF approaches were shown and evaluated. And using them significant results have been achieved.

The MEF analysis parameters presented in Table 5.5 show that the filtering approach with digital map presents improved precision and accuracy for the position estimates.

As a conclusion for the presented approaches a PF-based dynamic location estimator aided with map-matching technique was the selected methodology for the developed intelligent GNSS-based localisation system presented in Chapter 7.

TABLE 5.5: MEF parameters for deviation results of the dynamic filtering approaches

Parameter		**without digital map**	**with digital map**
Ellipses Center [m]	Easting	1.1937	0.0331
	Northing	0.1101	-0.0625
Semi-radii [m]	σ_A	0.6550	0.3554
	σ_B	0.6824	0.4867
Rotation	[deg]	-31.97	-44.09
LocAv 1σ	[%]	47.70%	44.99%

[4]Horizontal deviation lines might be caused by a biased orientation during zero speed instants.

[5]The converging deviation lines might be caused due to the most amount of present errors are tangential and projected on the segmented digital track map.

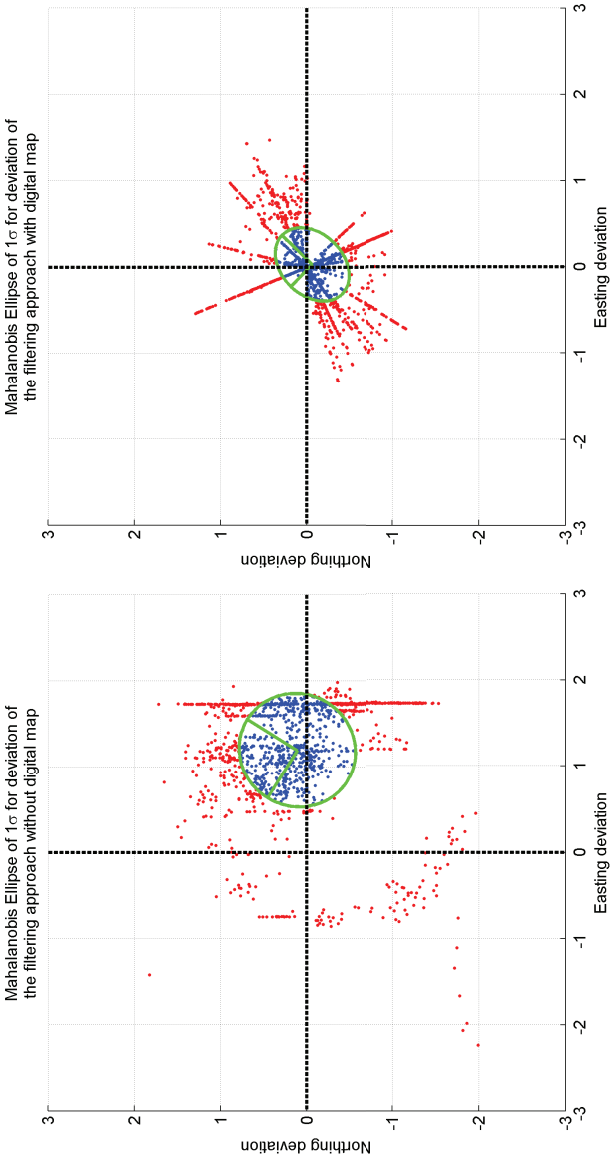

FIGURE 5.12: MEF plot of the proposed dynamic filtering approaches

Chapter 6

Validation Tool by means of Artificial Neural Network

"Let us assume that the persistence or repetition of a reverberatory activity (or "trace") tends to induce lasting cellular changes that add to its stability. When an axon of cell A is near enough to excite a cell B and repeatedly or persistently takes part in firing it, some growth process or metabolic change takes place in one or both cells such that A's efficiency, as one of the cells firing B, is increased."

Hebb's postulate, Donald Hebb, The Organization of Behavior.

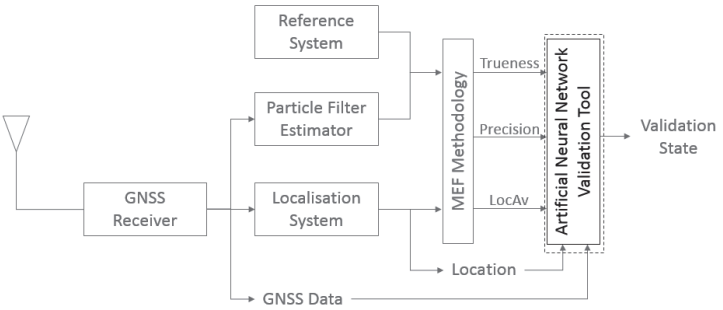

FIGURE 6.1: Graphical description of chapter 6: ANN Validation Tool

6.1 Introduction to AI-based approaches for GNSS quality validation tools

This chapter presents the bases for the development of an intelligent accuracy-based quality function (iAQF) to implement as part of a AI-based validation tool for GNSS-based localisation systems. The present method GNSS-Receivers' validation for extended accuracy evaluation of dynamic measurement of GNSS data presented in Chapter 4 is applied as iAQF, consisting on a set of ANN models with quantifiable measurements from GNSS-Receivers' data as inputs and post-processed accuracy-based deviation analysis results as targets. The applied deviation evaluation by means of MEF is explained in detailed in Chapter 4.

The basic ANN models used in this work are multilayer feed-forward neural networks. In a first step the feed-forward ANN models with log-sigmoid activated hidden layer and a pure-linear activated output layer are used in the quantification approximation stage, finding the quantifiable influences of GNSS data inputs to define their relevance in the trueness and precision resulting from the deviation analysis.

Then a separated set of feed-forward ANN models are used for the qualitative estimation as general function approximators to estimate the produced accuracy-based target functions, given the uncertainty measurement information by means of trueness and precision produced by the MEF methodology presented in Chapter 4.

This introductory section presents a brief description of the used ANN models for the developed iAQF validation tool.

The developed accuracy-based quality function (AQF) consists on the combination of quantifiable measurements for GNSS receivers' data and post processed accuracy-based deviation analysis, weighted by their importance to describe with numerical results the estimated GNSS quality of dynamic localisation systems. This is called the "white-box" AQF approach in [10].

The developed "intelligent" accuracy-based quality function (iAQF), on the other hand, consists on the combination of quantifiable measurements for GNSS receivers' data and post-processed accuracy-based deviation analysis for teaching AI-based systems to describe with numerical results the estimated GNSS quality of dynamic localisation systems. The resulting AI-based validation tools is therefore referred as the iAQF approach, or "black-box" AQF approach in [10], in contrast to the white-box AQF approach.

The AI-based certification process proposed in Chapter 3 can be achieved by the combination of both AQF and iAQF approaches to provide an attestation by means of complex decision-making machines. Due to this combination the AI-based certification proposal is called the "grey-box" AQF approach in [10].

6.2 Basic Artificial Neural Networks Models

There are two types of ANN models used for the development of AI-based validation tools. The "white-box" AQF approach in the present dissertation is a quantitative approximation that ponders the significant GNSS-Receivers' variables into numerical weights, regarding an accuracy-based GNSS Quality description. Once these variables and their related quantities have been established, the "grey-box" AQF approach can be applied; described as a qualitative approximation that describes accuracy as uncertainty measurements by means of trueness (as the magnitude analysis of the deviation) and precision (as the Mahalanobis Distance analysis of the calculated deviation dataset).
Both trueness and precision of the GNSS-Receiver are affected by different sources of error, as for example the current GNSS constellation. Therefore to correctly determine the used inputs to characterise the current GNSS constellation, all available GNSS information provided by the GNSS-Receiver must be quantified, regarding accuracy sources of error.

Table 6.1: Considered GNSS-Receiver variables

Input	**Description**
Gauss Krueger Easting	The Easting position provided by the receiver in GK coordinates.
Gauss Krueger Northing	The Northing position provided by the receiver in GK coordinates.
Number of Satellites in view	Satellites in direct line of sight from the current position.
Number of Used Satellites	Number of satellites used in the position solution.
HDOP	Horizontal Dilution of Precision.
Track Speed	The travel speed reported by the receiver in kilometres per hour.
Geometric mean of SNR	The geometric mean of the SNR from all the used satellites, in decibels.

6.3 ANN for accuracy-based Quantitative Approach

Proposed sources of error in GNSS data from [134] shown in the left row of Table 6.1 were considered during the search for the most significant sources of error in GNSS-Receivers, regarding the constellation information. These variables are taken into consideration as potential inputs for the AI-based approach for the quantitative approximation.

The "white-box" AQF approach is a quantitative approximation to weight the GNSS significant variables regarding the accuracy property of GNSS quality description. Using the weight finding strategy described in [85] these weights are calculated by means of a simple ANN model approximator.

From the proposed variables in Table 6.1, only the number of satellites in view was dismissed. The remaining variables showed significant correlation with the behaviour of the receiver for dynamic measurement accuracy evaluation.

Figure 6.2 presents a graphic description of the used architecture for the quantitative ANN models, using the MATLAB Neural Network Toolbox from MathWorks [82].

The hidden layer of each ANN is composed of six neurons with a log sigmoid activation function, while the output layer of each ANN is composed of one neuron with a linear activation function.

Two independent feed-forward ANN models were developed in order to achieve a combined pseudo-intelligent estimation of both trueness and precision.

After the training stage for both ANN models, the relevance of each input was found. The correspondent weights for both targets in Table 6.2 are adapted to percentage values to represent their influence on the target estimations.[1]

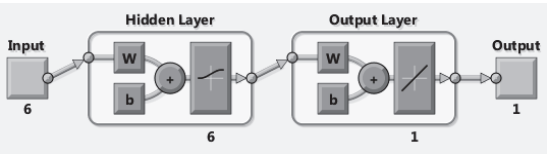

FIGURE 6.2: Architecture of the developed quantitative ANN models

[1]For the deviation module (Trueness) the most representative inputs are GK Northing and Geometric mean of SNR, while for the MD (Precision) are the GK coordinates and the HDOP.

TABLE 6.2: Quantitative approach: Analysis of weights of the proposed inputs

	Trueness (deviation module)	**Precision (Mahalanobis Distance)**
Gauss Krueger Easting	8.18 %	20.80 %
Gauss Krueger Northing	31.32 %	31.40 %
Number of Used Satellites	12.62 %	2.47 %
HDOP	19.18 %	31.29 %
Track Speed	0.05 %	7.56 %
Geometric mean of SNR	28.64 %	6.48 %

6.4 ANN for accuracy-based Qualitative Approach

The "grey-box" AQF approach is a qualitative estimation that describes the accuracy property of the GNSS quality as an uncertainty measurement by means of trueness and precision characteristics. Once the relevant inputs were established by means of the quantitative approach presented above, several ANN topologies were studied to determine the best possible estimator for safety-relevant applications. Not only proximity to the actual accuracy characteristic was taken into consideration, since the size of the ANN model is also an important factor for future implementation.

An exemplary dataset used for the training stage of the ANN models was extracted from the DemoOrt project, presented in [46]. This dataset contains GNSS data as well as GNSS signal information, along with an independent reference system based on data fusion techniques described in detailed in [46, 107], allowing a proper deviation analysis as starting point for the ANN models development.

Figure 6.3 presents a graphic description of the selected architecture to be used for the ANN validation tools for the qualitative approach. The hidden layer of each ANN is composed of 12 neurons with a log-sigmoid activation function, while the output layer of each ANN is composed of a neuron with a tan-sigmoid activation function.

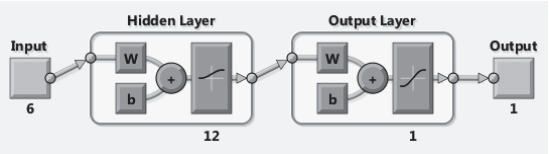

FIGURE 6.3: Architecture of the developed qualitative ANN models

TABLE 6.3: Qualitative approach: Characteristics of the training dataset

Date	*03.02.2009*	
Samples	*2709*	
Number of used satellites	**Minimum**	*4*
	Average	*6*
	Maximum	*10*
HDOP	**Minimum**	*1*
	Average	*2.04*
	Maximum	*14.4*
Track Speed [Km/h]	**Minimum**	*0*
	Average	*25.06*
	Maximum	*60.68*
Geometric mean of the SNR. [dB]	**Minimum**	*32*
	Average	*45.73*
	Maximum	*50*

Table 6.3 presents in detail the training dataset from [46] used for the learning stage in the following section.

6.5 ANN learning and validation stages

Once the topology for the quantitative and qualitative ANN models was defined, the details from inputs and targets were set and the results of the learning stage were presented. Using the MATLAB Neural Network Toolbox from MathWorks [82] several testings were performed until finding the best suitable[2] ANN model.

Figure 6.4 depicted the sections of the intelligent GNSS-based localisation system used for the learning stage. The part framed below presents the inputs for both the quantitative and qualitative approaches; while the part framed above presents the sources of the necessary targets for the qualitative approach.

For the developed Demonstrator-Tool presented in Chapter 7, the Figure 6.4 present the graphical description for the learning stage of the intelligent GNSS-based localisation system, while Figure 6.5 presents the graphical description for the validation stage.

The case study presented in the following section was created with the off-line mode of the developed Demonstrator-Tool from Chapter 7, since it has the possibility of using previously acquired GNSS data protocols to simulate the intelligent GNSS-based localisation system. Protocols from DemoOrt Project [46] were selected for this purposes.

[2]For the scope of this thesis it means the basic topologies required for the prototype.

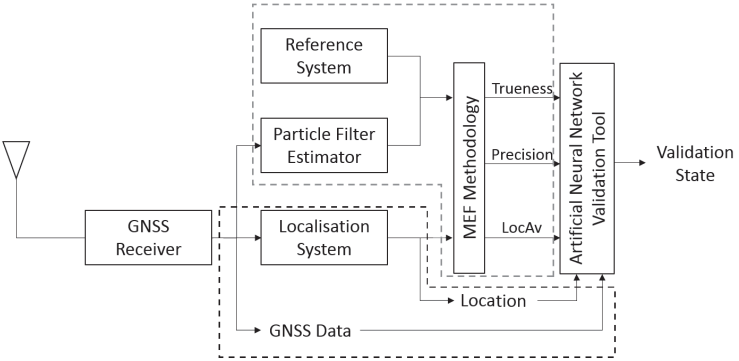

FIGURE 6.4: ANN Validation Tool: learning stage

6.6 ANN-based accuracy estimator - Case study

Figure 6.6 displays over a satellite image the case study dataset with coloured validation codes explained in the following sections. A different dataset from the one used in the training stage from [46] was selected for the validation stage of the developed ANN models. The characteristics of this validation dataset are depicted in Table 6.4.

The selected validation segments present characteristics of a "rural road" scenario, according to the classification in [134] detailed in Table 6.5 from [48].

The developed ANN tools are validated for different circumstances within the tested scenario[3]. Both the ANN models as well as the behaviour of the dynamic localisation system as a whole were tested. The considered "normal city - rural road" presented in Figure 6.6 has no complete open sky trajectories and presents a variable speed of the vehicle over time, as shown in the validation dataset from Table 6.4.

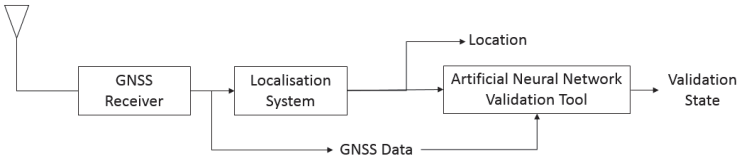

FIGURE 6.5: ANN Validation Tool: validation stage

[3]Such as changes in the values of the input variables.

FIGURE 6.6: Satellite picture of rural scenario location

TABLE 6.4: Qualitative approach: Characteristics of the validation dataset

Date	*29.05.2008*	
Samples	*2411*	
Number of used satellites	**Minimum**	*4*
	Average	*6*
	Maximum	*9*
HDOP	**Minimum**	*0.9*
	Average	*2.24*
	Maximum	*9.4*
Track Speed [Km/h]	**Minimum**	*0*
	Average	*27.99*
	Maximum	*60.77*
Geometric mean of the SNR. [dB]	**Minimum**	*37.95*
	Average	*47.08*
	Maximum	*50*

The dynamic measurements from the dataset are represented with coloured paths, distinguishing significant areas for the further analysis of the ANN models for accuracy-based validation, presenting a meaningful trade for safety-relevant land vehicle applications:

1. An area in **black**, corresponding to the trajectory of the vehicle with **normal behaviour** for both the localisation system and the ANN-based validation tools.

2. An area in **green**, corresponding to the dynamic measurement under **control**, deserving of special observations for further analysis.

3. An area in **orange**, corresponding to **uncontrolled** dynamic measurement ("Orange Alarm" for the intelligent GNSS-based localisation system), deserving of special observations for further analysis.

From all the normal behaviour from the validation dataset, the **controlled** dynamic measurement area plotted in green colour in Figure 6.6 presents two typical cases for the ANN-based validation tools. In both the ANN models estimate correctly the behaviour of the GNSS-based localisation system, although the separation into two regions respond to the two different behaviours of the localisation system as a whole:

1. **Green Area, Region 1:** where both the GNSS-based localisation system and the ANN-based validation tool work within small deviations (±5 meters).

2. **Green Area, Region 2:** where both the GNSS-based localisation system and the ANN-based validation tool work within big deviations (±10 meters).

TABLE 6.5: Scenario description based on number of satellites [48]

	Scenario Description
Scenario 1: Open Roads	Open sky, typically with constant speed of vehicle over time. The average Open sky number of used satellites is optimal.
Scenario 2: Normal City - Rural Road	One side shadowed with no complete open sky trajectories with variable speed of the vehicle over time. The average number of used satellites is normal, but not optimal.
Scenario 3: Narrow City Roads	Urban canyon, covered sky with variable speed of vehicle over time. The average number of used satellites is minimal.

On the other hand the **uncontrolled** dynamic measurement area plotted in orange colour in Figure 6.6 presents the case where the ANN-based estimation and the actual deviation differ significantly.

The colours in the results figures are selected to match the **controlled** and **uncontrolled** dynamic measurement areas as described above. These two selected areas are presented separately to describe the all possible responses of the ANN models as intelligent validation tools for dynamic measurements of GNSS-based localisation systems.

6.7 Green area: Controlled dynamic measurement

Figure 6.7 presents both ANN-based estimations and their correspondent real values over the number of samples. For the analysis of trueness the deviation module was estimated, while for the analysis of precision the MD was estimated.

Figure 6.7A presents the first region in the green area of the validation segment. This describes both trueness and precision of the dynamic measurement system in separated plots having similar behaviour to the estimations produced by the ANN models.

In Green Area Region 1 the expected normal behaviour of the system estimated by the ANN models coincides closely with the measured behaviour.

During this period of time both trueness and precision are provided within the requirements for the presented Scenario 2 in Table 6.5, validating the ANN models' estimation for good quality areas. The GNSS significant inputs during that period of time are depicted in Figure 6.7B. This safe state sets between ± 5 meters.

In Green Area Region 2 presented in Figure 6.8, both deviation module and MD increase, as seen in Figure 6.8A. This translates into a decrease on both trueness and precision of the dynamic measurements. Both ANN models responses are consequent with this decrease, providing a good estimation of the measured error. Figure 6.8B present the significant GNSS inputs during that period of time. This hazardous state sets between ± 10 meters. When the ANN validation tools achieve a correct estimation of the inaccurate behaviour of the dynamic measurement system an alarm is set, informing the lack of trueness and precision to be expected.

This driver's assistance feature of the intelligent GNSS-based localisation system presented in Chapter 7 is very relevant for safety-related issues and further risk analysis of intelligent transportation systems (ITS).

The AI-based validation tools are validated for this kind of cases, because their responses are according to the logical behaviour of the dynamic measurement system.

For bad accuracy-based GNSS quality areas, such as the presented "normal city - rural road" scenario in Green Area Region 2, the ANN tools provide important information, based on the intelligent interpretation of the GNSS variables of the system. Both correct and incorrect behaviour of the localisation system have proven to be properly estimated and validated by the developed ANN models.

6.8 Orange area: Uncontrolled dynamic measurement

The intelligent GNSS-based localisation system considers the area orange in Figure 6.6 as "cautionary alert" or "Orange Alarm", indicating the mismatch between the actual behaviour of the dynamic measurement system and the ANN model estimation. During these periods of time the ANN model estimation is providing an uncontrolled scenario, differing from the actual values. As seen in Figure 6.9A the logical behaviour of the dynamic measurement system for both trueness and precision (deviation module and MD) presented in orange as estimated by the ANN models, while the actual dynamic measurement system presents an unexpected increase in those values during that period of time. The intelligent GNSS-based localisation system interprets this as a potential risk; since all GNSS variables presented in Figure 6.9B indicate that the normal estimated behaviour of the dynamic measurement system should be correct.

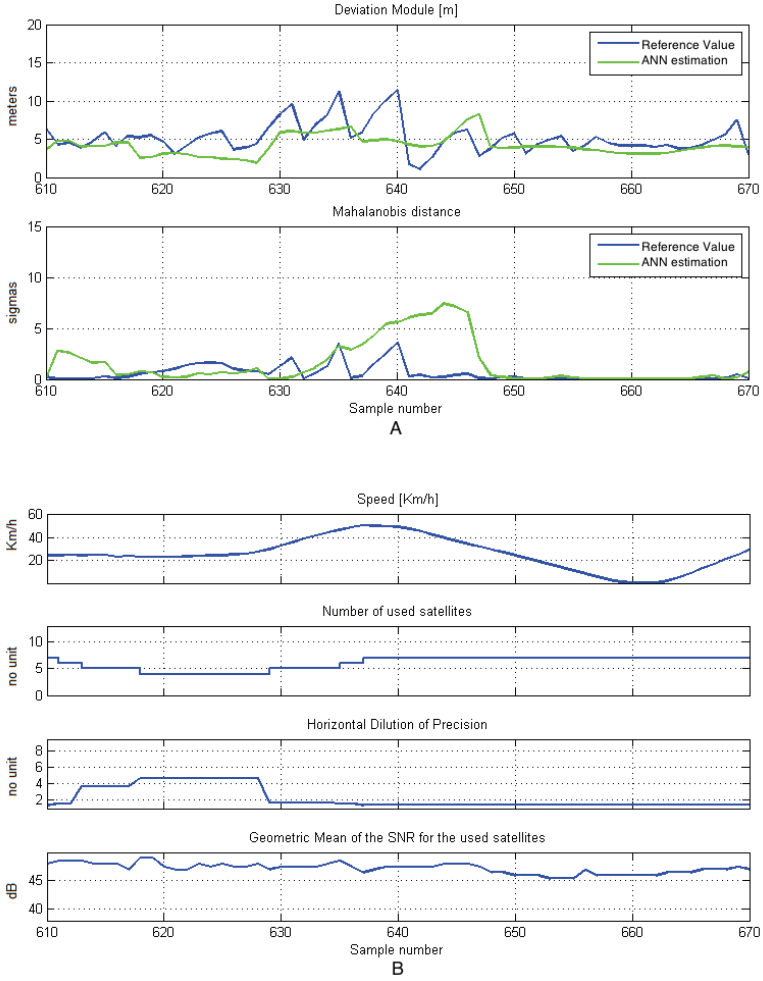

FIGURE 6.7: ANN-based models in Green Area, Region 1: (A) ANN-based models responses and real values comparison (B) Significant inputs for the ANN models

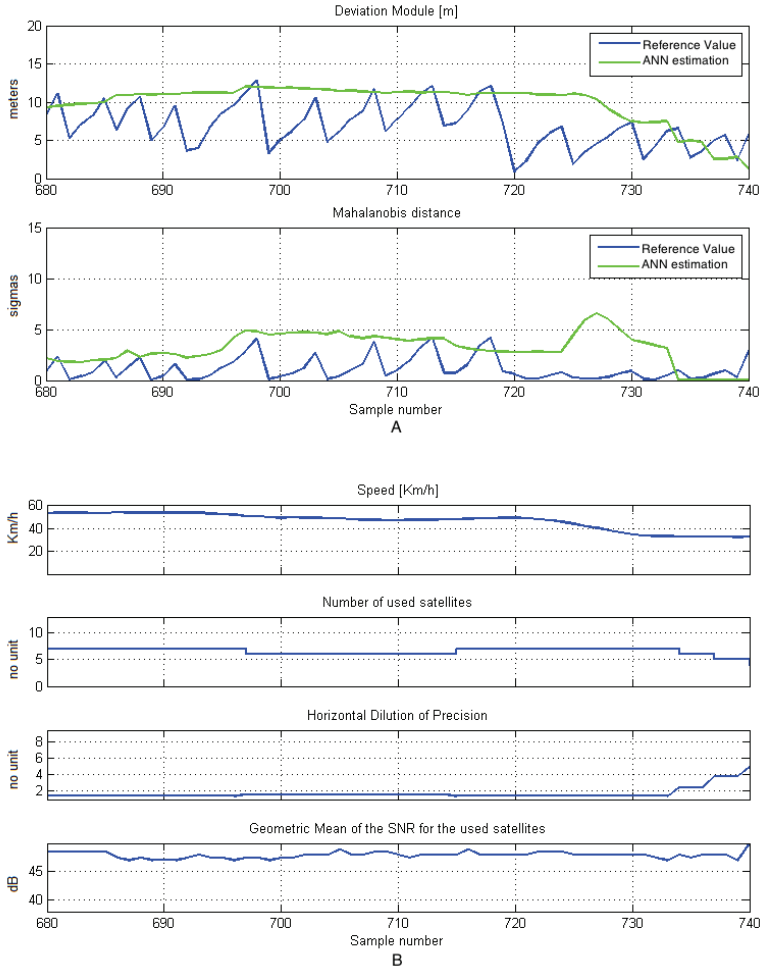

FIGURE 6.8: ANN-based models in Green Area, Region 2: (A) ANN-based models responses and real values comparison (B) Significant inputs for the ANN models

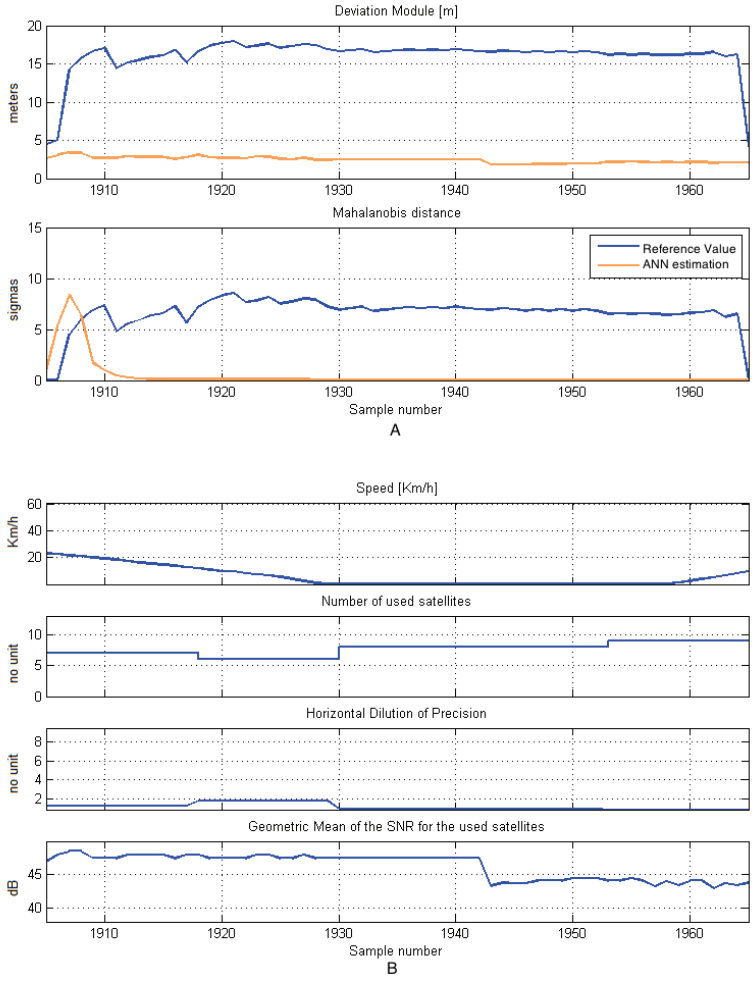

FIGURE 6.9: ANN-based models in Orange Area: (A) ANN-based models responses and real values comparison (B) Significant inputs

In this particular case, while the ANN models inform about the mismatch the dynamic measurement system remains within the requirements and only the "Orange Alarm" is set by the intelligent GNSS-based localisation system to make the driver aware of the potential decrease in trueness and precision.
This kind of uncertainty could lead to unexpected problems regarding the GNSS-based dynamic measurement system, but the developed ANN-based validation tool provides the necessary information to make this **uncontrolled** case into a "known risk" situation, reducing the actual potential risk.
This specific kind of problem, as depicted in Figure 6.9A, could be related to the lack of sequential learning in these basic ANNs models, ignoring unpredictable error by means of shadowing or multipath effect. This can be attributed to the limitations of the developed feed-forward ANN models for lacking sequential memory.

6.9 ANN validation tools summary

This chapter has presented the bases for the accuracy-based ANN models for validation of GNSS-based localisation systems.
Further work regarding special cases should be taken into consideration for future ANN-based accuracy characteristics estimation models.
Figure 6.10 shows a coloured coded trajectory with the results of the ANN-based validation for the considered cases. The controlled dynamic measurements areas are presented with two colours, green for small deviations and red for big deviations, while the uncontrolled dynamic measurements area is presented with orange colour.
The results have shown that the ANN-based methodology can be a promising significant contribution for further development in this research field, for future implementation of AI-based validation tools as an essential part of ITS.
In Chapter 7 the developed intelligent GNSS-based localisation system uses this ANN-based validation tools.

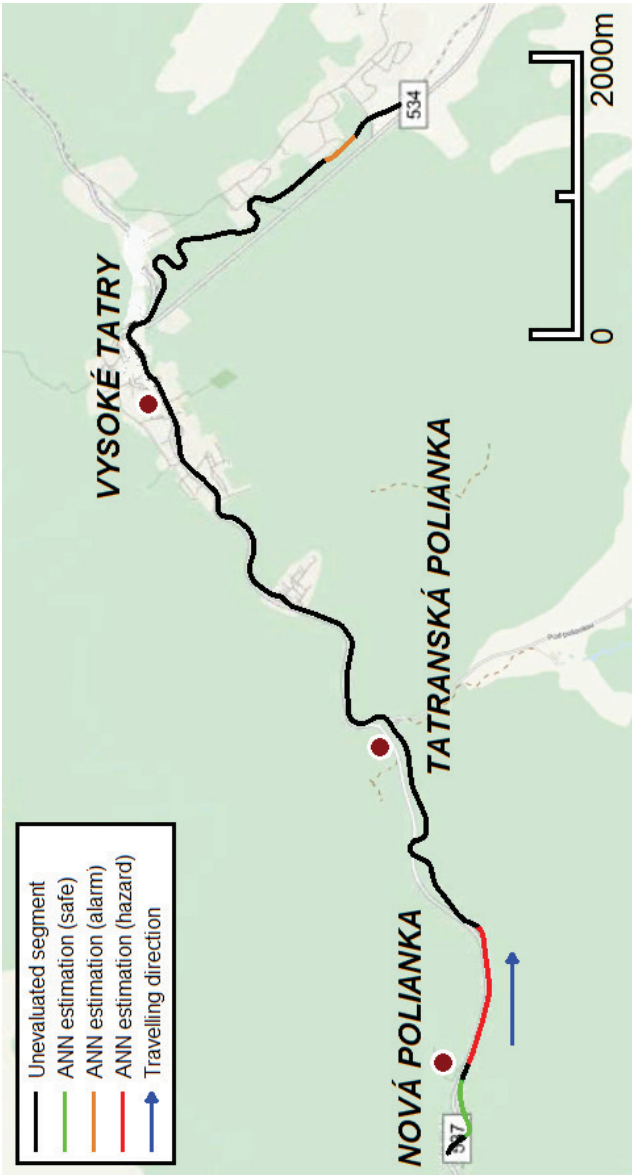

FIGURE 6.10: Vehicle trajectory with coded color GNSS-R validation state

Chapter 7

Intelligent GNSS-based localisation system

"It takes something more than intelligence to act intelligently."

Fyodor Dostoyevsky
Crime and Punishment

All together the intelligent GNSS-based Localisation system articulates many functional parts. This chapter presents the developed Demonstrator Tool in details.

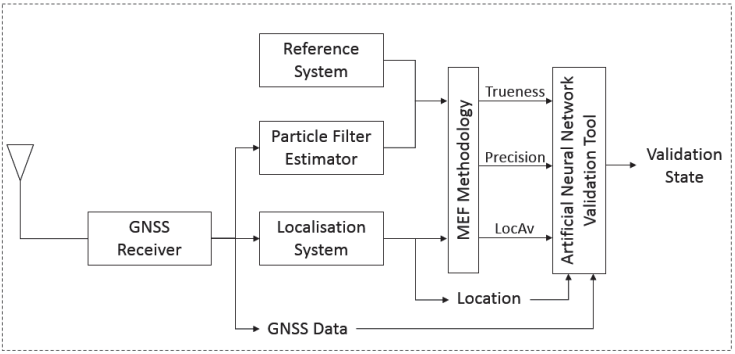

FIGURE 7.1: Graphical description of Chapter 7: Intelligent GNSS-based Localisation System - Demonstration Tool Architecture

This chapter presents the content of the architecture of the developed Demonstrator-Tool. While the off-line data simulation of this intelligent GNSS-based localisation system allows to process collected GNSS-data from the DemoOrt project [46], the on-line mode allowed test runs processing from the M3 tram line in Braunschweig, Germany during July 6^{th}, 2014.

7.1 Demonstrator-Tool description

Figure 7.2 presents a general block-diagram that describes the operations performed by the intelligent GNSS-based localisation system within the Simulink Framework of the Matlab software.
The developed Demonstrator-Tool is composed by the following blocks[1]:

- Data Acquisition Block
- Particle Filter Estimator Block
- MEF Methodology Block
- ANN Training Block
- ANN Prediction Block

The following subsections present a short description of all the blocks involved in the Demonstrator-Tool.

7.1.1 Data Acquisition Block

The Data Acquisition Block (DAB) is a hybrid module (software and hardware combined) composed of a Raspberry PI single-board computer handling low level communication with the reference input and evaluated GNSS-R, as well as the reference speed sensor, and its correspondent part as the block diagram-based software section of the Demonstrator-Tool.

[1]For further information in all blocks descriptions and development, refer to [137].

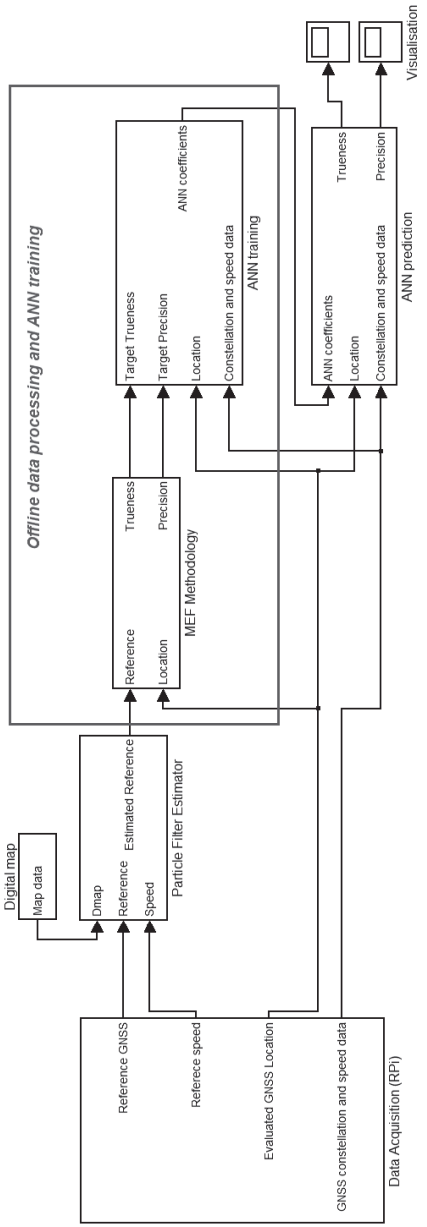

FIGURE 7.2: General block-diagram of the Demonstrator-Tool

The Raspberry Pi (RPi) is a credit card-sized single-board computer developed in the UK by the Raspberry Pi Foundation with the intention of promoting the teaching of basic computer science in schools [138]. RPi is regularly used for low-cost implementations, such as the developed compact demonstration cluster in [139].
The DAB module interacts within the Simulink framework as a host computer through an ad-hoc Wi-Fi connection, providing the output data of the Raspberry PI in the *Data Acquisition* block in Figure 7.2.

7.1.2 Particle Filter Estimator Block

The Particle Filter Estimator (PFE) module is executed as part of the Demonstrator-Tool with the block diagram based program in Simulink.
The PFE module is presented in Figure 7.2 as the *Particle Filter Estimator* block. It performs an estimation of the true position, providing a RS to be used in later stages of the Demonstrator-Tool.
The filter operation developed as a the PF-based location estimation combined with map-matching technique is described in Chapter 5, where the estimation process is based on the speed and position measurements provided by the reference GNSS receiver, and aided by a digital map of the vehicle's route by means of the map-matching technique presented in Chapter 5.

7.1.3 MEF Methodology Block

The MEF Methodology module is executed as part of the Demonstrator-Tool with the block diagram based program in Simulink.
The MEF module is presented in Figure 7.2 as the *MEF Methodology* block.
During the training operation of the ANN models for intelligent validation of the GNSS-based localisation system the *MEF Methodology* module applies the MD-based accuracy evaluation, as extensively described in Chapter 4 to obtain values of trueness and precision to be provided as targets for the *ANN Training* block.

7.1.4 ANN training Block

The ANN training module is executed as part of the Demonstrator-Tool with the block diagram based program in Simulink.
The ANN training module is presented in Figure 7.2 as the *ANN training* block.
The *ANN training* block performs the training stage of the ANN models for accuracy estimation by means of trueness and precision. The needed training stage to obtain the qualitative evaluation is described in Chapter 6.
The result of the training is the intelligent accuracy-based quality function (iAQF) or accuracy estimator by means of trueness and precision.

7.1.5 ANN prediction Block

The ANN prediction module is executed as part of the Demonstrator-Tool with the block diagram based program in Simulink.
The ANN prediction module is presented in Figure 7.2 as the *ANN prediction* block.
During the validation process, the *ANN prediction* block is operational providing qualification estimation of the iAQF, as described in Chapter 6.
Due to the on-line performance of the ANN-based validation tools, during test runs with already learned ANN no RS is required. Even though, the usage of an GNSS-based RS to verify the proper learning of the validation tools is presented in this chapter.

7.1.6 Summary of Simulink Blocks

All presented block in Figure 7.2 (Data Acquisition Block, Particle Filter Estimator, MEF methodology, ANN training, and ANN prediction) are performed within the Simulink host computer, providing the required computational power.
One of the main advantages of developing the Demonstrator-Tool is the flexibility of the Simulink framework that allows easily customised by means of block diagram modifications for specific safety-relevant applications.
The following section will present a test run example describing the behaviour of the developed intelligent GNSS-based localisation system.

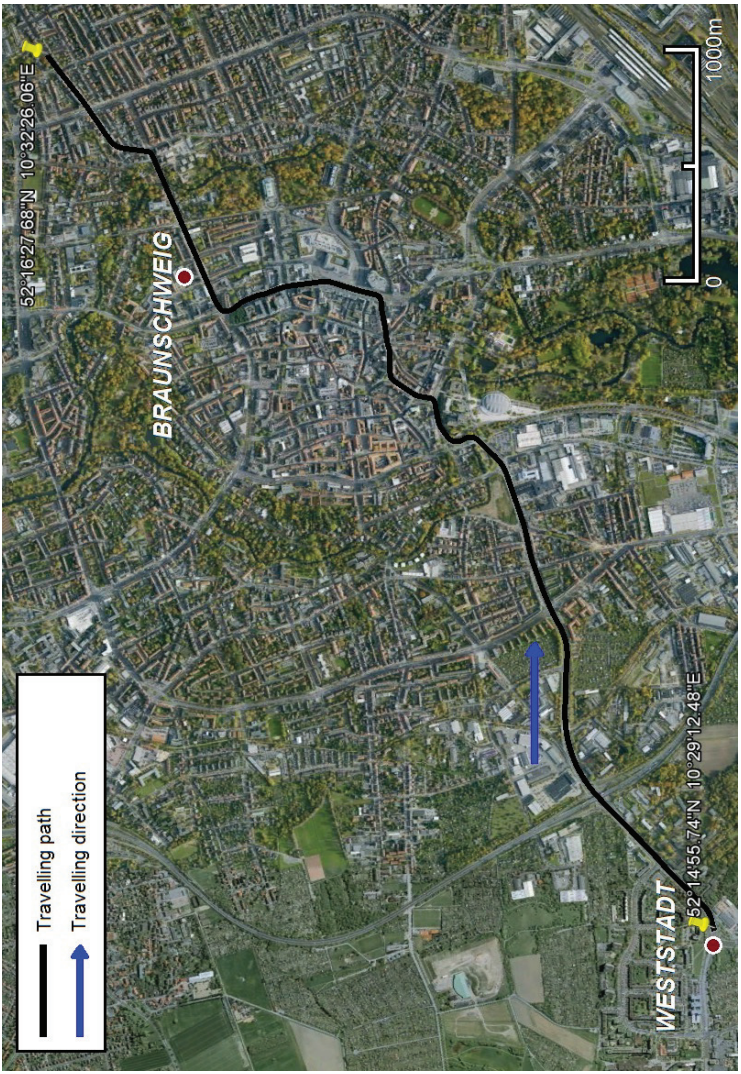

FIGURE 7.3: Satellite picture of the tram route section used in the Demonstrator-Tool

7.2 On-line Demonstrator-Tool performance example

This section presents a test run for the developed intelligent GNSS-based localisation system. The dataset collection, the learning stage and validation stage are explained in detail. Finally an evaluation of the intelligent GNSS-based localisation system is presented.

7.2.1 Dataset Description

In order to test the functionality of the combined methodologies involved in the developed intelligent GNSS-based localisation system a complex route should be take into consideration. Table 7.1 presents the general information of the datasets collected during July, 6*th*, 2014 from the M3 tram line in Braunschweig, Germany.

All datasets were collected by means of a RPi board during the route described in Figure 7.3. This route presents several different scenarios for the assessment of the whole system within several conditions for every recorded test.

The M3 tram line selected for the test runs and depicted in Figure 7.3 has a length of 5320 meters and it is set between the Tram stations of Donaustrasse and Bindestrasse in the city of Braunschweig, Germany.

During the collecting process depicted in Figure 7.4 the PF-Estimator produces the reference from the collected Reference GNSS Position and Speed, combined with the map-matching technique described in Chapter 5.

These collected datasets and the generated reference data are used for the learning and validation stages of the ANN models for AI-based validation tools, as presented in Chapter 6.

TABLE 7.1: Dataset description of test runs for Demonstrator-Tool

Test Run	**Starting Time**	**Duration [m]**	**Sampling Frequency**	**Number of Samples**	**Speed [km/h]**		
					Min	**Mean**	**Max**
M3B1	09:14 AM	26	1 Hz	1579	0	11	54
M3B2	10:14 AM	23	1 Hz	1366	0	13	55
M3B3	11:14 AM	24	1 Hz	1426	0	13	53
M3B4	12:14 AM	24	1 Hz	1419	0	12	58

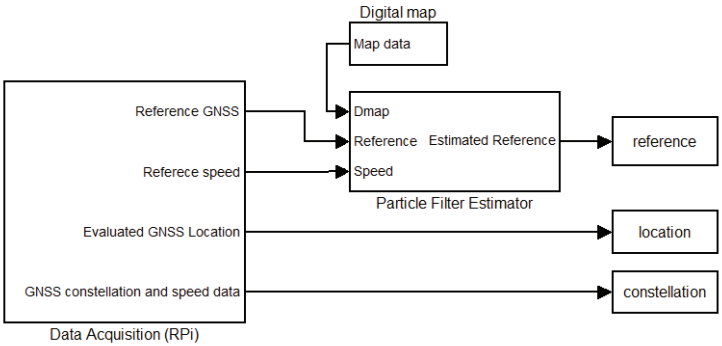

FIGURE 7.4: Block-diagram of the on-line data acquisition and reference generation for ANN training

7.2.2 Learning Stage

The learning stage for the Demonstrator-Tool is similar to the already presented quantitative and qualitative approach for ANN modelling of the quality of the GNSS-based system by means of accuracy evaluation.

During this period the ANN models learn the behaviour of the accuracy characteristics (trueness and precision) of the collected GNSS data. The ANN models produce the so-called learning coefficients. The structure of the ANN-based validation tools produced by this learning stage is depicted in Figure 7.5.

The six inputs are processed by the hidden layer, composed by 12 neurons with log-sigmoid activation functions, while the output layer of each ANN is composed of one neuron with a tan-sigmoid activation function.

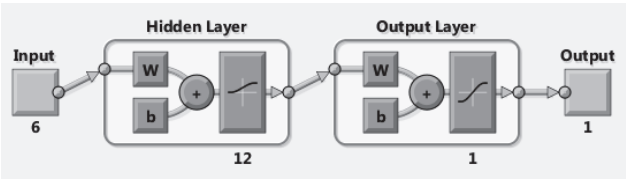

FIGURE 7.5: Structure of the ANN-based validation tool for the Demonstrator-Tool

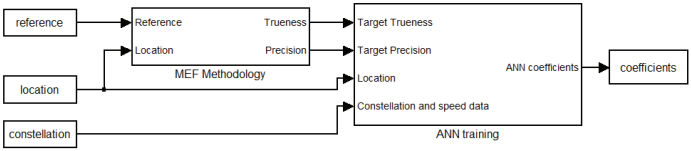

FIGURE 7.6: Block-diagram of the off-line data processing and ANN training operation

Figure 7.6 presents the Simulink scheme for the Learning stage of the Demonstrator-Tool. The ANN training block in the Simulink scheme performs the training of two ANNs with the structure presented in Figure 7.5, for later estimation of trueness and precision respectively.

7.2.3 Validation stage

Once the learning stage is done, the validation stage must be performed.
The coefficients learned by the ANN models during the learning stage are applied and the AI-based validation tools produce estimations for the accuracy characteristics of the GNSS acquired data.
Figure 7.7 presents the Simulink diagram block involved in the validation process.
The ANN models received the position and the constellation information collected and produce an intelligent estimation of the accuracy that allows the validation of the GNSS-based localisation system.

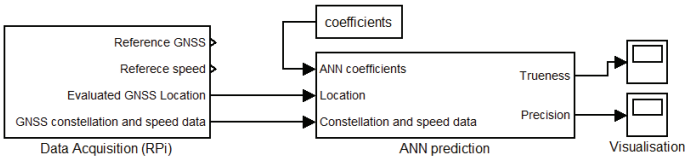

FIGURE 7.7: Block-diagram of the on-line GNSS receiver validation process

7.3 Demonstrator-Tool Results Evaluation

The evaluation of the Demonstrator-Tool can be seen in the following figures. While Figure 7.8 presents the global dataset coded colored estimations, Figure 7.9, Figure 7.10 and Figure 7.11 present specific sections with:

1. **Safe controlled scenario:** where deviation module estimation is under 10 meters and MD estimation is lower than 3σ.
2. **Hazardous controlled scenario:** where deviation module estimation is over 10 meters or MD estimation is higher than 3σ.
3. **Uncontrolled scenario:** where deviation module and MD estimations differ from actual values, hence the estimations cannot be trusted.

In the section shown in Figure 7.9 both real and estimated accuracy parameters present values corresponding to small deviations, therefore this section is classified as a safe controlled scenario and the estimation curve is traced with green color code.
In the section shown in Figure 7.10 both real and estimated accuracy parameters present values corresponding to big deviations, therefore this section is classified as a hazardous controlled scenario and the estimation curve is traced with red color code.
On the other hand, the section shown in Figure 7.11 presents a case where the magnitude of the estimated accuracy parameters differs from the magnitude of the real accuracy parameters, therefore this section is classified as an uncontrolled scenario and the estimation curve is traced with yellow color code. The results presented here show the useful application of the Demonstrator-Tool developed during the present dissertation.
The global M3 tram line collected GNSS dataset, presented as estimations of trueness by means of deviation module and precision by means of Mahalanobis Distance in Figure 7.8, can also be seen over the route map in Figure 7.12, retracing the route section marked in the satellite picture from Figure 7.3. The coding for the color is as following:

- **Color code green:** safe controlled scenario for the GNSS-based system.
- **Color code red:** hazardous controlled scenario for the GNSS-based system.
- **Color code yellow:** uncontrolled scenario for the GNSS-based system (also called alarm scenario).

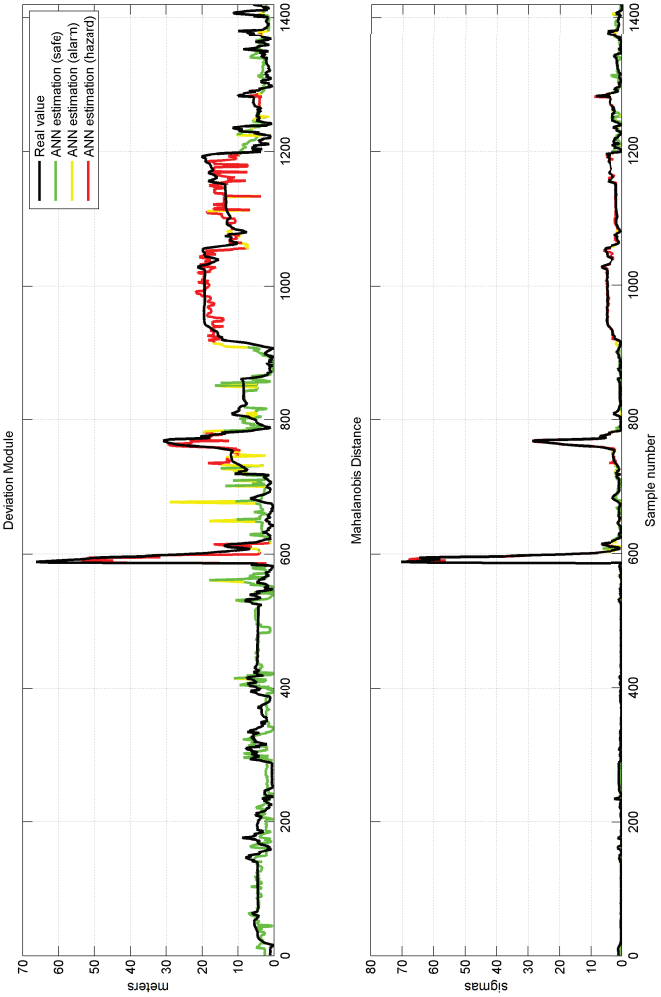

FIGURE 7.8: Coded color ANN-based estimation of GNSS-R validation state for the global dataset

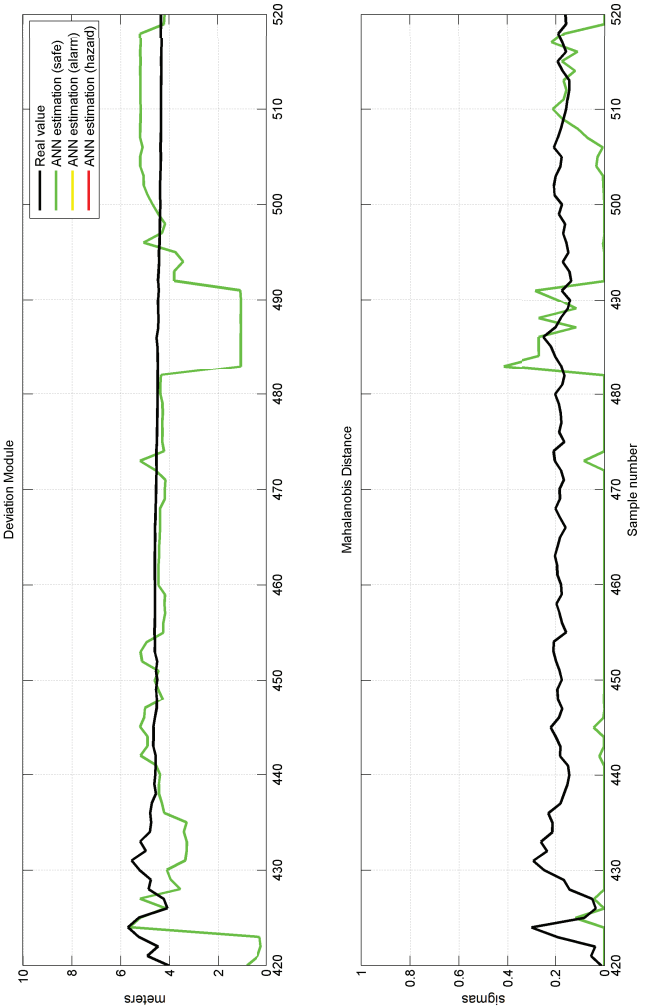

FIGURE 7.9: ANN estimation with coded color for safe controlled dynamic measurement section

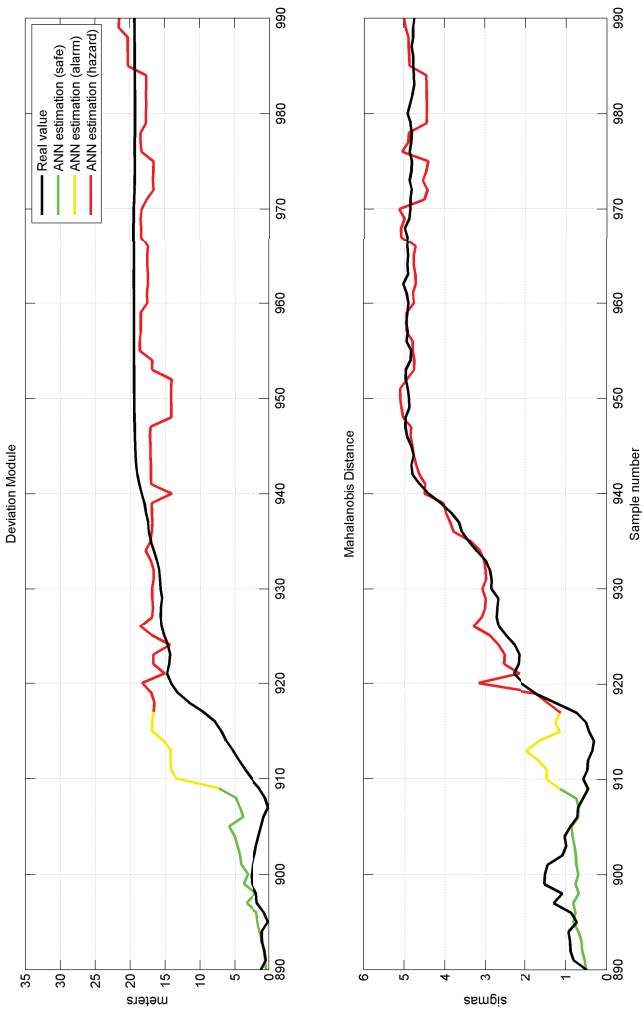

FIGURE 7.10: ANN estimation with coded color of GNSS-R validation state for a section with hazardous controlled dynamic measurement

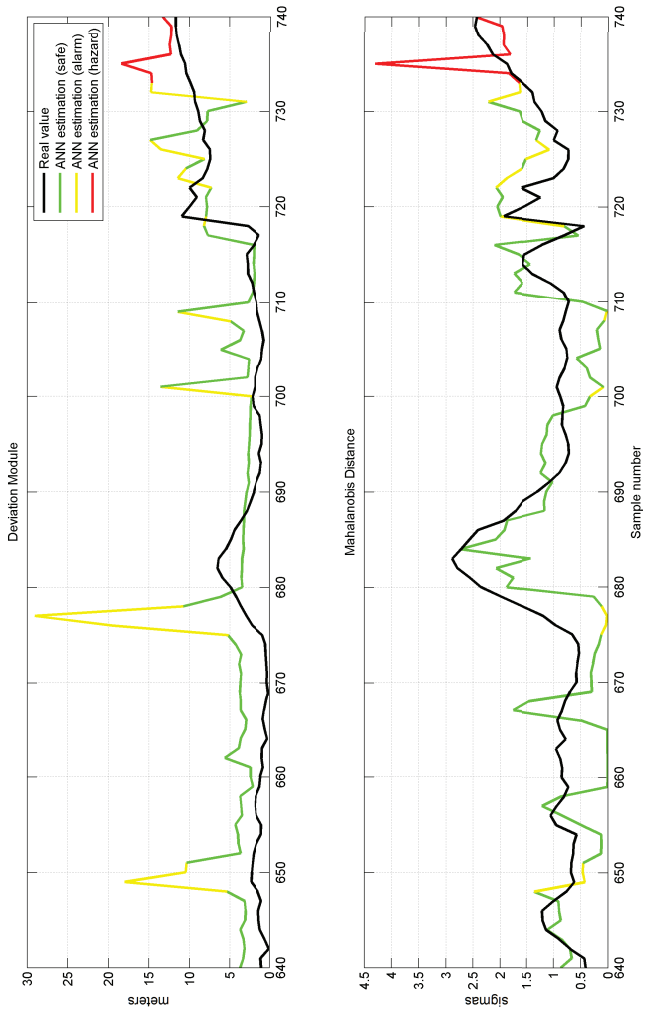

FIGURE 7.11: ANN estimation with coded color of GNSS-R validation state for a section with uncontrolled dynamic measurement

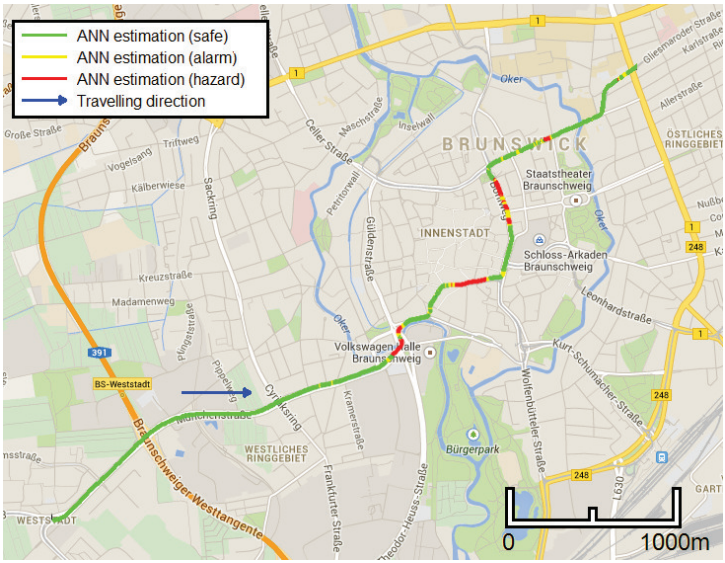

FIGURE 7.12: Vehicle trajectory with coded color GNSS-R validation state

Also, as a final report from Demonstrator-Tool after the GNSS-data has been collected a MEF methodology evaluation is performed (as described in Chapter 4), resulting on the MEF parameters presented in numerical values in Table 7.2 and the MEF plot for the deviation evaluation of the collected dataset and their correspondent validation state from the ANN estimators (as described in Chapter 6) in Figure 7.13.[2]

TABLE 7.2: MEF parameters for location deviation of the input dataset

Parameter		**Value**
Ellipses Center [m]	Easting	-3.5800
	Northing	2.0089
Semi-radii [m]	σ_A	4.7407
	σ_B	8.2545
Rotation	[deg]	-51.76
LocAv 1σ	[%]	60.82%
LocAv 2σ	[%]	75.62%
LocAv 3σ	[%]	82.38%
LocAv 4σ	[%]	86.96%

[2]These plots are a good evidence against the CEP approach. As already mentioned in this thesis an elliptical error approach should be considered.

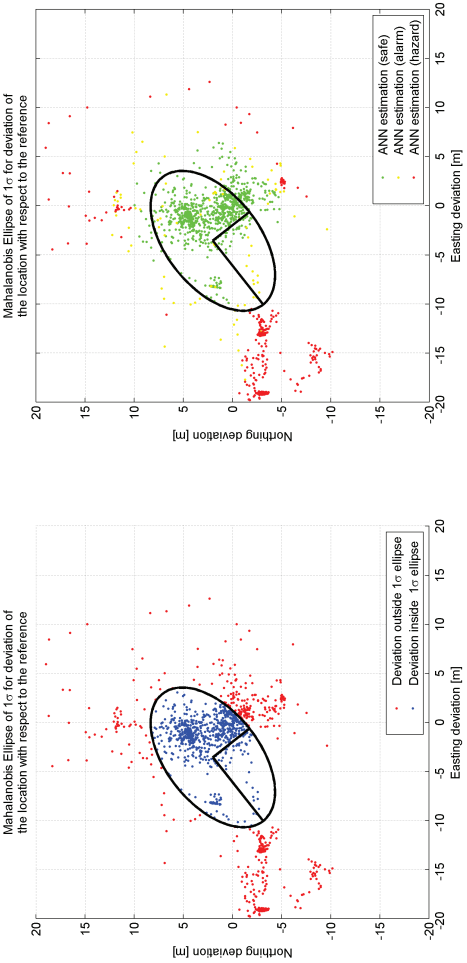

FIGURE 7.13: MEF plot of the input dataset position deviation

Chapter 8

Conclusions and further work

"I don't exactly know what I mean by that, but I mean it."

J.D. Salinger
The Catcher in the Rye

8.1 Major scientific contributions and achievements:

The general achievement of the present dissertation is a significant contribution for intelligent GNSS-based localisation systems.
The system described, modelled and applied corresponds to the first step of AI-based applications for GNSS-based localisation system evaluation and verification, within the research field of ITS.
The significant scientific contributions presented in this dissertation are summarised in the following subsections, with their correspondent description and potential applications, as well as their related further works.

8.1.1 New certification process for GNSS-Receivers

The contribution of a new standarised quality-based GNSS-Receivers certification process presented in Chapter 3 can be already applied by means of quality-based reports, as presented in [15].

The resulting process is the practical application of the abstract process proposed in [44] oriented particularly for safety-relevant GNSS-Receivers usages.
The certified receivers must be tested within the frame of the mentioned accredited laboratories following the procedures also described in Chapter 3.
This process insures the future applications of the attested receivers as part of intelligent GNSS-based localisation systems within a significant range of aimed qualities and prices, allowing low-cost intelligent localisation systems, as presented in [140].
Finally, a robustness analysis should be taken into consideration to ensure this proposal as a certification process.

8.1.2 New Mahalanobis Ellipses Filter methodology

The MEF methodology for accuracy-based receivers quality description by means of deviation evaluation presented in Chapter 4 is a simple mathematical methodology that allows multiple applications, such as GNSS-Receivers certifications (as presented in Chapter 3) and GNSS-Receivers statistical quality control procedures (as presented in Chapter 4).
This newly developed accuracy-based evaluation methodology allows the ITS systems to be tested in tangential (along the road/track) and perpendicular (across the road/track) from land vehicle reference.
These vehicle-referenced coordinates and the proposed elliptical error probability approach can easily result in better detailed requirements for future ITS applications.

8.1.3 New Particle Filter estimator

In Chapter 5 the PF-based dynamic location estimator aided with map-matching technique was the selected methodology for the developed intelligent GNSS-based localisation system in Chapter 7, after the detailed development of many PF-based estimators, better suited for other applications.
This new approach for PF-based estimators can be applied in many estimation problems, beyond the usage for location estimation. Further work in intelligence calibration field is recommended.
The selected approach by means of combination of PF techniques and map-matching also allows a GNSS-dependent reference system for validation tools, as presented in

this dissertation in the developed Demonstrator-Tool from Chapter 7, and it can also be applied for validation purposes for independent reference measurement systems for GNSS-based localisation systems.
Finally, repeatability tests should be taken into consideration to ensure this approach as part of the certification process.

8.1.4 Artificial Neural Networks validation tools for quantitative and qualitative accuracy-based analysis

The presented ANN-based quantitative and qualitative approaches for accuracy-based analysis and estimation in Chapter 6 can be used for any kind of intelligent validation, as well as for calibration purposes.
The present usage as part of the developed intelligent GNSS-based localisation systems from Chapter 7 proves these approaches to be a useful tools for future AI-based applications. Many other intelligent calibration applications can be developed following the methodology presented in this thesis.
Finally, repeatability tests to achieve certifiable status should be taken into consideration to ensure this kind of validation tools as part of the certification process.

8.1.5 Developed software and hardware Demonstrator-Tool

The developed Demonstrator-Tool, both in software and hardware levels for the intelligent GNSS-based localisation system from Chapter 7 are milestones for further AI-based localisation systems, by means of GNSS or any other kind of localisation technique.
The presented results validate the ANN-based estimators as a useful strategy for further development of intelligent GNSS-based localisation systems, within ITS applications such as driver's assistance systems, line or track selectivity systems, and any other localisation-based applications.

8.1.6 Basis for requirements and risk analysis of intelligent GNSS-based localisation system

The basis for intelligent GNSS-based localisation systems requirements, for safety-relevant GNSS-based applications, within the safety theory of [141] can be achieved.

Further work focused on the calculation of the beta factor (β), as suggested in [142]. By adjusting the requirements for safety-relevant GNSS applications, both tangential and perpendicular β factors can be described as:

$$\beta_T = \frac{\overline{X_T}}{\sigma_T} \qquad \beta_P = \frac{\overline{X_P}}{\sigma_P}$$

Where both β factors depend on the trueness (mean value of deviation represented by $\overline{X}$) and precision (standard deviation represented by σ).

8.2 Suggested further work

Even though many of the scientific contributions from the present dissertation can be already applied for safety-relevant applications, there are many improvements or further analyses that can be performed in many of the involved fields.
The following subsections will present suggested paths for future research in these fields.

8.2.1 Certification process for GNSS-Receivers

The certification process for GNSS-Receivers presented in Chapter 3 should be further developed into a legal frame for standarisation purposes within the European territory, since outside Europe standardisation status is unclear.

8.2.2 MEF methodology

Focusing especially on the technical aspects of the proposed certification process for GNSS-Receivers the MEF methodology developed during the present dissertation in Chapter 4 should be defined and written within a normative frame.
A potential DIN could be developed describing the methodology as well as standardised procedures, modelling techniques and accuracy-based quality reports composition.

8.2.3 PF-based estimator development

The achieved GNSS-dependent reference system by means of PF combined with map-matching from the Chapter 5 can be improved towards the inclusion of modelling vehicle

techniques as part of the PF-based estimator.
Further analysis of this kind of improvement is recommended.

8.2.4 ANN-based validation tools development

Further development of the ANN-based validation tools in Chapter 6 can be analysed. The usage of sequential ANN topologies might be useful to improve the accuracy-based estimation, taking into consideration shadowing and multi-path effects on the trueness and precision estimations.
Also an important application for anti-jamming (A-J) and anti-spoofing (A-S) techniques by means of ANN-based validation tools is open for further studies.

8.2.5 Demonstrator-Tool development

A substantial improvement that can be easily applied in the developed prototype from Chapter 7. The usage of better GNSS-Receivers' technologies, such as Differential Global Positioning System (DGPS) or Precise Point Positioning (PPP) modules would allow a potential second version of the Demonstrator-Tool, presenting new adaptability challenges or advantages for ITS applications.

8.2.6 Requirements and risk analysis development

Further work focused on the β factors addition to the requirements for GNSS-based localisation systems should be developed.
And finally a risk analysis of the developed system by means of Petri Nets (PN) modeling and Monte Carlo Simulations (MCS), as well as a second version of the Demonstrator-Tool should allow future ITS applications, within safety-relevant considerations.

Bibliography

[1] Office for Outer Space Affairs of the United Nations. *Report on Current and Planned Global and Regional Navigation Satellite Systems and Satellite-based Augmentation Systems*. International Committee on Global Navigation Satellite Systems Provider's Forum, 2010.

[2] UNITED STATES NAVAL OBSERVATORY. Block 1 satellite information, 1996.

[3] GLOBAL NAVIGATION SATTELITE SYSTEM GLONASS. *INTERFACE CONTROL DOCUMENT. Navigation radio signal in bands L1, L2 (Version 5.1)*. Russian Federation, 2008.

[4] G. W. Hein, et al. Status of Galileo frequency and signal design, 2002.

[5] S. Luan. China puts new navigation satellite into orbit, 2007.

[6] R. Toledo-Moreo and M. A. Zamora-Izquierdo. High-integrity IMM-EKF-based road vehicle. *IEEE Transactions on Intelligent Transportation Systems*, 8(3), 2007.

[7] J. M. Fraile. Advanced GNSS-based localisation system for railway applications. In *Proc. 7th World Congress on Intelligent Systems*, 2000.

[8] P. Gutierrez. EGNSS for road transport: On Galileo's home field. *Inside GNSS*, pages 74–75, February 2014. http://www.insidegnss.com/node/3917.

[9] F. Grasso Toro and E. Schnieder. Basis for certification of GNSS receivers by means of accuracy analysis. In *POSNAV ITS 2013 - Positionierung und Navigation für Intelligente Transportsysteme 2013*, 2013.

[10] F. Grasso Toro, D.E. Diaz Fuentes, and E. Schnieder. Dynamic localisation validation by ANN-based accuracy function. On-going research, 2015.

[11] Wikipedia®. Satellite navigation - comparison of GNSS systems. URL `http://en.wikipedia.org/wiki/Satellite_navigation`.

[12] European Commission. *TEN guidelines Decision Council /EP 1996*. European Commission, 1996.

[13] F. Grasso Toro, D. Lu, and E. Schnieder. Accuracy evaluation of GNSS for a precise vehicle control. In *CTS 2012 13th IFAC Symposium on Control in Transportation Systems*, 2012.

[14] F. Grasso Toro and E. Schnieder. Basis for certification of GNSS receivers by means of reliability analysis. In *CERGAL 2014*, 2014.

[15] F. Grasso Toro and E. Schnieder. Basis for certification of GNSS receivers by means of quality analysis. On-going research, 2014.

[16] F. Grasso Toro, D. E. Diaz Fuentes, and E. Schnieder. New filter by means of Mahalanobis distance for accuracy evaluation of GNSS. In *POSNAV ITS 2013 - Positionierung und Navigation für Intelligente Transportsysteme 2013*, 2013.

[17] D.J. Salmond N.J. Gordon and A. Smith. Novel approach to nonlinear/non-Gaussian Bayesian state estimation. In *Radar and Signal Processing, IEE Proceedings*, volume 140, pages 107–113, 1993.

[18] M. S. Arulampalam, S. Maskell, and N. Gordon. A tutorial on particle filters for online nonlinear/non-Gaussian Bayesian tracking. *IEEE TRANSACTIONS ON SIGNAL PROCESSING*, 50:174–188, 2002.

[19] J. Puchyova. Minimizing of target localization error using multi-robot system and particle filters. In *International Conference on Digital Information Processing, Turkey. World Academy of Science, Engineering and Technology*, pages 856–860, 2013.

[20] J. Puchyova. Behaviour of multiagent system with defined goal. *Information Sciences and Technologies: bulletin of the ACM Slovakia*, 5(4):15–25, 2013.

[21] F. Grasso Toro, M. Hodon, and J. Puchyova. Quality control of GNSS-receivers by accuracy-based analysis. In *SMTDA 2014*, 2014.

[22] E. Schnieder. *Methoden der Automatisierung*. Vieweg Verlag, 1999.

[23] S. Arndt, et al. iglos. the intelligent glossary - terminology management as knowledge network. In *EURO-ZEL 2013 - 21st International Syposium*, 2013.

[24] A. Yurdakul and E. Schnieder. Multilingual problems in navigation terminology. In *TIA - 10th International Conference on Terminology and Artificial Intelligence*, 2013.

[25] A. Yurdakul and E. Schnieder. Standardisierung internationaler terminologien in diversen national-und fachsprachen. In *tekom-Jahrestagung*, 2013.

[26] L. Schnieder and M. Wegener. Transgression of semantic boundaries by methodical terminology management. In *Accuracy 2010 - The Ninth International Symposium on Spatial Accuracy Assessment*, pages 425–428, 2010.

[27] F. Saussure. *Grundfragen der allgemeinen Sprachwissenschaft*. Degruyter, 2006.

[28] P.R. Lutzeier. *Lexikologie*. Tübingen: Stauffenberg, 1995.

[29] W. Wolski. *Das Lemma und die verschiedenen Lemmatypen*. Walter de Gruyter, 1989.

[30] ISO 1087-1/2000. Terminology work vocabulary. theory and application, 2000.

[31] R. Arntz, H. Picht, and F. Mayer. *Einführung in die Terminologiearbeit*. OLMS, 2004.

[32] B. Bessé. *Terminological definitions*. John Benjamins, 1997.

[33] R. Dubuc and A. Lauriston. *Terms and contexts*. John Benjamins, 1997.

[34] A. Yurdakul and E. Schnieder. Solving definition and relation problems in english navigation terminology. In *ICFLTAL 2014 - International Conference on Foreign Language Teaching and Applied Linguistics*, 2014.

[35] B. Hofmann-Wellenhof, K. Legat, and M. Wieser. *Navigation. Principles of positioning and guidance*. Springer Verlag, 2003.

[36] ISO 19133. Geographic information - location-based services - tracking and navigation, 2005.

[37] CENELEC EN50126. Railway applications - the specification and demonstration of reliability, availability, maintainability and safety (RAMS), 2007.

[38] M. E. Peters. *2008 FEDERAL RADIONAVIGATION PLAN.* Department of Transportation USA, 2008.

[39] IEC 60050-191. International electrotechincal vocabulary (IEV) - part 191: Dependability and quality of service, 2002.

[40] D. Lu. *GNSS for Train Localisation Performance Evaluation and Verification.* PhD thesis, Technische Universität Braunschweig, 2014.

[41] F. Haensel, et al. Methods and platforms for certification of satellite based localisation systems in transportation. In *Proceedings of the 6th International Conference on ITS Telecommunications Proceedings*, 2006.

[42] DIN 1319-1. Grundlagen der Messtechnik - Teil 1: Allgemeine Grundbergriffe, 1995.

[43] M. Wegener. *Über die metrologische Qualität der Fahrzeugortung.* PhD thesis, Technische Universität Braunschweig, 2013.

[44] F. Haensel. *Zur Formalisierung technischer Normen.* PhD thesis, Technische Universität Braunschweig, 2008.

[45] DIN EN ISO/IEC 17000. Konformitätsbewertung - Begriffe und allgemeine Grundlagen, 2005.

[46] K. Lemmer, et al. *Entwicklung eines Demonstrators für Ortungsaufgaben mit Sicherheitsverantwortung im Schienengüterverkehr DemoOrt Abschlussbericht der Phasen 1 und 2.* Deutsches Zentrum für Luft- und Raumfahrt, Braunschweig, 2009.

[47] M. Wegener and E. Schnieder. Design of a mobile GNSS reference system for road vehicle localisation. In *20th ITS World Congress*, 2013.

[48] D. Spiegel, F. Grasso Toro, and E. Schnieder. A new methodology towards GNSS-receiver evaluation in non-perfect signal reception environments. In *ENC-GNSS 2014 - European Navigation Conference*, 2014.

[49] D. Spiegel, F. Grasso Toro, and E. Schnieder. A satelite independent high dynamic test bed and first measurement results. In *ION GNSS 2014*, 2014.

[50] D. Niehues. *Ein Beitrag zur hochgenauen Positionsbestimmung von Fahrzeugen als Grundlage autonomer Fahrregime im Hochgeschwindigkeitsbereich.* PhD thesis, Technische Universität Dresden, 2013.

[51] B. Stadlmann, S. Mairhofer, and G. Hanis. Field experience with GPS based train control system. In *ENC-GNSS 2010*, 2010.

[52] J. Poliak, et al. Reference measurement platforms for satellite based safety applications. In *Proceedings on the International Symposium on Operational Space Applications*, 2006.

[53] D. Lu, D. Wu, and E. Schnieder. Hazard analysis for GNSS-based train localisation unit with model based approach according to EGNOS SoL and railway RAMS. In *IAIN 2012 - 14th International Association of Institutes of Navigation Congress 2012*, 2012.

[54] D. Lu, F. Grasso Toro, and E. Schnieder. RAMS evaluation of GNSS for railway localisation. In *ICIRT 2013 - IEEE International Conference on Intelligent Rail Transportation*, 2013.

[55] D. Lu, F. Grasso Toro, and E. Schnieder. Hazard analysis of a satellite-based localisation unit for train. In *WCRR 2013 - World Congress on Railway Research*, 2013.

[56] D. Lu and E. Schnieder. Real-time verification of GNSS receiver measured train location. In *CERGAL 2014*, 2014.

[57] F. Reinbold, M. Wegener, and E. Schnieder. QualiSaR - development of a qualification procedure for the usage of Galileo satellite receivers for safety relevant applications. In *ENC GNSS 2012 - European Navigation Conference*, 2012.

[58] A. Resch, R. Pfeil, and A. Stelzer. Review of the LPM local positioning measurement system. In *IEEE International Conference on Localization and GNSS*, 2012.

[59] M. Wegener, M. Huebner, and E. Schnieder. Entwicklung eines referenzmesssystems für ortungssysteme im straßenverkehr unter berücksichtigung des qualitätsbegriffs. In *AAET 2011 - Automatisierungs-, Assistenzsysteme und eingebettete Systeme für Transportmittel 2011*, 2011.

[60] M. Wegener, F. Reinbold, and E. Schnieder. Anforderungen an ein referenzmesssystem zur untersuchung der GPS-messqualität. *tm – Technisches Messen*, 78:354–363, 2011.

[61] M. Wegener and E. Schnieder. A measurement standard for vehicle localization and Its ISO-compliant measurement uncertainty evaluation. In *IEEE Transactions on Instrumentation and Measurement*, 2012.

[62] M. Wegener, M. Huebner, and M. Brahmi. Requirements on reference systems for vehicle localisation. *ATZelektronik worldwide*, October 2012.

[63] PTB Data Analysis and Measurement Uncertainty Working Group 8.42. Analysis of dynamic measurements, 2014.

[64] M. Wegener and E. Schnieder. State-space based adaptation of the ISO GUM to time-dependent uncertainties of dynamically measured quantities. In *XX IMEKO World Congress 2012*, 2012.

[65] M. Wegener, F. Grasso Toro, and E. Schnieder. Enhancement of the GUM method to dynamical systems: A straightforward approach. In *ADM 2014 - 8th Workshop on Analysis of Dynamic Measurements*, 2014.

[66] F. Grasso Toro, D.E. Diaz Fuentes, and E. Schnieder. Extended accuracy evaluation of GNSS for dynamic localisation in railways. In *WCRR 2013 World Congress on Railway Research 2013*, 2013.

[67] J. Kaipio and E. Somersalo. Statistical and computational inverse problems. *Applied Mathematical Sciences 160*, 2004.

[68] P. Maybeck. *Stochastic models, estimation and control*. Academic Press, 1979.

[69] M. J. Colaco, et. al. *Kalman and Particle filters, METTI V - Thermal Measurements and Inverse Techniques; Volume: I.* Roscoff, 2011.

[70] R. Winkler. *An Introduction to Bayesian Inference and Decision*. Probabilistic Publishing, 2003.

[71] R. Kalman. A new approach to linear filtering and prediction problems. *ASME Journal Basic Engineering*, 82:35–45, 1960.

[72] J. Kaipio, et. al. *State Estimation for Process Imaging, Chapter in Handbook of Process Imaging for Automatic Control*. CRC Press, 2005.

[73] H. Sorenson. Least-squares estimation: from Gauss to Kalman. *IEEE Spectrum*, 7:63–68, 1970.

[74] B. Ristic, M. S. Arulampalam, and N. Gordon. *Beyond the Kalman Filter*. Artech House, 2004.

[75] A. Doucet, N. Freitas, and N. Gordon. *Sequential Monte Carlo Methods in Practice*. Springer, 2001.

[76] J. Carpenter, P. Clifford, and P. Fearnhead. An improved particle filter for nonlinear problems. *IEEE Proc. Part F: Radar and Sonar Navigation*, 146:2–7, 1999.

[77] L. A. Zadeh. Optimum nonlinear filters. *Journal of Applied Physics*, 24:396–404, 1953.

[78] R. S. Bucy. Linear and nonlinear filtering. *Proc. IEEE*, 58(6):854–864, 1970.

[79] H. W. Sorenson and A. R. Stubberud. Nonlinear filtering by approximation of the a posteriori density. *Int. J. Contr.*, 8:33–51, 1968.

[80] R. L. Stratonovich. Conditional Markov processes. *Theor. Prob. Appl. (USSR)*, 5:156–178, 1960.

[81] A. Gelfand and A. F. M. Smith. Sampling-based approaches to calculating marginal densities. *Journal of American Statistic Association*, 85:398–409, 1990.

[82] M. Hudson Beale, et al. *NeuralNetwork Toolbox User's Guide Version 8.2 (Release 2014a)*. The MathWorks, Inc, 2014.

[83] M. Matteucci. *ELeaRNT: Evolutionary Learning of Rich Neural Network Topologies*. PhD thesis, Carnegie Mellon University, 2002.

[84] R. D. Reed and R. J. Marks. *II. Neural Smithing: Supervised Learning in Feedforward Articial Neural Networks*. The MIT Press, 1998.

[85] Y. Liu. The research on the analysis of main parameters affecting GNSS accuracy. Internal report TU-BS, 2013.

[86] K.O. Stanley and R. Miikkulainen. Efficient evolution of neural network topologies. In *IEEE Proceedings of the 2002 Congress on Evolutionary Computation (CEC'02)*, 2002.

[87] K.O. Stanley and R. Miikkulainen. Continual coevolution through complexification. In *In Proceedings of the Genetic and Evolutionary Computation Conference (GECCO-2002)*, 2002.

[88] J. Leitner, et al. Artificial neural networks for spatial perception towards visual object localisation in humanoid robots. In *IEEE International Joint Conference on Neural Networks (IJCNN)*. IEEE, 2013.

[89] H. Mehmood, N. K. Tripathi, and T. Tipdecho. Seamless switching between GNSS and WLAN based indoor positioning system for ubiquitous positioning. *Earth Science Informatics*, 5:1–11, 2014.

[90] National Marine Electronics Association. *NMEA 0183 Standard for Interfacing Marine Electronic Devices Version 2.1*. NMEA National Office, 1995.

[91] Department of Defense, Department of Homeland Security, and Department of Transportation. *2012 FEDERAL RADIONAVIGATION PLAN*. US Government, 2012.

[92] United States Department of Transportation. Research and innovative technology administration: Positioning, navigation and timing and spectrum management, 2007. URL `http://www.rita.dot.gov/pnt/about`.

[93] National Imagery and Mapping Agency. *World Geodetic System 1984: Its definition and relationships with Local Geodestic Systems*. Department of defense, 2000.

[94] ITU Radiocommunication Assembly. Standard-frequency and time-signal emissions. In *International Telecommunications Union. Retrieved 2011*, 2011.

[95] ISO 15725. Accuracy (trueness and precision) of measurement methods and results, 2011.

[96] D. Kaplan and C. J. Hegarty. *Understanding GPS. Principles and applications*. Artech Verlag, 2006.

[97] M. Hodon. GNSS-receiver quality investigation estimated from the implemented standards analysis. In *ICTIC 2012 - The 1st International Virtual Conference*, 2012.

[98] Rong-Tsorng Wang. *"Reliability Evaluation Techniques" (Chapter of "Energy Efficient Fault Tolerant Systems").* Springer, 2014.

[99] J. Liu, et. al. Integrity assurance of GNSS-based train integrated positioning system. *Science China - Technological Sciences*, 54:1779–1792, 2011.

[100] MEFISTO Project. Air traffic control definitions, 1997. URL `http://giove.isti.cnr.it/projects/mefisto/atc_definitions.html`.

[101] A. Filip, H. Mocek, and L. Bazant. GPS-GNSS based train positioning for safety critical applications. *Signal Draht*, 3:51–55, 2001.

[102] U.I. Bhatti, W. Ochieng, and S.J. Feng. Integrity of an integrated gps/ins system in the presence of slowly growing errors. *GPS Solutions*, 11:173–181, 2007.

[103] W. Ochieng, et al. User level integrity monitoring and quality control for high accuracy positioning using GPS/INS measurements. *JGPS*, 7:104–114, 2008.

[104] K. Ping-Ya. *GPS-based precision approach and landing navitagion emphasis on inertial and pseudolite augmentation and differential ionosphere effect.* PhD thesis, Stanford University, 2000.

[105] U.I. Bhatti. *Improved integrity algorithms for integrated GPS/INS systems in the presence of slowly growing errors.* PhD thesis, Imperial College London, 2007.

[106] M. Quddus, W. Ochieng, and R. Noland. Integrity of map-matching algorithms. *Transp Res C Emer*, 14:283–302, 2006.

[107] J. Poliak. *Validierung von satellitenbasierten Eisenbahn-ortungssystemen.* PhD thesis, Technische Universität Braunschweig, 2009.

[108] United States Department of Transportation. *NAVSTAR GPS USER EQUIPMENT INTRODUCTION.* Department of Homeland Security, 1996.

[109] R. Knauf and A. Gonzalez. A TURING test approach to intelligent system validation. In *Leipziger Informatik-Tage*, pages 71–76, 1997.

[110] R. Knauf, K.P. Jantke, and T. Abel. Fundamentals of a TURING test approach to validation of AI systems. In *4nd International Scientific Colloquium, Ilmenau University of Technology*, volume 2, pages 59–64, 1997.

[111] A.M. Turing. Computing machinery and intelligence. *Mind*, pages 433–460, 1950.

[112] B. MOHAN REDDY and RANJAN GUPTA. Introduction: P.C. Mahalanobis and the Symposium on Frontiers of Anthropology. *Human Biology*, pages 819–825, 1995.

[113] P.C. Mahalanobis. On tests and measures of group divergence. *Journal of the Asiatic Society of Bengal*, 26:541–588, 1930.

[114] P.C. Mahalanobis. On the generalized distance in statistics. *Proceedings of the National Institute of Sciences (Calcutta)*, 2:49–55, 1936.

[115] P.C. Mahalanobis. Normalisation of statistical variates and the use of rectangular coordinates in the theory of sampling distributions. *Sankya*, 3:35–40, 1937.

[116] G.J. McLachlan. Mahalanobis distance. *Resonance*, pages 20–26, 1999.

[117] R. De Maesschalck, et al. Tutorial: The Mahalanobis distance. *Chemometrics and Intelligent Laboratory Systems*, 50:1–18, 2000.

[118] J.K. Ghosh and P. P. Majumder. P.C. Mahalanobis' contributions to biometry: a note written on the occasion of his birth centenary. *Annals of Human Biology*, pages 287–289, 1994.

[119] G.J. McLachlan. *Discriminant Analysis and Statistical Pattern Recognition*. Wiley, 1992.

[120] P.C. Mahalanobis. Distribution of the muslims in population of India. *Sankya*, 7: 4–9, 1946.

[121] K. De Vogeleera, et al. Estimation of quality of experience in 3G networks with the Mahalanobis distance. In *CTRQ 2011 - The Fourth International Conference on Communication Theory, Reliability, and Quality of Service.*, 2011.

[122] T. Kamei. Face retrieval by an adaptive Mahalanobis distance using a confidence factor. In *2002 International Conference on Image Processing*, 2002.

[123] W. Trochim. *Research Methods Knowledge Base 3e.* PhD thesis, Cornell University, 2004.

[124] E. Novak. *Deterministic and Stochastic Error Bounds in Numerical Analysis.* Springer, 1988.

[125] C. Andrieu, et. al. Particle methods for charge detection, system identification and control. In *Proceedings of IEEE*, pages 423–438. IEEE, 2004.

[126] O. Pink and B. Hummel. A statistical approach to map matching using road network geometry, topology and vehicular motion constraints. In *Proc. of 11th International IEEE Conference on Intelligent Transportation Systems*, 2008.

[127] Y. Lou, et al. Map-matching for low-sampling-rate GPS trajectories. In *17th ACM SIGSPATIAL International Conference on Advances in Geographic Information Systems*, 2009.

[128] C. Smaili, et. al. A Hybrid Bayesian Framework for Map Matching: Formulation Using Switching Kalman Filter. *Journal of Intelligent Robot Systems*, 74:725–743, 2014.

[129] S. Syed and M.E. Cannon. Fuzzy logic based-map matching algorithm for vehicle navigation system in urban canyons. In *ION National Technical Meeting*, 2004.

[130] M. E. El Najjar and P. Bonnifait. A Road-Matching Method for Precise Vehicle Localization Using Belief Theory and Kalman Filtering. *Autonomous Robots*, 19: 173–191, 2005.

[131] P. Davidson, J. Collin, and J. Takala. Application of particle filters to a map-matching algorithm. In *Gyroscopy and Navigation*, pages 285–292, 2011.

[132] S. Dmitriev, et al. Optimal map-matching for car navigation system. In *Proceedings of 6th International Conference on Integrated Navigation Systems*, 1999.

[133] P. Revesz. Random walk in random and non-random environments. *World Scientific*, 1990.

[134] F. Y. Ming. *DILUTION OF PRECISION CALCULATION FOR MISSION PLANNING PURPOSES.* PhD thesis, NAVAL POSTGRADUATE SCHOOL, 2009.

[135] J. R. Clynch. *GPS Accuracy Levels - Major Accuracy Divisions*. PhD thesis, Naval Postgraduate School, 2001.

[136] u-blox Holding AG. NEO-6. u-blox 6 GPS modules data sheet, 2011.

[137] Damian Eduardo Diaz Fuentes. Development of a simulink based prototype for real-time intelligent GNSS-based localisation. Master's thesis, Technische Universität Braunschweig, 2015.

[138] R. Cellan-Jones. A 15 pound computer to inspire young programmers.

[139] S. J. Cox, et al. Iridis-pi: a low-cost, compact demonstration cluster. *Cluster Computing*, 2013.

[140] F. Grasso Toro, D. E. Diaz Fuentes, and E. Schnieder. Low-cost satellite based localisation system. On-going research.

[141] L. Schnieder and E. Schnieder. *Verkehrssicherheit*. Springer Verlag, 2013.

[142] K. Bierbrauer. *Ein Beitrag zur Bestimmung der Biegetragfähigkeit bestehender Stahlbetonbauteile*. PhD thesis, Universität der Bundeswehr München, 2008.